International Surfaces,
Coatings and Interfaces Conference

SURFCOAT KOREA 2021

Graphene Korea 2021
International Conference

GRAPHENE KOREA 2021

BOOK OF ABSTRACTS

26 - 28 MAY, 2021

VIRTUAL JOINT CONFERENCES

Organizer

SETCOR
Conferences & Exhibitions

SurfCoat / Graphene Korea 2021 Joint Virtual Conferences Preliminary Program

26 - 28 May 2021 (GMT + 2 Time Zone)

26 May, 2021		
SurfCoat Korea 2021 Session I.A **Surface treatments and coatings deposition, functionalization, modelling and characterization**		
Session's Chairs: **Prof. Hee-Jung Im, Jeju National University, Rep. of Korea** **Prof. Christopher Berndt, Swinburne University of Technology, Australia**		
09:00 - 09:30	Highly durable, transparent and superwetting multifunctional nanocoating **J. Yang**	**Prof. Jinglei Yang**, The Hong Kong University of Science and Technology, **Hong Kong**
09:30 - 10:00	Icephobic materials: Current research advances and application challenges **J. Tao**, Y. Shen and Z. Chen	**Prof. Jie Tao**, Nanjing University of Aeronautics and Astronautics, **China**
10:00 - 10:30	Trends and spray pattern flattening by optimizing nozzle shape in cold spray **K. Sakaki**	**Prof. Kazuhiko Sakaki**, Shinshu University, **Japan**
10:30 - 11:00	**Morning Break**	
11:00 - 11:30	High power impulse magnetron sputtering: a flexible tool for synthesis of high performance materials **T. Kubart**	**Prof. Tomas Kubart**, Uppsala University, **Sweden**
11:30 - 11:45	Plasma Treatment of Polytetrafluoroethylene in Nitrogen with Water/Ethanol Vapor Dielectric Barrier Discharge Plasma **S.W. Fitriani**, H. Yajima, F. Hisroshi and A. Hatta	**Ms. Sukma Wahyu Fitriani**, Kochi University of Technology, **Japan**
11:45 - 12:00	Cefazolin- chitosan composite coatings on titanium implant with antibacterial ability **H-M. Huang**	**Ms Hui-Min Huang**, National Kaohsiung University of Science and Technology, **Taiwan**
12:00 - 13:30	**Lunch Break**	
Graphene Korea 2021 Session I: **Graphene and 2D Materials, Growth, synthesis, modification and functionalization and Characterization**		
Session's Chairs: **Dr. Artem Mishchenko, Manchester University, UK** **Dr. Elena Polyakova, Graphene Laboratories Inc, NY, USA**		
13:30 - 14:00	Is the Tipping Point for Graphene Commercialisation Approaching? **R. Collins**	**Dr. Richard Collins**, IDTechEx, **UK**
14:00 - 14:30	Graphene Oxide and Graphene-like Materials: Finding Their Place in the World of Commercial Carbon Materials **E. Polyakova**	**Dr. Elena Polyakova**, Graphene Laboratories Inc, NY, **USA**
14:30 - 15:00	Twistronics and stacking control in van der Waals materials **A. Mishchenko**	**Dr. Artem Mishchenko**, Manchester University, **UK**
15:00 - 15:15	Nacre Shell Inspired Self Assembly of Graphene Oxide-Lipid Nanocomposites **C R Greeshma**, D; Baskaran and A. Mishra	**Ms. Greeshma C. Raghuvaran**, ITT Gandhinagar, **India**
15:15 - 15:30	Disclinations in Graphene and Pseudo-Graphenes **A.E. Romanov**, A.L. Kolesnikova and M.A. Rozhkov	**Prof. Aleksei Romanov**, ITMO University, **Russia**
15:30 - 15:45	A Scalable Method for the Layer-by-layer Thinning of 2D Materials **J. Sun**, G. Giorgi, M. Palummo, P. Sutter, M. Passacantando and L. Camilli	**Dr. Jianbo Sun**, Technical University of Denmark, **Denmark**
15:45 - 16:00	2D-germanium: a structural investigation of germanene on Ag(111) by means of photoelectron spectroscopy and diffraction **L. Kesper**, M. Schmitz, J. A. Hochhaus, M. G. H. Schulte, U. Berges and C. Westphal	**Mr. Lukas Kesper**, TU Dortmund University, **Germany**
16:00 - 16:15	Monolayers in ultrafast intense optical pulses: topological phenomena **S. A. Oliaei Motlagh**, V. Apalkov and M. I. Stockman	**Dr. Seyyedeh A. Oliaei Motlagh**, Georgia State University, **USA**

16:15 - 16:45	Afternoon Break	
SurfCoat Korea 2021 Session I.B: Surface treatments and coatings deposition, functionalization, modelling and characterization		
Session's Chairs: Prof. Tomas Kubart, Uppsala University, Sweden Dr. Mark D. Soucek, University of Akron, USA		
16:45 - 17:15	Investigation of the Non-Isocyanate Urethane Functional Monomer in Latexes: Hydronomers **M.D. Soucek**	**Dr. Mark D. Soucek**, University of Akron, **USA**
17:15 - 17:30	Structure and phase formation of ion-plasma vacuum-arc Zr-B-Si-C-Ti-(N) coatings during deposition **D.S Belov**, I.V. Blinkov, V.S. Sergevnin, A.V. Chernogor, B.Yu. Kuznetsov	**Mr. Dmitry Belov**, National University of Science and Technology MISiS, **Russia**
17:30 - 17:45	Synthesis of Superhydrophobic Fluoropolymer Coatings by Hot Wire Chemical Vapor Deposition **A.I. Safonov**, V.S. Sulyaeva, S.V. Starinskiy and N.I. Timoshenko	**Dr. Alexey Safonov,** Kutateladze Institute of Thermophysics, **Russia**
17:45 - 18:00	Fluorine-free omniphobic slippery surfaces made of PDMS-like molecules: surface structure and wetting properties **M. Callau**, C. Fajolles and P. Guenoun	**Ms. Marion Callau**, Paris-Saclay University/ CEA, **France**
18:00 – 18:15	Development of Bioglass Incorporated Plasma Electrolytic Oxidation (PEO) Coating on Titanium Surfaces for Biomedical Application A. Sukrey and **B.A. Razak**	**Dr. Bushroa Abd Razak**, University of Malaya, **Malaysia**

27 May, 2021		
Graphene Korea 2021 Session II: **Graphene for electronic, photovoltaic and magnetic applications**		
Session's Chairs: **Prof. Kuan Eng Johnson Goh, Institute of Materials Research and Engineering (IMRE), Singapore** **Dr. Debananda Mohapatra, Yeungnam University, Rep. of Korea** **Dr. Mindaugas Lukosius, Inst. for High Performance Microelectronics, Germany**		
08:30 - 09:00	Rediscovery of existing materials through 3D structuring of graphene and carbon nanotubes: case for elastic polyurethane foam J. Lee, J. Kim, Y. Shin and **I. Jung**	**Prof. Inhwa Jung**, Kyung Hee University, **Rep. of Korea**
09:00 - 9:30	Unveiling predominant electrical performance of nitrogen-doped graphene thin film transistors **S-G. Yoon**	**Prof. Soon-Gil Yoon**, Chungnam National University, **Rep. of Korea**
09:30 - 10:00	Natural Graphite and Solvent Processed Bulk Graphene Nanoplatelets For Clean Energy Harvesting **D. Mohapatra,** J.-J. Shim and S. S. Nemala	**Dr. Debananda Mohapatra**, Yeungnam University, **Rep. of Korea**
10:00 - 10:30	Engineering Qubits in 2D Semiconductors **K.E. Johnson**	**Prof. Kuan Eng Johnson Goh**, Institute of Materials Research and Engineering (IMRE), **Singapore**
10:30 - 11:00	**Morning Break**	
11:00 - 11:15	Mass production of soluble graphite that shows ultra-high exfoliation efficiency in liquid **Y. Arao** and M. Kubouchi	**Dr. Yoshihiko Arao**, Tokyo Institute of Technology, **Japan**
11:15 - 11:30	Roll-to-roll process based fabrication of large-area wrinkled graphene on flexible substrates **P. Narute**, C. Jun Lee, R. S. Sharbidre and S-G. Hong	**Mr. Prashant Narute**, University of Science and Technology-Daejeon, **Rep. of Korea**
11:30 - 11:45	XUV-laser induced detachment of multi-layer graphene from silicon carbide substrate **V. Vozda**, T Burian, J. Chalupský, J. Čechald, V. Hájková, L. Juha, M. Krůs, J. Kunc and N. Medvedev	**Mr. Vojtech Vozda**, Institute of Physics- Czech Academy of Sciences, **Czech Republic**
11:45 - 12:00	Chloride Migration in Graphene Oxide Concrete **B. Kim** and M. Ambrose	**Dr. Boksun Kim**, University of Plymouth, **UK**
12:00 - 12:15	Graphene as a standard material for accurate dimensional measurement of the focal volumes of Raman microscopes **A. Sacco**, C. Portesi, A. M. Giovannozzi and A. M. Rossi	**Dr. Alessio Sacco,** INRiM-Turin, **Italy**
12:15 - 14:00	**Lunch Break**	
SurfCoat Korea 2021 Session II: **Surface treatments and coatings deposition, functionalization, modelling and characterization**		
Session's Chairs: **Prof. Uroš Cvelbar, Jozef Stefan Institute, Slovenia** **Prof. Xin Tu, University of Liverpool, UK** **Dr. Ana Ferraria, University of Lisbon, Portugal** **Prof. Irena Kratochvilova, Czech Academy of Sciences, Czech Republic**		
14:00 - 14:30	Plasma engineering of graphene nanowalls and other 2D structures beyond graphene **U. Cvelbar**	**Prof. Uroš Cvelbar**, Jozef Stefan Institute, **Slovenia**
14:30 - 15:00	Insights into oxidation processes of protective coatings from AIMD modelling F. Guo, T. Glechner, N. Koutná, Y. Du, H. Riedl, P.H. Mayrhofer and **D. Holec**	**Prof. David Holec**, Montanuniversitat Leoben, **Austria**
15:00 - 15:30	A route to complexity: sputter deposition using target powders **D. Depla**	**Prof. Diederik Depla**, Ghent University, **Belgium**
15:30 - 15:45	Formation of multiphase synthesized coatings on TiNi substrate **G. Baigonakova**, S. Gunther and A.Shishelova	**Dr. Gulsharat Baigonakova**, Tomsk State University, **Russia**

15:45-16:00	Ultra-Thin Topological Insulator Films for Thermoelectrical Applications: Deposition and Properties. **J. Andzane**, K. Niherysh, E. Kauranens, U. Malinovskis, A. Felsharuk and D. Erts	**Dr. Jana Andzane**, University of Latvia, **Latvia**
16:00 - 16:30	**Afternoon Break**	
16:30 - 16:45	Sol-Gel Surface Coating of 3D Printed Parts **H.G Manning**, J. Mohan, M.Culleton, B. Duffy and J. Kennedy	**Dr. Hugh Manning**, Trinity College Dublin, **Ireland**
16:45 - 17:00	Investigation of Electroless Copper Plating on Textiles using Different Catalysts **G. Taghavi Pourian Azar**, D. Fox, L. Krishnan and A.J. Cobley	**Dr. Golnaz T. Pourian Azar**, Coventry University, **UK**
17:00 - 17:15	Characterization of solid devices using quadrupole SIMS **N. Wehbe**	**Dr. Nimer Wehbe**, King Abdullah Univ. of Sci. & Tech. (KAUST), **Saudi Arabia**
17:15 - 17:30	Finite element simulation of residual stresses and failure mechanism of plasma sprayed thermal barrier coating considering real interface. A. Abdelgawad and **K. Al-Athel**	**Dr. Khaled Al-Athel**, King Fahd University of Petroleum and Minerals, **Saudi Arabia**
17:30 - 17:45	One Structure – Three functionalizations: Laser based microstructures on aluminium with superhydrophobic, ice-repellent and self-cleaning properties **S. Milles**, M. Soldera and A.F. Lasagni	**Mr. Stephan Milles**, Technische Universität Dresden, **Germany**
17:45 - 18:00	Durable polymeric nanocomposite coatings with remarkable icephobic performance **H. Memon**, J. Liu, D. Focatiis, K. Choi and X. Hou	**Mr. Halar Memon**, University Of Nottingham, **UK**
18:00 - 18:15	Friction level control of pneumatic rod seals by surface texturing **M. Brase** and M. Wangenheim	**Mr. Markus Brase**, Leibniz Univ. Hannover, **Germany**
18:15 - 18:30	Mechanical and tribological characteristics of carbon- and nitrogen-based thin films prepared by bottom-up approach **L. Kolodziejczyk**, W. Szymanski, D. Martínez-Martínez, R. Parkhomenko, O. De Luca, M. Knez, P. Rudolf and L. Cunha	**Dr. Lukasz Kolodziejczyk**, Lodz University of Technology, **Poland**

28 May, 2021		
SurfCoat Korea 2021 Session III.A: Surface engineering / coatings for environment, energy, electric, photovoltaic and magnetic applications		
Session's Chairs: Prof. Diederik Depla, Ghent University, Belgium Prof. Kazuhiko Sakaki, Shinshu University, Japan Dr. Alfred Tok Ling Yoong, Nanyang Technological University, Singapore		
08:00 - 08:30	Development of ceramic coatings with hydrogen, corrosion, irradiation, and electrical resistance **T. Chikada**	**Prof. Takumi Chikada**, Shizuoka University, **Japan**
08:30 - 09:00	Tribological performance of novel water-based nano-lubricants used for hot steel rolling **Z. Jiang**	**Prof. Zhengyi Jiang**, University of Wollongong, **Australia**
09:00 - 09:30	Thermal Spraying of Biomaterials: Matching Process Conditions to Phase Structure and Biocompatibility **C. Berndt**	**Prof. Christopher Berndt**, Swinburne University of Technology, **Australia**
09:30 - 09:45	Adsorption Study on The Porphyrin Aggregates Formed at the Toluene/Water Interface **T.A. Gusman** and S. Tsukahara	**Mrs. Tania Gusman**, Osaka University, **Japan**
09:45 - 10:00	Fundamental Analysis of Lignin Molecular Binding Mechanism using Surface Forces Apparatus (SFA) **D. Lee**, Y. Song, S. Lee, J. Park, H. Kwon, J. Lee and C. Lim	**Mr. Dong Woog Lee**, Ulsan National Inst. of Science and Technology, **Rep. of Korea**
10:00 - 10:15	General Trends in Core-shell Preferences of Bimetallic Nanoparticles **N. Eom**, M. E. Messing, J. Johansson and K. Deppert	**Dr. Namsoon Eom**, Lund University, **Sweden**
10:15 - 10:30	Zr alloy protection against high-temperature oxidation: coating by a double-layered structure with active and passive functional properties **I.Kratochvílová**, J. Škarohlíd,, R. Škoda and P. Ashcheulov	**Prof. Irena Kratochvilova**, Institute of Physics of the Czech Academy of Sciences, **Czech Republic**
10:30 - 11:00	**Morning Break**	
Session's Chairs: Prof. David Holec, Montanuniversitat Leoben, Austria Prof. Zhengyi Jiang, University of Wollongong, Australia Prof. Tomas Kubart, Uppsala University, Sweden		
11:00 -11:15	Penetration behaviour of different blasting particles at composite peening **M. Seitz** and K. A. Weidenmann	**Mr. Michael Seitz**, Karlruhe Institute of Technology (KIT), **Germany**
11:15 - 11:30	A new method for testing the abrasive wear of cementitious materials loaded with a spinning wheel S. Czarnecki, **K. Krzywiński**, M. Moj, A. Chowaniec and Ł. Sadowski	**Mr. Kamil Krzywiński**, Wroclaw University of Science and Technology, **Poland**
11:30 - 11:45	The effect of the addition of granite powder to the primer on the pull-off strength of epoxy resin coatings **Ł. Kampa** and Ł. Sadowski	**Mr. Łukasz Kampa**, Wroclaw Univ. of Science and Technology, **Poland**
11:45 - 12:00	Self-protective Paste Nitriding Process of AISI 304 SS for Sea Water Applications **G. Vargas** and L. López	**Dr. Gregorio Vargas**, Center for Research and Advanced Studies (CINVESTAV), **Mexico**
12:00 - 12:15	Amorphous carbon nitrogen-modified layers for light emitting diodes **K. Dyndał**, G. Lewińska, J. Sanetra, S. Kluska and K.W. Marszalek	**Dr. Katarzyna Dyndał**, AGH University of Science and Technology, **Poland**
12:15 - 12:30	Electrostatic discharge behaviors of Diamond-like Carbon on Alumite **S.Yamamoto** and H.Ezaki	**Dr. Shuji Yamamoto**, Japan Coating Center Co., LTD, **Japan**
12:30 - 12:45	Abnormal Aging and Recovery Processes in Perovskite Solar Cells with Metal Electrodes **D.G. Lee**, M-C. Kim, S. Wang, B. Jo Kim, Y.S. Meng and H.S. Jung	**Mr. Dong Geon Lee**, Sungkyunkwan University, **Rep. of Korea**

12:45 - 13:00	Mechanisms for electron emission in ion surface interactions **P. Riccardi**	**Dr. Pierfrancesco Riccardi**, University of Calabria, **Italy**
13:00 - 14:00	**Lunch Break**	
SurfCoat Korea 2021 Session III.B **Bio-interfaces/ Biomedical/ Bioactive surfaces and coatings**		
Session's Chairs: **Prof. Christopher Berndt, Swinburne University of Technology, Australia** **Dr. Mark D. Soucek, University of Akron, USA**		
13:30 - 14:00	Atomic Layer Deposition of Noble Metals with Low Concentration Ozone **A. Ling Yoong**	**Dr. Alfred Tok Ling Yoong**, Nanyang Technological University, **Singapore**
14:00 - 14:15	Development of Electrically Activable Phosphonium Self-Assembled Monolayers to Efficiently Kill and Tackle Bacterial Infections **S. Auditto**, S. Carrara, F. Rouvier, F. Brunel, C. Janneau, M. Camplo, M. Sergent, I. About, J.-M. Bolla and J.-M. Raimundo	**Ms. Sanjana Auditto**, Aix-Marseille Univ, **France**.
14:15 - 14:30	Synthesis of 5,15-A2BC-Type Porphyrins to modify a Field-Effect Transistor for Detection of Gram-Negative Bacteria **L. Neumann**, L. Könemund, F. Hirschberg, R. Biedendieck, D. Jahn, H.-H. Johannes and W. Kowalsky	**Ms. Laurie Neumann**, TU Braunschweig, **Germany**
14:30 - 14:45	Modification of a Field-Effect Transistor for Gram-negative Bacteria Detection Using Porphyrin SAMs **L. Könemund**, L. Neumann, F. Hirschberg, R. Biedendieck, D. Jahn, H.-H. Johannes and W. Kowalsky	**Ms. Lea Könemund**, TU Braunschweig, **Germany**
Graphene Korea 2021 Session III **Graphene for electronic, photovoltaic and magnetic applications**		
Session's Chairs: **Prof. Cecilia Mattevi, Imperial College London, UK** **Prof. Cristiane Morais Smith, University of Utrecht, The Netherlands**		
14:45 - 15:15	Ink formulations of 2D materials for 3D printed energy devices **C. Mattevi**	**Prof. Cecilia Mattevi**, Imperial College London, **UK**
15:15 - 15:45	Research of graphene in 200 mm pilot line: from theory to devices **M. Lukosius**	**Dr. Mindaugas Lukosius,** Inst. for High Performance Microelectronics, **Germany**
15:45 - 16:15	Atom-by-atom design of graphene-like structures **C. Morais Smith**	**Prof. Cristiane Morais Smith**, University of Utrecht, **The Netherlands**
16:15 - 16:45	**Afternoon Break**	
16:45 - 17:15	Graphene, chemistry and single molecule devices **G. Schneider**	**Prof. Grégory F. Schneider**, Leiden Univ., **The Netherlands**
17:15 - 17:30	Large-dimensional MoS2 Transistors Array Fabricated by RF Sputtering and Its Applications **H. Park**, N. Liu, B.H. Kim, Y.J. Yoon and S. Kim	**Ms. Heekyeong Park**, Sungkyunkwan University, **Rep.of Korea**
17:30 – 17:45	Enhanced sensitivity of humidity and soil moisture sensor using liquid exfoliated MoS2 nanosheets **M.S. Siddiqui**, V.S. Palaparthy, H. Kalita, M.S. Baghini and M. Aslam	**Mr. Mohd Salman Siddiqui**, Indian Institute of Technology-Bombay, **India**
17:45 - 18:00	Conductive cationized cotton yarns coated with graphene sheets: in-situ mechanical and electrical properties **L. Maneval**, A. Serghei, N. Sintes-Zydowicz and E. Beyou	**Mrs. Léa Maneval**, University of Lyon, **France**
18:00 - 18:15	Superconducting Dirac point in proximetized graphene **G.N. Daptary**, E. Walach, E. Shimshoni and A. Frydman	**Dr. Gopi Nath Daptary**, Bar-Ilan University, **Israel**

Posters Virtual Session

Posters are being displayed through the Virtual event solution.
Discussions are to be done through the system chat features available to the attendees.

N.	Poster Title	Author, Affiliation, Country
1.	Al2O3 and TiO2 Atomic Layer Deposition on Die Casting Mold Steel for Surface Engineering **R.M. Silva**, F.Oliveira and R.F. Silva	**Prof. Rui Silva**, University of Aveiro, **Portugal**
2.	Fabrication of hierarchical TiO2@NiO nanocomposite electrode with outstanding cycle durability for electrochromic application **J-H. Yu**, R.H. Jeong, D. In Kim, J.W. Lee, J.W. Yang, S. Park, S-H. Nam and J-H. Boo	**Mr. Jung-Hoon Yu**, Sungkyunkwan University, **Rep. of Korea**
3.	Effect of Heat Treatment Temperature on the Microstructure and Properties of Thermally Sprayed Ni-Cr-Mo-Al Alloy Coating **A. Srichen** and C. Banjongprasert	**Ms. Aradchaporn Srichen,** Chiang Mai University, **Thailand**
4.	Evaluation of self-cleaning efficiency of laser-structured aluminum surfaces contaminated with organic and inorganic particles **S. Milles**, M. Soldera and A.F. Lasagni	**Mr. Stephan Milles**, Technische Universität Dresden, **Germany**
5.	GaN epitaxy on graphene/sapphire substrate C-Y. Chiang, Y-C. Chang and **W-C. Ke**	**Mr. Wen-Cheng Ke**, Nat. Taiwan Uni of Science & Technology, **Taiwan**
6.	Hydrogel Based Adsorption Particle Shuttling on Aqueous System while Removing Co Nuclides **H-J. Kim**, S-J. Kim, C.W. Park and H-M. Yang	**Dr. Hyung-Ju Kim**, Korea Atomic Energy Research Institute- Daejeon, **Rep. of Korea**
7.	Surface protection of concrete surfaces with anti-graffiti systems **S. Jäntsch**, C. von Laar and H. Bombeck	**Mrs. Sandra Jäntsch**, University of Rostock, **Germany**
8.	Comparison of wear and cavitation erosion resistance of the cermet coatings sprayed by HVOF **E. Jonda**, L. Łatka, M. Szala and M. Walczak	**Dr. Ewa Jonda**, Silesian University of Technology, **Poland**
9.	Optical sensing properties of citrate-reduced gold nanoparticle thin films **G.J. Lee**, M.A. Yewale, L. N. Nguyen, E.H. Choi, D.G. Kim, T.Y. Kim, and C. K. Hwangbo	**Prof. Geon Joon Lee**, Kwangwoon University, **Rep.of Korea**
10.	Facile fabrication of Cuprous Oxide QDs-Afr 2D array as a sensor media for neurotransmitter **H.K. Lee** and S. J. Park	**Mr. Ho Kyung Lee**, Gachon University, **Rep. of Korea**
11.	Photoluminescence and structural defects of ZnO films deposited by reactive magnetron sputtering with unconventional Ar-O2 gas mixture formation **K. Bockute**, E. Demikyte, S. Tuckute, M. Urbonavicius, S.Varnagiris, G. Laukaitis and M. Lelis	**Dr. Kristina Bockute**, Kaunas University of Technology, **Lithuania**
12.	Study on the Quantum Dot Organic-Inorganic Hybrid Photodetector Using Low Temperature Conbustion Process Based NiOx as an Electron Blocking Layer **K-T. Kim**, W-S. Kim and S-Y Oh	**Dr. Kee Tae Kim**, Sogang University, **Rep. of Korea**
13.	Improved Dark Current of Organic Photodetector By inserting of Hf-SnO2 Layer as an Electron Transport Material **S. Lee**, G-M. Kim and S. Oh	**Ms. Seri Lee**, Sogang University, **Rep. of Korea**
14.	Water-processable LiFePO4/graphene hybrid cathodes for high power Lithium Ion Batteries **J-W. Jeon** and M. Biswas	**Dr. Ju-Won Jeon**, Kookmin University, **Rep. of Korea**
15.	Immobilization of viable proteins onto plasma modified nanofibers investigated by XPS analysis **A. Manakhov** and A. Solovieva	**Dr. Anton Manakhov**, Research Institute of Clinical and Experimental Lymphology– Branch of the ICG SB RAS, **Russia**
16.	Phototransistor with Heterogeneous Double Layer Consisted of Inorganic CsPbIxBr3-x Perovskite and In-Ga-Zn-O Semiconductor for Visible Light Detection **H-J. Na**, S-E. Lee and Y.S. Kim	**Mr. Hyun-Jae Na**, Seoul National University, **Rep. of Korea**
17.	Enhanced wear performance of surface layer of some cold working tool steels after combined finishing processes **D. Toboła** and A. Łętocha	**Dr. Daniel Toboła**, Łukasiewicz Research Network - Krakow Institute of Technology, **Poland**

18.	Phosphate and Flouride Bath Electrolyte for Low-energy PEO Coatings on Mg-based Biodegradable Materials **Y. Husak** and B. Dryhval	**Dr. Yevheniia Husak**, Sumy State University, **Ukraine**
19.	Temperature and Iodine Effects on Hydrogen Oxidation **H-J. Im** and J-W. Yeon	**Prof. Hee-Jung Im**, Jeju National University, **Rep. of Korea**
20	Stability of polyacid-doped polyaniline-based layer-by-layer films **J.W. Jeon**, P.B. Dea Firda and Y. Trianzar Malik	**Dr. Ju-Won Jeon**, Kookmin University, **Rep. of Korea**

SurfCoat Korea 2021 SessionI.A

Surface treatments and coatings deposition, functionalization, modelling and characterization

Highly durable, transparent and superwetting multifunctional nanocoating

Man Kwan Law, Jinglei Yang*

Department of Mechanical and Aerospace Engineering, The Hong Kong University of Science and Technology, Clear Water Bay, Hong Kong SAR, China

Abstract:

Herein, a durable multifunctional nanocoating applied for glazing and cement-based substrates was developed by a simple sol-gel approach with the incorporation of isocyanate silane-modified surfactant. This organic-inorganic hybrid nanocoating integrated a lot of advanced properties, such as high transparentness (Vis transmittance above 85%), extremely super wetting (water contact angle, WCA=4.4±0.3°), and effective de-frosting and anti-fogging performances. It presented a strong adhesion behavior and remained the lowest WCA=5.14±0.2°on the glass after 0.6 m/s water flowing for 30 times (150 mins) under 0.4 Mpa, it also exhibited excellent resistance to 10 weeks of UV aging on the glass and cement substrates with WCA=9.2±2.1°and 14.7±2.3°, respectively. After the test, it demonstrated the durable self-cleaning performance on the cement surface with a low 2.9±0.7% reflectance reduction rate. Most interestingly, this novel nanocoating containing Sb-doping SnO_2 particles showed significant abilities to thermal insulation property, achieving an effective IR shielding performance.

Keywords: Nanocoating; Highly transparent; Superwetting; Durability; Multifunction; Organic-inorganic hybrids; Sol-gel approach.

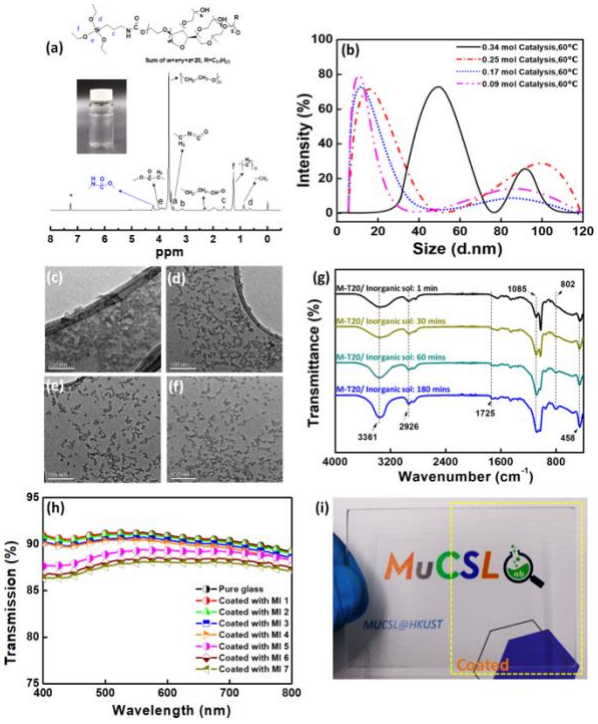

Figure 1 (a) NMR spectra of T20 synthesized from 1:1 molar ratio of ICPTMS and Tween-20; (b) The particle size distribution of prepared inorganic sol #5 with different catalysis concentrations (e.g., 0.34/ 0.25/ 0.17/ 0.09 mol) under a constant temperature 60°C, obtained by DLS measurement; TEM images of Sb-doped SnO_2-SiO_2 NPs (Specimen: inorganic sol #5) obtained with concertation of catalysis (c) 0.34 mol, (d) 0.25 mol,(e) 0.17 mol and (f) 0.09 mol under 60°C; (g) FTIR spectra at different times during synthesis of organic-inorganic hybrid nanocoating; (h) Comparison of transparency properties between the pure glass and different formulas of hybrid nanocoatings with 100 nm thickness; (i) Visual images of pure glass (left side) and glass coated with MI 4 nanocoating (right side).

References:

1. Lee, H.; Alcaraz, M. L.; Rubner, M. F.; Cohen, R. E., Zwitter-Wettability and Antifogging Coatings with Frost-Resisting Capabilities. *ACS Nano* **2013,** *7* (3), 2172-2185.

Icephobic materials: Current research advances and application challenges

J. Tao,[1,*] Y. Shen,[1,2] Z. Chen[2,*]

[1] Nanjing University of Aeronautics and Astronautics, College of Materials Science and Technology, Nanjing, China
[2] Nanyang Technological University, School of Materials Science and Engineering, Singapore

Abstract:
Ice accretion may cause malfunction or serious performance degradation in outdoor facilities and structures, such as aircraft, ship, locks and dams, offshore platforms, solar panels, wind turbines, power transmission towers and lines, and sports facilities, leading to huge economic loss or even loss of human lives. Icephobic materials, typically applied in the form of coatings, have received growing attention in the last decade. We will focus on recent research progress in water wetting state, ice nucleation, and ice adhesion from both theoretical and application perspectives. After a short introduction, static and dynamic water wetting behaviors are discussed, with an emphasis on reducing the water adhesion at low temperatures. Ice nucleation theories have been applied to investigate how the surface texture affects the ice nucleation behavior, which in turn could be used to explain various observed icing delays. Icephobic performance tests at lab scale are then introduced, before several application examples of icephobic materials are illustrated. This presentation ends up with discussions of some outstanding issues and challenges faced by this research community, keeping in mind the complexity of different environment in which practical applications are taking place.

Keywords: icephobic, anti-icing, superhydrophobic, ice nucleation, ice adhesion, icing delay, application.

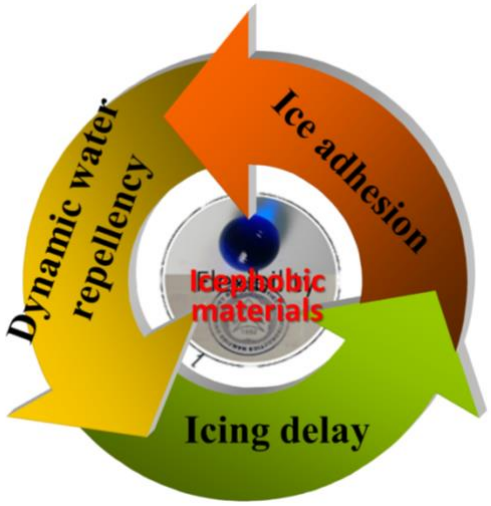

Figure 1: The icephobicity should be systematically discussed and confirmed around the three aspects of dynamic water repellency, icing-delay time, and ice adhesion.

References:

1. Shen, Y., Wu, X., Tao, J., Zhu, C., Lai, Y., Chen, Z. (2019), Icephobic materials: fundamentals, performance evaluation, and applications, *Prog. Mater. Sci.*, 103, 509-557.
2. Xu, Y., Shen, Y., Tao, J., Lu, Y., Chen, H., Hou, W., Jiang, B. (2020), Selective nucleation of ice crystals depending on the inclination angle of nanostructures, *Phys. Chem. Chem. Phys.*, In Press.

Atomic Layer Deposition of Noble Metals with Low Concentration Ozone

Abstract

Noble metal thin films have several potential applications in electronics, protective coating, and catalyst industries. The atomic layer deposition (ALD) of noble metal films are currently achieved using either oxygen or hydrogen as precursors or annealing agents, requiring high temperatures leading to increased risks of explosion and fire. ALD methods not using oxygen or hydrogen as precursors or annealing agents have so far resulted in noble metal oxides instead of pure metal films. An ALD process has been developed for noble metal thin films preparation utilizing low concentration ozone (1.22 g/m^3) as a reactant, without the need for any oxygen or hydrogen. This process has been successfully demonstrated for the fabrication of Rhodium (Rh) and Palladium (Pd) thin films. Both metal films exhibited extremely uniform surface with the root mean square (RMS) surface roughness below 0.2 nm. The 20 nm thick metal films had very low resistivity of 12μΩ cm for rhodium and 63 μΩ cm for palladium, showing the deposited metal films had a high purity. The reaction mechanism of palladium ALD from $Pd(hfac)_2$ and low concentration ozone was also studied by density functional theory (DFT). The simulation results show that $Pd(hfac)_2$ dissociative chemisorbed on Si (100) surfaces. Subsequently, ozone reacted with Pd(hfac)* by cleaving its C-C bond to produce gaseous oxygen and adsorbed CF_3-OC and CF_3-CO-CHO with a relatively low activation barrier. Hence, the reaction was kinetically favourable. The adsorbed complex carbide was then depleted by the excess ozone. The calculated results reveal that pure palladium can be prepared by $Pd(hfac)_2$ and ozone in low concentration without oxygen or hydrogen. All the results indicate that this low concentration ozone based ALD process could yield high quality noble metal films in low temperature and safer way.

Trends and spray pattern flattening by optimizing nozzle shape in cold spray

K. Sakaki [1,*]

[1] Faculty of Engineering, Shinshu University, Nagano, Japan

Abstract:
Cold spray (CS), that is one of the thermal spraying methods, uses a high-pressure process gas that is lower than the melting point of the material particles at a supersonic velocity with a convergent divergent nozzle. The material particles are injected into the flow, are accelerated, and collide with the substrate at high velocity to form a coating. Since the gas temperature is lower than the melting point of the material particles, it has the advantage of suppressing thermal stress, oxidation, and thermal degradation.
Recently, significant requirements have pushed the application of cold spray from a coating process to an AM process which is normally termed as cold spray additive manufacturing (CSAM) [1]. CSAM can be manufactured in the atmosphere, does not dissolve powder, has a large production size, a short production time, and has high flexibility in using the equipment.
In the cold spray process, cross-sectional shape of the nozzle has a significant effect on spray pattern of coatings. The goal of this investigation is to establish a design for the cold spray gun nozzle to gain more uniform spray profile of coatings. We have investigated the influence of expansion ratio, nozzle total length and the ratio of nozzle length of divergent section and parallel section of rectangular nozzle on behaviors of gas and particle by the computational fluid dynamics (CFD) in high pressure cold spraying. We have studied copper particles so far. In this study, we will examine aluminum particles. First, we investigate the influence of the size and shape of the rectangular section nozzle on the velocity, temperature, and particle distribution of aluminum particles by CFD (Figure 1). When the inlet gas pressure rises from 3 to 5 MPa, the overall particle impact velocity increases and the number of particles exceeding the critical velocity increases in CFD results. However, at any gas pressure, the particle impact velocity becomes significantly lower toward the end of the nozzle wall and becomes lower than the critical velocity. After that, the rectangular section nozzles were fabricated and coating formation experiments were conducted, spray patterns and coating cross-sectional structures were observed, and coating adhesion was also evaluated.

Keywords: cold spray, spray pattern, aluminum coating, rectangular cross-section nozzle, CFD.

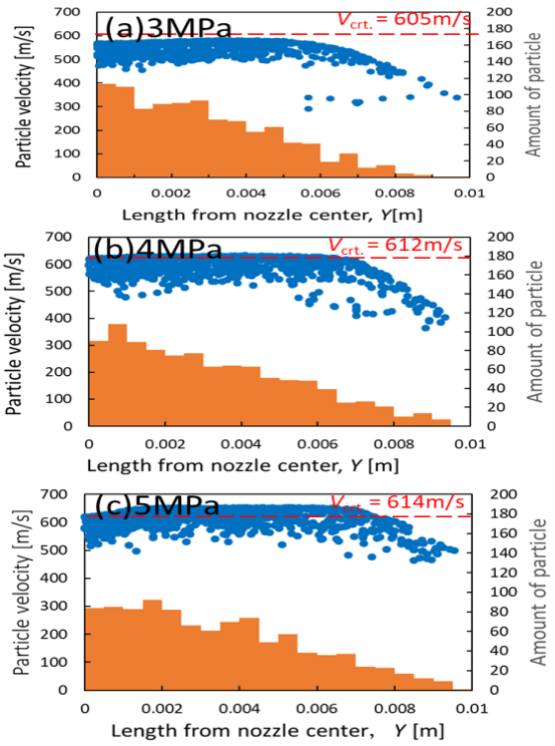

Figure 1: CFD results of influence of gas inlet pressure on distributions of particle impact velocity in the Z-axis direction and particle number on the substrate with 1000 particles (from the center to the end of the nozzle cross section) (P_i=3, 3.5, 4MPa, T_{gi}=623K) V_{crt}: Calculated critical velocity for each gas inlet pressure in cold spray) [2].

References:

1. For example, Li, W., Caroms., Yin, S. (2020), Solid-state cold spraying of Ti and its alloys, *J. Progress in Materials Science*, 110,100633.
2. Sakaki, K., *et al*. (2021) Spray pattern of aluminum coatings with the rectangular cross-section nozzle calculated by the computational fluid dynamics (CFD) in high-pressure cold spraying, *Proc. of International Thermal Spray Conference 2021, In Press.*

High power impulse magnetron sputtering: a flexible tool for synthesis of high performance materials

T. Kubart,[1, *]

[1] Solid State Electronics, Uppsala University, Uppsala, Sweden

Abstract:
Magnetron sputtering is a widely used deposition technique suitable for synthesis of various thin film materials. With increasing demands on the performance, there is a need for techniques that can provide even better materials. This can be achieved using ionized deposition methods where a large fraction of the deposited atoms are ionized. High power impulse magnetron sputtering (HiPIMS) is an ionized variant of magnetron sputtering that combines the advantages of the traditional magnetron sputtering such as flexibility and scalability with improved material quality achieved in an ionized deposition process.
In HiPIMS, the magnetron discharge is operated in a pulsed manner at a low duty cycle (often below 1 %) and at a low frequency (commonly on the order of 100 Hz) to achieve a very high peak power density (0.5–10 kW/cm^2). This leads to increased plasma densities during the pulse on-time (about 10^{19} m^{-3}) that are sufficient to ionize the sputtered atoms. After an intense research effort, HiPIMS is becoming more common in industrial applications.
This contribution gives several examples of thin films synthesized by HiPIMS, highlighting the advantages of the ionized deposition. In the case of diamond-like carbon, the mechanical properties can be significantly improved with a huge reduction in the wear rate for films deposited by HiPIMS as compared to classical magnetron sputtering [1]. Thin metal films for metallization also benefit both with respect to the resistivity, especially at low thicknesses, and by improved surface coverage [2]. The latter is very important for metallization of nanostructured surfaces. Reactive HiPIMS is another exciting area where the growth temperature of various materials can be reduced while keeping the same performance as demonstrated for thermochromic VO_2 [3].
There remain, however, several aspects of HiPIMS that still require further research. For instance, although the discharge characteristics provide information useful for process control, the underlying physical mechanism are not clear. This is especially true in the case of reactive deposition.
In summary, HiPIMS is a deposition technique that is very interesting for applications as well as an exciting research topic.

Keywords: Magnetron sputtering, HiPIMS, Thin film materials, Surface engineering, Pulsed discharges

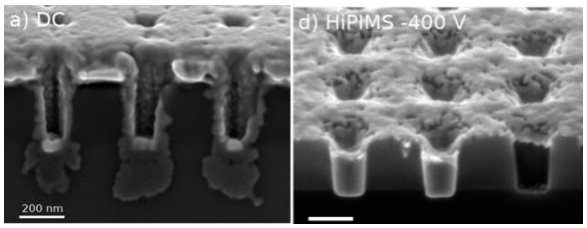

Figure 1: An example illustrating ionized deposition of Cu. The HiPIMS process shows excellent filling inside nanosized holes (right hand side) as compared to poor filling in classical sputtering (left) [2].

References:

1. Aijaz, A.; Ferreira, F.; Oliveira, J.; Kubart, T. Mechanical properties of hydrogen free diamond-like carbon thin films deposited by high power impulse magnetron sputtering with Ne. *Coatings* 2018, 8, 385.
2. Jablonka, L.; Kubart, T.; et al. Metal filling by high power impulse magnetron sputtering. *J Phys D* 2019, 52, 365202.
3. Aijaz, A.; Ji, Y.-X.; Montero, J.; Niklasson, G.A.; Granqvist, C.G.; Kubart, T. Low-temperature synthesis of thermochromic vanadium dioxide thin films by reactive high power impulse magnetron sputtering. *Sol Energ Mat Sol C* 2016, 149, 137-144.

Plasma Treatment of Polytetrafluoroethylene in Nitrogen with Water/Ethanol Vapor Dielectric Barrier Discharge Plasma

Sukma Wahyu Fitriani[1*], Hideki Yajima[2], Furuta Hisroshi[3,4], Akimitsu Hatta[3,4]

[1]Graduate School of Engineering, Kochi University of Technology, Kami, Japan
[2] ORC Manufacturing, Co. Ltd., Chino, Japan
[3]School of System Engineering, Kochi University of Technology, Kami, Japan
[4]Center for Nanotechnology, Research Institute, Kochi University of Technology, Kami, Japan

Abstract:
Surface modification of polytetrafluoroethylene (PTFE) to improve adhesion properties has gained more interest. Several studies investigated plasma treatment on the PTFE using different kinds of plasma (e.g., low-pressure plasma, atmospheric pressure plasma) and gas reaction (e.g., helium, oxygen, nitrogen, argon, argon/water-ammonia) showed an interesting result. In contrast, plasma treatment of PTFE by water-ethanol vapor with nitrogen gas has not yet been studied in detail. In this study, surface treatment of PTFE was carried out by using dielectric barrier discharge (DBD) plasma of nitrogen mixture with water-ethanol vapor, which ethanol concentration was varied form 0% - 100%. Nitrogen gas was bubbled into water/ethanol solution, then the mixture gas was introduced in between a pair of glass plates with a 2 mm gap. The DBD plasma was generated by applying 15 kV and 25 kHz sinusoidal wave to the electrodes on the pair of glass plates. Water contact angle (WCA) measurement and XPS analysis were performed before and after plasma treatment. In addition, stabilization of modification was analyzed by dipping plasma-treated PTFE into water.
Plasma treatment has successfully enhanced the wettability of PTFE, which showed by reduction of WCA from 110^{o} of the original PTFE to 12^{o} after plasma treatment. The spectrum of XPS shows that functional polar groups were formed on the PTFE surface after plasma treatment. The oxygen-containing functional groups and the nitrogen-containing functional group were detected on the modified PTFE, carboxyl group at 288.5 eV (O-C=O), carbonyl group at 287.7 eV (C=O), hydroxyl groups at 286.6 eV (C-O) and amine group at 285.6 eV (C-N). Appearances of the functional groups correspond to the decreasing of water contact angle. Degradation of the WCA was occurred after dipping plasma-treated PTFE in water. It might be due to the creation of low molecular weight oxidized materials (LMWOM) on the PTFE surface as a thin film which is dissolved in water. Furthermore, it was challenging to reduce the creation of LMWOM by DBD plasma treatment.

Keywords: DBD plasma, PTFE, surface functionalization, nitrogen-water/ethanol

References:

1. N. Inagaki, S. Tasaka, K. Narushima and K. Teranishi (2002), Surface Modification of poly(tetrafluoroethylene) with Pulsed Hydrogen Plasma, *J. Appl. Polym. Sci.*, 83, 340
2. J. Hubert, T. Dufour, N. Vandencasteele, S. Desbief, R. Lazzaroni and F. Reniers (2012), Etching Processes of Polytetrafluoroethylene Surface Exposed to He and He-O2 Atmospheric Post-discharge, *Langmuir*., 28, 9466
3. W. Hai, T. Hi, K. Shimizu and T. Yajima (2015), Preparation of Super Hydrophilic Polytetrafluoroethylene Surface using Gaseous Ammonia-Water Low-Temperature Plasma, *J. Photopolym. Sci. Technol.*, 28, 479

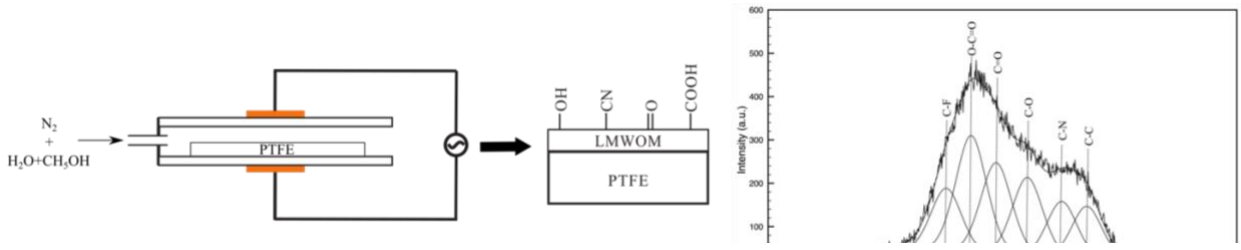

Figure 1: Illustration figure of present study: highlight from the experiment and the result

Cefazolin–chitosan composite coatings on titanium implant with antibacterial ability

Hui-Min Huang[1], Shih-Fu, Ou[1*]
[1] National Kaohsiung University of Science and Technology, Department of Mold and Die Engineering, Kaohsiung, Taiwan

Abstract:
According to the National Joint Registry in the United Kingdom, the number of hip and knee replacements increased by 19.47% and 27.72% respectively over the last decade [2]. At least 5% of these surgeries are subject to complications associated with infections, which usually have serious consequences to the patient's health, such as implant extraction. Infections are mainly caused by Staphylococcus aureus (S. aureus) andStaphylococcus epidermidis (S. epidermidis), Escherichia coli (E. coli), Pseudomonas aeruginosa (P. aeruginosa) and proteus [2]. This study aims to fabricate a drug-delivery coating on a Ti implant which provides antibacterial ability on E. coli. The cefazolin drug carried by chitosan was deposited on Ti surface by electrophoretic deposition. Before deposition, Ti was alkali-treated for the improved coating adhesion. Schematic illustration of the coating process was shown in Figure.1. The morphology, composition, adhesion, and antibacterial ability of the coating was identified. Results show that the cefazolin-chitosan coating has good adhesion which attained 5B grade evaluated by adhesion test. The cefazolin with needle shape was distributed in the chitosan matrix on Ti. The cefazolin-chitosan coating exhibited almost 100% antibacterial activity against E. coli after 8 h incubation, because cefazolin has a high release rate after 8 hours. In addition, the antibacterial activity of the cefazolin-chitosan coating (up to 89%) was higher than the chitosan coating (53%) after 24 h incubation.

Keywords: drug; Ti; surface

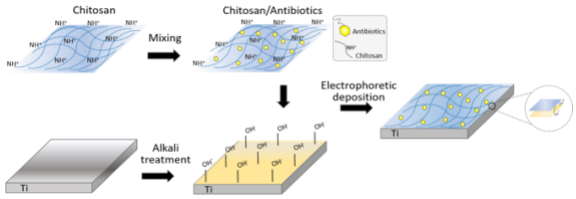

Figure.1: Schematic illustration of the coating process

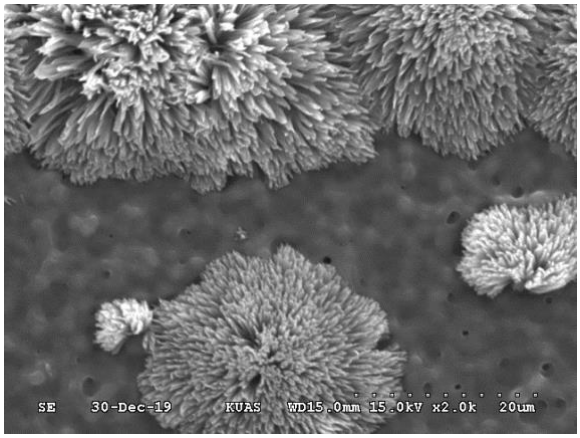

Figure 2: SEM micrograph of the cefazolin-chitosan coating.

References:

1. Agarwal R., García A.J. (2015), Biomaterial strategies for engineering implants for enhanced osseointegration and bone repair, *Adv. Drug Deliv. Rev.* 94, 53–62.
2. Melero H., Fernández J., Dosta S., Guilemany J.M. (2011), Caracterización de nuevos recubrimientos biocompatibles de hidroxiapatita-TiO_2 obtenidos mediante *Proyección Térmica de Alta Velocidad, Cerámica y Vidr* 50 (2), 59–64.

Graphene Korea 2021 Session I:

Graphene and 2D Materials, Growth, synthesis, modification and functionalization and Characterization

Is the Tipping Point for Graphene Commercialisation Approaching?

Dr. R. Collins, IDTechEx, Boston, USA

Abstract:
As the hype for graphene fades the revenue increase reaches its inflection point. Graphene offers tremendous opportunities in numerous sectors. Indeed, IDTechEx forecast that it will become a *ca.* $700m market for the material alone by 2031. Despite this, many graphene companies are in that crucial step where they finally must convert their numerous leads into sales.
Significant orders have been observed for graphene powders and nanoplatelets in enhanced polymers, heat spreaders, wear resistant liners, anti-corrosion coatings, and energy storage devices. And this is just the start. Numerous sectors will adopt this material over the next 5-years after a prolonged period of in-house testing and supply chain immaturity. Market leaders and beginning to emerge and a period of consolidation over the next decade is inevitable.
In this talk, IDTechEx outline the past, present and future of graphene whilst considering trends in production capacity, price, revenues, and applications.
Graphene commercialization, in many ways, is following in the footsteps of CNTs. This technology too experienced a hype cycle but now is making a steady but quiet commercial progress. Indeed, it has entered the phase of rapid volume growth partially thanks to its falling price over the past few years. In this talk, we will consider the past, present and future of CNTs in terms of the evolution of industry production capacity, price, revenues, and applications.
This talk will conclude with a look at the developments of CVD grown graphene and the emerging field of 2D materials beyond carbon.

Keywords: Graphene, 2D materials, Nanoplatelets, Graphene oxide, Nanomaterial, Graphene Powders, Graphene Applications, Commercialisation

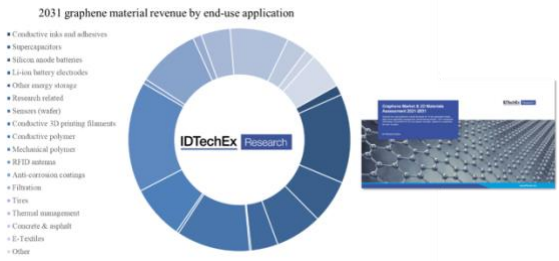

Figure 1: Graphene Market and 2D Material Assessment 2021-2031. Source: IDTechEx.

Graphene Oxide and Graphene-like Materials: Finding Their Place in the World of Commercial Carbon Materials

Dr. Elena Polyakova, CEO, Graphene Laboratories Inc.
A subsidiary of G6 Materials Corp (GGG.V)

Abstract

Carbon atoms are the backbone of organic chemistry. A combination of these atoms can lead to the creation of an infinite variation of complex organic structures. For example, soot particles can form in nature and be synthesized in the lab quite easily, while each particle possesses a unique, complex geometric structure. Mankind produces a broad spectrum of carbon materials that are available in industrial qualities at reasonable prices including carbon fiber, carbon black, acetylene black, vapor grown carbon fibers, micronized graphite, expanded graphite, spherical graphite, activated carbon, glassy carbon, synthetic graphite, fullerenes and carbon nanotubes.

Over the last 15 years, a plethora of new materials marketed as "graphene" has emerged. It should be noted that graphene itself is an ideal rather than a real object, therefore it is more appropriate to label such materials as being 'graphene-like' in nature. Graphene-like materials can be broadly classified as structures with a high aspect ratio and having thickness of less than 10 nanometers. They are produced by various techniques that involve the exfoliation of graphite and synthesis using various forms of hydrocarbon sources. Graphene-like materials currently face fierce competition from commercially available carbon materials. For every new graphene-like material produced, there are a number of low-cost carbon alternatives that make it difficult to enter to the commercial marketplace. We will provide a general overview of the similarities and differences between these materials as well as suitable experimental techniques for their characterization.

Graphene Oxide is an emerging material that has been initially considered as a precursor for graphene production. Now, it is finding applications due its unique chemical nature as well as its ability to be further chemically modified by a variety of chemical moieties. We will overview the revolutionary potential of this material as well as the challenges associated with its production and practical use.

Twistronics and stacking control in van der Waals materials

A. Mishchenko

The University of Manchester, UK

Abstract:
I will present our recent progress in quantum properties of van der Waals materials. The advent of Van der Waals technology has allowed the development of many materials that did not exist before and has led to the observation of many exciting new physical phenomena in these materials due to the unique electronic, optical and mechanical properties of 2D atomic crystals. In particular, I will discuss how interlayer twist angle and stacking order can be used for deterministic control of the properties of van der Waals materials. Tuning twist angle (twistronics) became recently a huge field since electronic bands of 2D materials, their nontrivial topology, electron-electron interactions, and other structural and electronic degrees of freedom can be dramatically changed by a moiré pattern induced by twist angles between different layers. On the other hand, control of the stacking order provides an alternative approach to program quantum properties, and without the need of a moiré superlattice.

Controlling stacking order in multilayer graphite films allowed us to discover the quantum Hall effect in hexagonal graphite and to find strong electronic correlations in rhombohedral graphite films.

Nacre Shell Inspired Self Assembly of Graphene Oxide-Lipid Nanocomposites

C R Greeshma [1], Dhyanesh Baskaran [1], Abhijit Mishra [1]
[1] Materials Science and Engineering, Indian Institute of Technology, Gandhinagar, Gujarat, India

Abstract:
Nanoscale graphene oxide-lipid composites have shown wide applications in the field of biosensing and nanosafety. While macroscopic free-standing membranes of this combination potentially offer excellent mechanical properties which can be attributed to the inherent strength of graphene oxide. Previous experimental studies have mostly dealt with monolayer or bilayer interactions of lipids with graphene and graphene oxide surfaces. In our study, we report for the first time, a simple and scalable fabrication method where Small Unilamellar Vesicles (SUVs) of L-α-Phosphatidylcholine(PC) and 1,2-dioleoyl-sn-glycero-3-phosphocholine(DOPC) combine with graphene oxide to produce stable nanocomposites via self assembly. Scanning Electron Microscopy (SEM) images of the composite revealed layer-by-layer structures, reconfirmed by X-Ray Diffraction(XRD) results which show a proportional increase in the interlayer separation with increasing ratio of lipid in graphene oxide. The nanocomposite thus fabricated mimics naturally occuring nacre shell structures where graphene oxide substitutes the strong aragonite layers, and the intermediate lipid layers provide the necessary elasticity pertaining to protein-chitin in nacre. The addition of lipids to graphene-based nanocomposites also serve as a biodegradable alternative to using polymers as a popular reinforcement agent. The ease of fabrication method reported facilitates the production of stable GO-Lipid membranes in variable scales and geometries.

Keywords: self-assembly, graphene oxide, bionanocomposite, lipids, nacre shell, biomimetics, free standing membrane

Disclinations in Graphene and Pseudo-Graphenes

A.E. Romanov,[1,*] A.L. Kolesnikova,[1,2] M.A. Rozhkov,[1]

[1] ITMO University, Laser Photonics and Optorlrvtronics Department, St. Petersburg, Russia
[2] Instiitute of Problems of Mechnical Engineering, RAS, St. Petersburg, Russia

Abstract:
The role of disclinations in graphene and graphene-like crystals, is considered. First, we briefly review the properties of disclinations in conventional crystals and elastic continuum [1]. Then, the disclination approach is used to model the structural features and energetics of 2D crystalline materials. For graphene, we introduce disclination networks – periodic distributions of disclination defects. Disclinations manifest themselves as 4-, 5-, 7- or 8-member carbon rings in otherwise 6-member ideal 2D graphene crystal lattice. Limiting cases of graphene-like 2D carbon lattices without 6-member motives, i.e. pseudo-graphenes, are discussed [2] (Fig. 1). The geometry and energy of disclinated 2D carbon configurations are analyzed with the help of molecular dynamics simulation technique. A comparison of the obtained modeling results with analytical calculations within the framework of the theory of defects of elastic continuum is presented. We also investigate the properties (geometry and energy) of grain boundaries in polycrystalline graphene and demonstrate the similarity with the results of disclination description used for conventional 3D polycrystals [3].

Keywords: graphene; disclination; disclinated carbon ring; grain boundary; molecular dynamics; pseudo-graphene; disclination network.

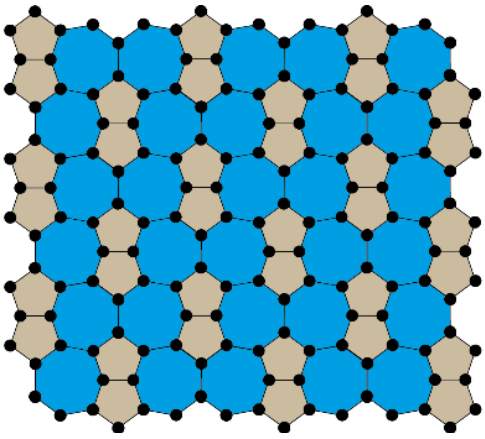

Figure 1: Figure presenting the example of pseudo-graphene crystal consisting of 5- and 7-member carbon rings shown in grey and blue color, respectively.

References:

1. Romanov, A.E., Kolesnikova, A.L. (2009) Application of disclination concept to solid structures, *Prog. Mater. Sci.*, 54, 740-769.
2. Romanov, A.E., Rozhkov, M.A.. Kolesnikova, A.L. (2018) Disclinations in polycrystalline graphene and pseudo-graphenes. Review, *Lett. Mater.*, 8, 384-400.
3. Romanov, A.E., Kolesnikova, A.L., Orlova,T.S., Hussainova, I., Bougrov, V.E., Valiev, R.Z. (2015) Non-equilibrium grain boundaries with excess energy in graphene, *Carbon*, 81, 223-231.

A Scalable Method for the Layer-by-layer Thinning of 2D Materials

J. Sun,[1,*] G. Giorgi,[2] M. Palummo,[3] P. Sutter,[4] M. Passacantando,[5] L. Camilli[1]

[1] Technical University of Denmark, Department of Physics, Lyngby, Denmark
[2] CNR-ISTM, Perugia, Italy
[3] Dipartimento di Fisica, Università degli studi di Roma "Tor Vergata", Dipartimento di Fisica, and Istituto Nazionale di Fisica Nucleare, Roma, Italy
[4] University of Nebraska-Lincoln, Department of Electrical and Computer Engineering, NE, USA
[5] University of L'Aquila, Department of Physical and Chemical Science, and CNR-SPIN L'Aquila, L'Aquila, Italy

Abstract:
The physical properties of two-dimensional (2D) materials depend strongly on the number of layers [1], [2]. Hence, methods for controlling their thickness with atomic layer precision are highly desirable, yet still too rare, and demonstrated for only a limited number of 2D materials [3]. Here we present a simple and scalable method for the continuous layer-by-layer thinning that works for a large class of 2D materials, notably the germanium-based 2D materials. It is based on a simple oxidation/etching process, which selectively occurs on the topmost layers. Through a combination of atomic force microscopy, X-ray photoelectron spectroscopy, Raman spectroscopy and X-ray diffraction experiments, we demonstrate this layer-by-layer thinning method on germanium arsenide (GeAs), germanium sulfide (GeS) and germanium disulfide (GeS_2). Our strategy, which we believe could be applied to other classes of 2D materials upon proper choice of the oxidation/etching reagent, could pave the way for the realization of 2D material-based devices, such as electronic or opto-electronic ones, where a precise control over the number of layers (hence over the material's physical properties) is needed. Finally, we also show that this method can be used to make precise patterns in 2D materials when combining with lithography.

Keywords: 2D materials, oxidation, layer-by-layer thinning, GeAs, GeS, GeS2, black phosphorous, transition metal dichalcogenides

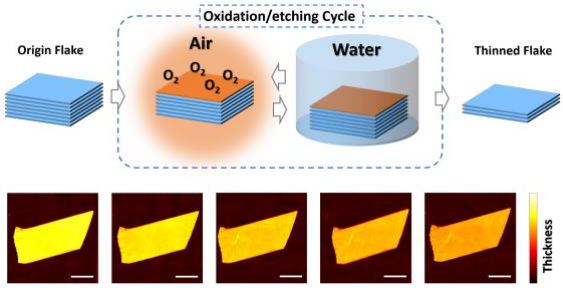

Figure 1. Upper: Schematic illustration of the oxidation/etching process for the layer-by-layer thinning of 2D materials; Bottom: AFM images showing continuous thinning of a GeAs flake by using the oxidation/etching method.

References:

1. S. Z. Butler et al., ACS Nano, vol. 7, no. 4, pp. 2898–2926, 2013.
2. X.-L. Li et al., Adv. Funct. Mater., vol. 27, no. 19, p. 1604468, 2017.
3. Y. Liu et al., ACS Nano, vol. 7, no. 5, pp. 4202–4209, 2013.

2D-germanium: a structural investigation of germanene on Ag(111) by means of photoelectron spectroscopy and diffraction

L. Kesper[1,2,*], M. Schmitz[1,2], J. A. Hochhaus[1,2], M. G. H. Schulte[1,2], U. Berges[1,2], and C. Westphal[1,2]

[1] TU Dortmund University, Experimental Physics 1, Dortmund, Germany
[2] Center for synchrotron radiation DELTA, TU Dortmund University, Dortmund, Germany

Abstract:
The discovery of graphene in 2004 opened a new field of two-dimensional materials in solid state physics. Stepping down the carbon group, so-called Dirac-materials beyond graphene, like silicene and germanene, also obtain outstanding electronic properties in two-dimensional structures due to their Dirac-characteristic. According to the report of the first synthesis of germanene in 2014 [1], even the realization of the germanene-based field-effect transistors (FET) has been succeeded [2]. Beside its tunable bandgap germanene shows strong spin-orbit coupling, just like large buckling, which allows to observe quantum spin hall effect (QSHE) or features known from topological insulators [8, 9]. Since the surface and interface structure of 2D-materials has a major influence on the electronic properties of the material, we focus on the analysis of chemical and atomic structures at the interfaces.

Here we present a first detailed structural model of germanene on Ag(111), as well as an investigation of the structural evolution of two-dimensional germanium phass. We use physical vapor deposition (PVD) to grow thin germanium films on Ag(111). Various phases of low-dimensional germanium at different layer thicknesses can be found, that have been structurally and electronically characterized by LEED, XPS, and XPD (figure 1). Thus, the evolution towards the famous honeycomb phase of germanene can be sketched to facilitate the understanding of its structural formation and development. In particular, the interface structure between adsorbate and substrate is of great interest with respect to technological applicability. One milestone of this work is to clear up the disagreement in literature whether germanium forms (quasi-)freestanding germanene on Ag(111) or a surface alloy [5, 6]. Therefore we use the powerful methods of XPS and XPD to distinguish a chemically freestanding germanene phase from a surface alloy. These techniques allow a separate study of chemical bondings of the internal and interface structure and additionally provide a complete structural model of the system, which has not been done, yet. The germanium forms strongly buckled honeycomb phases with different interface structures, as concluded from XPS and XPD measurements. All measurements are performed at beamline 11 at DELTA, Dortmund, using soft synchrotron radiation.

In this contribution we will present a new structural model for epitaxially grown germanene on Ag(111), as well as our new findings on structural formation and development via preliminary and transitional phases of germanium.
K**eywords**: 2D materials, Dirac cone, germanene, Ag(111), structural model, FET, synchrotron radiation, interface, surface, PVD, XPS, XPD.

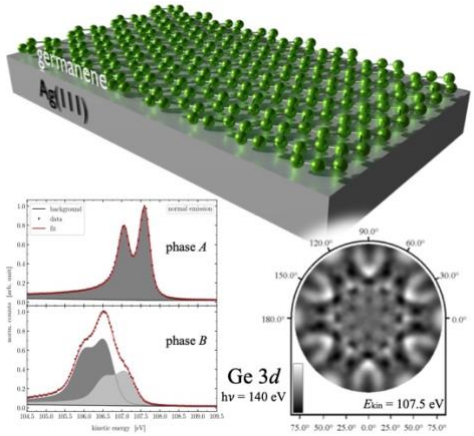

Figure 1: Epitaxially grown germanene on Ag(111) in honeycomb structure. We use XPS and XPD measurements to resolve the chemical and electronic structure at the surface and interface.

References:

1. M. E. Dávila *et al.*, New J. Phys. **16**, 095002 (2012).
2. B. N. Madhushankar *et al.*, 2D Mater. **4**, 021009 (2017).
3. C. C. Liu *et al.*, Phys. Rev. Lett. **107**, 076802 (2011).
4. M. Ezawa *et al.*, J. Phys. Soc. Japan **84**, 1 (2015).
5. C. Lin *et al.*, Phys. Rev. Mater. **2**, 1 (2018).
6. K. Zhang *et al.*, Phys. Rev. B **102**, 125418 (2020).

Monolayers in ultrafast intense optical pulses: topological phenomena

S. A. Oliaei Motlagh, V. Apalkov, M. I. Stockman

Physics and Astronomy Department, Georgia State University, Atlanta, USA

Abstract:
Interactions of ultrafast intense optical pulses, 0.1-1 V/Å, with solids create unique platforms to study highly nonlinear phenomena such as ultrafast field-driven currents, optical absorption and reflection, extreme UV absorption, high-harmonic generation, and ultrafast ionization.

We report our findings on ultrafast phenomena defined by nontrivial topological properties of two-dimensional solids in the reciprocal space. The studied monolayers are graphene, surfaces of topological insulators, and transitional metal dichalcogenides (TMDCs). Particularly for TMDCs monolayers, we predict a new ultrafast phenomenon induced by intense circularly polarized optical pulses, and we call it a topological resonance. The topological resonance results in a significant valley polarization in TMDC monolayers. This is extended to other two-dimensional materials with the same symmetry, like gapped graphene and hexagonal boron nitride. This strong valley polarization can be written and read out by a single cycle of an optical pulse with a few femtoseconds duration.

The applied linearly polarized pulses generate ultrafast electric current in the monolayers of gapped graphene and TMDC. When the polarization of the pulse is perpendicular to the axis of symmetry of gapped graphene and TMDC monolayers, it generates currents both along the direction of the pulse polarization and along the perpendicular direction. The current which flows in perpendicular direction is a nontrivial current which is absent in the pristine graphene where both time and inversion symmetries are conserved and the Berry curvature is concentrated as a delta function at Dirac points.

The predicted phenomena can be applied to ultrafast all-optical classical and quantum storage and processing of information.

Keywords: light-matter interaction, ultrafast pulse, valley polarization, nonlinear phenomena, topological phenomena, topological resonance, gapped graphene, transitional metal dichalcogenides, TMDC, hexagonal boron nitride.

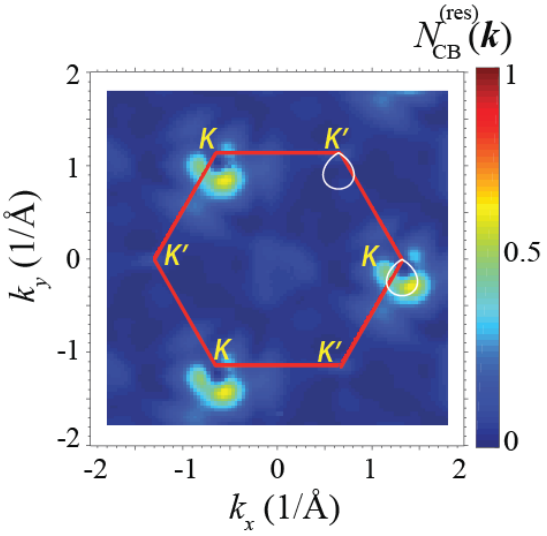

Figure 1: Figure illustrating Residual conduction band population and the strong valley polarization induced by a single cycle of an ultrafast pulse for a monolayer of MoS_2. The pulse is a right-handed circular pulse with amplitude of 0.2 V/Å and the duration of 4 fs. The red solid line shows the boundary of the first Brillouin zone of this monolayer and K, K_0 points indicated in its boundary.

References:

1. Motlagh, S. A. O., A., Apalkov, V., Stockman, M.I. (2021), Transition metal dichalcogenide monolayers in an ultrashort optical pulse: Femtosecond currents and anisotropic electron dynamics, *Phys. Rev. B* 00, 005400, *In Press*.
2. Motlagh, S. A. O., Zafar, A. J., Mitra, A., Apalkov, V., Stockman, M.I. (2020), Ultrafast strong-field absorption in gapped graphene, *Phys. Rev. B* 101 (16), 165433.
3. Motlagh, S. A. O., Nematollahi, F., Mitra, A., Zafar, A. J., Apalkov, V., Stockman, M.I. (2020), Ultrafast optical currents in gapped graphene, *J. Phys.: Condens. Matter* 32 065305.
4. Motlagh, S. A. O., Nematollahi, F., Apalkov, V., Stockman, M.I. (2019), Topological resonance and single-optical-cycle valley polarization in gapped graphene, *Phys. Rev. B* 100 (11), 115431.

SurfCoat Korea 2021 Session I.B:

Surface treatments and coatings deposition, functionalization, modelling and characterization

Investigation of the Non-Isocyanate Urethane Functional Monomer in Latexes: Hydronomers

M.D. Soucek

Department of Polymer Engineering, Akron, OH. USA

Abstract:
A series of new urethane methacrylate (UMA) and diurethane monomers were synthesized with the reaction of ethylene carbonate and aliphatic amines, followed by the reaction with methacrylic anhydride. Urethane latexes were prepared by monomer-starved semibatch polymerization of the new urethane methacrylates with methyl methacrylate (MMA) and butyl acrylate (BA). A uniform morphology and a unimodal particle distribution were observed by a combination of dynamic light scattering (DLS), ultrasound acoustic attenuation spectroscopy (UAAS), and transmission electron microscopy (TEM). The thermal stability, minimum film formation temperature (MFFT) and thermo-mechanical properties of the urethane latexes were also studied. The inclusion of urethane monomers appeared to have lowered the MFFT via a water plasticization effect, while enhancing the Tg of the final film properties.
Two of urethane methacrylate monomers, 2-[(butylcarbamoyl)oxy]ethyl methacrylate (BEM) and 2-[(methylcarbamoyl)oxy]ethyl methacrylate (MEM), were used to prepare model latexes. The Urethane functional (BEM) latexes were evaluated by FT-IR, solid state nuclear magnetic resonance (SS-NMR), dynamic light scattering (DLS), gas chromatography (GC), differential scanning calorimetry (DSC), tensile and dynamic mechanical thermal analysis (DMTA). This accounted for the higher modulus and tensile strength in latexes derived from batch polymerization. Both homogeneous and core-shell structures were prepared. The tensile modulus, tensile strength and elongation-at-break were all dependent on BEM or MEM content. A proposed mechanism for film formation will be presented.

Structure and phase formation of ion-plasma vacuum-arc Zr-B-Si-C-Ti-(N) coatings during deposition

D.S Belov, I.V. Blinkov, V.S. Sergevnin, A.V. Chernogor, B.Yu. Kuznetsov

Functional Nanosystems and High-Temperature Materials Department,
National University of Science and Technology MISiS, Moscow, Russia

Abstract:
Thermal spray ZrB_2 – SiC coatings are being investigated to study the possibility of their application for protection against high-temperature oxidation of structural materials. However, the high porosity of coatings, low adhesive strength with the substrate, realized by this method, do not make it possible to consider them as simultaneously increasing the wear-resistant characteristics of rubbing structural elements operating in an oxidizing environment at high temperatures. This work is devoted to studying the possibilities of forming this system coatings by the arc-PVD method, which is widely used to create coatings with a variety of functional properties, making it possible to use them as wear-resistant in various operating conditions.
The evaporated cathode was made of a combined cylindrical powder composite insert ZrB2 (80 vol.% or 88.4 wt.%) - SiC (20 vol.% or 11.6 wt.%) diameter – 58 mm and height – 15 mm, prepared by the spark plasma sintering method, which was pressed into a metal base made of titanium (titanium alloy, Ti ~ 99,7 wt.%) with a diameter of 62 mm. The current and voltage of the evaporating arc were 110A and 20V. A negative bias potential of 120V was applied to the substrate. The partial pressure of nitrogen during Zr-B-Si-C-Ti-N coatings formation was 0.8 Pa. The argon pressure during the deposition of Zr-B-Si-C-Ti coatings was 0.4 Pa.
The XPS study of the Zr-B-Si-C-Ti-N coating indicates that the maximum of the Zr3d spectral line corresponds to 180.0 eV, which belongs to zirconium carbide. The Si2p spectrum contains a line with an energy of ~ 101.1 eV. This value is in the range of reference values for SiC (100.2 eV) and Si_3N_4 (101.8 eV) and corresponds, apparently, to silicon carbonitride. The Ti2p spectrum consists of one doublet, E_b (Ti2p3) - 454.7 eV, that is slightly lower than for titanium nitride (454.9 eV). Perhaps this is determined by the formation of Ti-Ti, Ti-B bonds. The spectrum of boron B1s is located at E_b 188.2 eV, which characterizes the energy of Zr-B bonds. In the Zr-B-Si-C-Ti coating for the Ti2p spectrum, a peak of 454.8 eV is observed, which can be interpreted as titanium with a mixed type of Ti-Ti, Ti-C bond. The spectrum of Zr3d + B1s contains a peak at 179.7 eV, which corresponds to zirconium carbide. The presence of a boron peak with an energy of 188.2 eV can be explained by the presence of Zr – B bonds. The Si2p spectrum has two peaks: 99.9 and 101.1 eV. The main peak at 99.9 eV can be attributed to silicon carbide with a small fraction of Si – Si bonds. The second peak exceeds the SiC reference value (100.2 eV), so it can be attributed to SixOyCz, which is consistent with the presence of oxygen in the coating.
The Zr-B-Si-C-Ti-N coating has a predominantly amorphous structure, formed mainly on the basis of nitride, carbide, boride phases and complex compounds Zr, Si, Ti. The Zr-B-Si-C-Ti coating is characterized by an amorphous-nanocrystalline structure. The amorphous component of this coating is formed mainly by phases based on Zr and Si. The nanocrystalline structure is formed by a complex carbide (Zr, Ti) C. The increased degree of the structure amorphization of the Zr-B-Si-C-Ti-N coatings can be associated with a higher cooling rate of the forming coating due to the higher thermal conductivity of the residual nitrogen atmosphere as compared to argon.

Keywords: amorphus structure, nanocrystalline structure, complex carbide, arc-PVD, phase formation, functional coatings, bonds energy.

Synthesis of Superhydrophobic Fluoropolymer Coatings by Hot Wire Chemical Vapor Deposition

A.I. Safonov,[1,2,*] V.S. Sulyaeva,[3] S.V. Starinskiy,[1,2] N.I. Timoshenko,[1]

[1] Kutateladze Institute of Thermophysics SB RAS, Laboratory of rarefied gases, Novosibirsk, Russia
[2] Novosibirsk State University, Novosibirsk, Russia
[3] Nikolaev Institute of Inorganic Chemistry SB RAS, Novosibirsk, Russia

Abstract:
Fluoropolymer coatings are promising for creating hydrophobic and superhydrophobic surfaces due to their low surface energy. Such surfaces can be used for intensification of heat exchange, creation of self-cleaning surfaces, separation of water-oil emulsions, etc. [1,2]. The applicability of hydrophobic and superhydrophobic fluoropolymer coating is dependent on its stability and durability. Coatings meeting these requirements may be obtained by the HW CVD method used in the present work. The method details and experimental setup are described in the paper [3]. A lot of synthesis parameters, such as the activator filament temperature, precursor gas pressure, substrate temperature, precursor gas flow, allows us to finely control of coating morphology, wettability and durability. So it is obtained several different type of morphology: smooth, porous, dendridic and powder. The contact angle varies in the range of 110 – 173° with a change in morphology. The change of morphology may be explained by dependence of polymerization rates on flow of active radicals reaching the substrate. It is shown that namely the generation of free radicals moving to substrate determine by synthesis parameters. Based on these results the compromise synthesis conditions lead to formation of resistant coatings with contact angles in range of 160° - 173° were obtained. The Figure 1 shows the morphology of typical coatings and result of its wettability measurements.
The work was supported by the Russian Science Foundation (project No. 18-79-10119).

Keywords: superhydrophobic coating, wettability control, fluoropolymer coatings, polymer, surface structure, different surface structure, hexafluoropropylene oxide, deposition, hot-wire chemical vapor deposition, HWCVD.

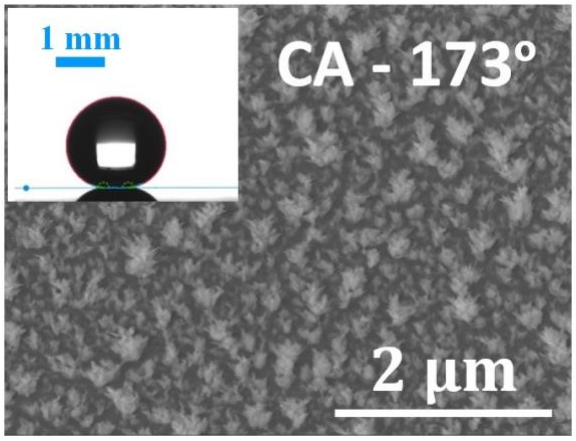

Figure 1: SEM image of the surface of fluoropolymer obtained coating and the measured contact angles. The insets show photograph of a water droplet on the surface coating.

References:

1. Surtaev, A., Serdyukov, V., Pavlenko, A., (2016) Nanotechnologies for Thermophysics: Heat Transfer and Crisis Phenomena at Boiling, *Nanotechnologies in Russia*, 11, 696–715.
2. Drelich, J., Marmur, A., (2014), Physics and applications of superhydrophobic and superhydrophilic surfaces and coatings, *Surface Innovations*, 2, 211–227.
3. Safonov, A., Sulyaeva, V., Gatapova, E., Starinskiy, S., Timoshenko, N., Kabov, O. (2018), Deposition features and wettability behavior of fluoropolymer coatings from hexafluoropropylene oxide activated by NiCr wire, *Thin Solid Films*, 653, 165–173.

Fluorine-free omniphobic slippery surfaces made of PDMS-like molecules: surface structure and wetting properties

M. Callau [1], C. Fajolles [1], P. Guenoun [1]

[1] Université Paris-Saclay, CEA, CNRS, NIMBE, LIONS, 91190 Gif-sur-Yvette, France

Abstract:

Surfaces covered with omniphobic coatings are investigated for many applications from anti-icing, anti-corrosive to self-cleaning uses as they allow droplets of many liquids to easily slide without pinning. To this end, during the past decades, fluorine-based molecules have been widely used since their deposition induces a very low surface energy. However, these molecules will soon be banned from the industrial market due to health and environnemental issues. To replace these molecules, Wang and McCarthy have demonstrated in 2016 that PDMS-like molecules can be grafted onto glass substrates by specific process conditions[1]. These molecules are supposedly covalently grafted to the substrate, leading to the fabrication of omniphobic surfaces with low sliding angles and low hysteresis (< 10 °) for a broad range of liquids. By adapting their process and studying the surface structure by different microscopies and x-ray reflectivity (Table 1 and Figure 1), we highlight here the key features that lead to a highly slippery coating. The coating process is found to lead to very specific surface topographies (Figure 2), which are process dependent and can be related to different wetting properties of the substrates (contact angles, hysteresis and sliding angles). The understanding of the grafting mechanism at the molecular level and of specificities of these molecules can pave the way to the fabrication of optimized eco-friendly omniphobic coatings for a full range of surface treatement applications.

Keywords: omniphobic, wetting, PDMS, slippery, topography, polymers, grafting.

Layer	ρ_e (e.Å^{-3})	Thickness (Å)
PDMS layer 3	0.1369	22.0
PDMS layer 2	0.6073	33.9
PDMS layer 1	0.4382	18.5
SiO_2 (oxide)	0.6751	19.9
Si (substrate)	0.7173	-

Table 1: Layer-by-layer composition of the PDMS film by fitting the X-ray reflectivity data with the Reflex software [2].

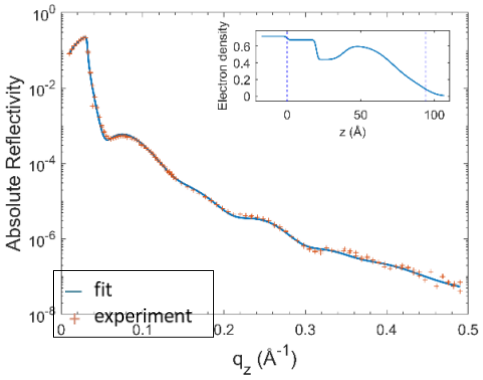

Figure 2: X-ray reflectivity spectrum of a silicium wafer covered with an omniphobic PDMS-based coating.

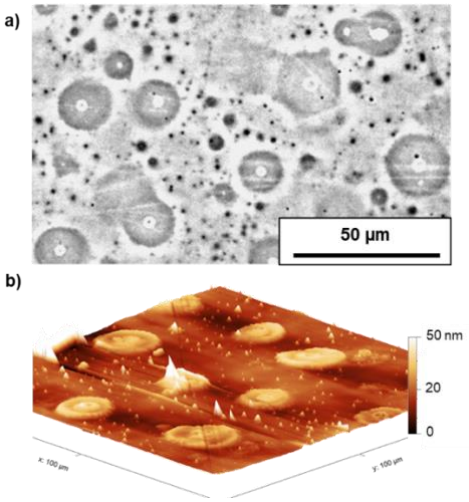

Figure 2: a) Phase contrast microscopic observation and b) Atomic Force Microscopy image of a glass substrate covered with an omniphobic PDMS-based coating.

References:

1. Wang L, McCarthy TJ. Covalently Attached Liquids: Instant Omniphobic Surfaces with Unprecedented Repellency. *Angew Chemie - Int Ed*. 2016;55(1):244-248.
2. Vignaud G, Gibaud A. REFLEX: A program for the analysis of specular X-ray and neutron reflectivity data. *J Appl Crystallogr*. 2019;52:201-213.

Development of Bioglass Incorporated Plasma Electrolytic Oxidation (PEO) Coating on Titanium Surfaces for Biomedical Application

Athirah Sukrey [1,2], Bushroa A. Razak [1,2,*]
[1] Department of Mechanical Engineering, Faculty of Engineering, University of Malaya, 50603 Kuala Lumpur, Malaysia
[2] Centre of Advanced Manufacturing and Materials Processing (AMMP), Department of Mechanical Engineering, Faculty of Engineering, University of Malaya, 50603 Kuala Lumpur, Malaysia

Abstract:
Titanium and its alloys have been extensively used in various fields listed as aerospace, manufacturing, architectural, and biomedical industries due to their excellent mechanical properties and corrosion resistance, low elastic modulus, low density, high biocompatibility, and relatively high melting point [1-3]. However, continuous research should be carried out to improve the mechanical properties for better resilience, and bioactivity and antibacterial activity enhancement. In this work, the surfaces of titanium substrates are altered by incorporating bioglass (BG) into the oxide coating produced during the Plasma Electrolytic Oxidation (PEO) treatment. In general, BG is a known bioactive material possessing the ability to induce an apatite layer formation at the interfaces of bone and implant and the improvement of interaction between the implant and ambient body fluid [4]. The PEO technique is utilized in this work due to the simple equipment set-up, a brief treatment period, and the excellent adherent and uniformity of bio-functional hydroxyapatite incorporated oxide coatings on the metallic substrates' surfaces [5]. The PEO coating produced demonstrates a good adhesion strength with critical load at 696.23 mN load and uniform distribution of bioglass components throughout the coated sample. The relatively short treatment time of PEO has successfully produced a thin BG incorporated oxide coating with an average thickness valued at 17.1167 μm. The bioactivity of the sample is demonstrated with the inducement of a new apatite layer after the simulated body fluid (SBF) immersion, which confirmed by the observation of a scabrous layer on the previously formed PEO coating. The inducement of this new apatite layer demonstrates the PEO technique's ability to produce a porous bio-functional coating that can enhance the biocompatibility of biomedical implant material.

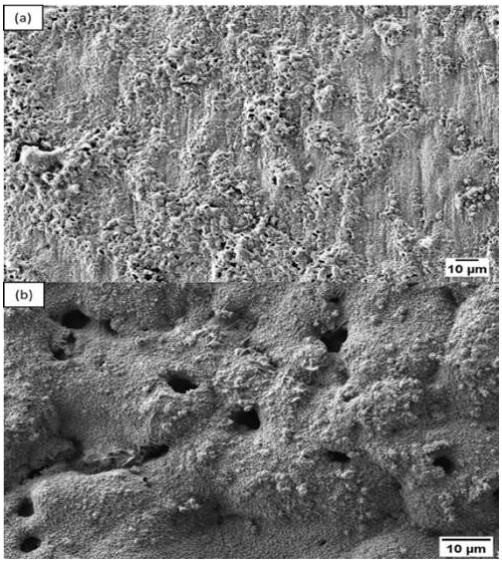

Keywords: plasma electrolytic oxidation, bioglass, electrolyte concentration, adhesion strength, NaOH concentration,

Figure 1: The figure above illustrates a new apatite layer formation on the previously formed PEO coating after the immersion in simulated body fluid (SBF) for 14 days. The formation of apatite layer demonstrates the feasibility of the PEO technique in incorporating bioactive materials into the oxide coating.

References:

1. A. Kurup, P. Dhatrak, N. Khasnis, Surface modification techniques of titanium and titanium alloys for biomedical dental applications: A review, Mater. Today Proc. (2020) 0–6.
2. D. Quintero, O. Galvis, J.A. Calderón, J.G. Castaño, F. Echeverría, Effect of electrochemical parameters on the formation of anodic films on commercially pure titanium by plasma electrolytic oxidation, Surf. Coatings Technol. 258 (2014) 1223–1231.
3. H.J. Rack, J.I. Qazi, Titanium alloys for biomedical applications, Mater. Sci. Eng. C. 26 (2006) 1269–1277.
4. BS. Necula, I. Apachitei, L.E. Fratila-Apachitei, E.J. Van Langelaan, J. Duszczyk, Titanium bone implants with superimposed micro/nano-scale

porosity and antibacterial capability, Appl. Surf. Sci. 273 (2013) 310–314.
5. SA Adeleke, S. Ramesh, A.R. Bushroa, Y.C. Ching, I. Sopyan, M.A. Maleque, S. Krishnasamy, H. Chandran, H. Misran, U. Sutharsini, The properties of hydroxyapatite ceramic coatings produced by plasma electrolytic oxidation, Ceram. Int. 44 (2018) 1802–1811.

Graphene Korea 2021 Session II:

Graphene for electronic, photovoltaic and magnetic applications

Rediscovery of existing materials through 3D structuring of graphene and carbon nanotubes: case for elastic polyurethane foam

J. Lee,[1], J. Kim,[1], Y. Shin,[1], I. Jung, [1,*]
[1] Kyung Hee University, Department of Mechanical Engineering, Yongin, South Korea

Abstract:
The effect of graphene oxide loading on sound-absorbing properties of open cell polyurethane foam was investigated. GO was impregnated into PU foam by a step-by-step vacuumassisted process. Sound-absorbing properties can be greatly enhanced by GO impregnation. Especially, sound-absorbing properties can be tuned to be maximized to specific frequency range by controlling GO impregnation density. The averaged sound absorption coefficient from 800 Hz to 6300 Hz was increased more than four times by impregnating 15 wt% of GO into 5-mm-thick PU foam with a bulk density of 51 kg/m3. Foam parameters such as porosity, Young's modulus, and flow resistivity were determined as a function of GO concentration. Elastic porous material theory was used to model sound-absorbing properties of GO impregnated PU foam, which showed good agreement with measurements at every GO loading condition. The pore tortuosity, which was determined using a fitting procedure, exhibited a good linear relationship with GO loading. It was found that impregnation of GO significantly increased tortuosity. The results given here suggest theoretical and experimental guidelines for use of GO to improve and optimize the sound-absorbing properties of PU foam.
This material further modified to measure interfacial pressure. The developed sensor have a characteristic of coated with silicone rubber, which has widened pressure measurement range and improved response time. The sensor is capable of measuring pressures lower than 100Pa and higher than 200 kPa and can measure oscillating pressure well above 50 Hz. The sensor showed high repeatability and durability and operated normally after 1000 cycles at 360 kPa applied pressure. The sensor was made by coating polyurethane foam with silicone rubber and further dip-coated with MWCNT dispersed TPU ink. The use of TPU as a binding material helped MWCNT strongly attach to the foam skeleton and reduced the interfacial electrical resistance. As a result, low hysteresis (6.4%) was achieved. By controlling amount of silicone rubber impregnated, the sensitivity can be controlled from 0.013 kPa^{-1} to 0.032 kPa^{-1}. These sensors were used for measuring both subtle pressures such as the pulse and large pressures such as the pressure beneath a heel. Additionally, wide range of pressure distributions were measured using the array sensors.

Keywords: graphene oxide, carbon nanotube, polyurethane foam, sound absorption coefficient, elastic porous material theory, pressure sensor, silicone rubber, thermoplastic polyurethane

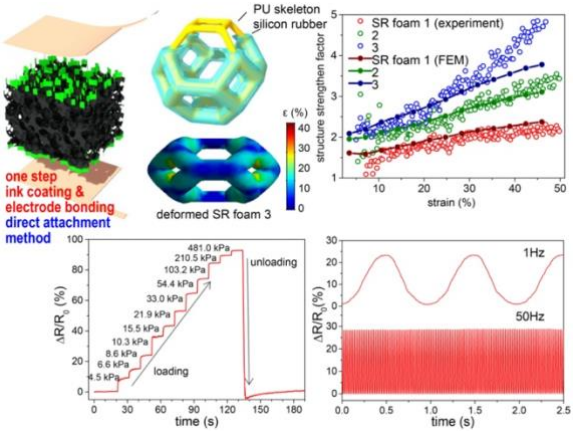

Figure 1: Illustration of the bonding procedure a CNT/TPU/SR foam pressure sensor, Kelvin cell model for SR foam, the maximum principal strain distributions of SR foam at 31.8% compressive strain by finite element analysis, measured and calculated structure strengthen factors, resistance change upon step-wise increase of pressure from 4.5 kPa to 481.0 kPa, resistance response of a sensor upon applying a repetitive pressure of 12.6 kPa at 1 Hz, 11.2 kPa at 50 Hz

References:

1. Lee, J., Jung, I. (2019), Tuning sound absorbing properties of open cell polyurethane foam by impregnating graphene oxide, *Amer. Appl. Acoustics*, 151, 10-21.
2. Lee, J., Kim, J., Shin, Y., Jung, I. (2019), Ultra-robust wide-range pressure sensor with fast response based on polyurethane foam doubly coated with conformal silicone

rubber and CNT/ TPU nanocomposites islands, *Compos. B*, 177, 107364.

Unveiling predominant electrical performance of nitrogen-doped graphene thin film transistors

Yire Han[1], Byeong-Ju Park,[1], Ji-Ho Eom[1], Ha-Rim Ahn[2], Cheolho Jeon[2], Sungmi Yoo[3], Yun-Ho Kim[3] and Soon-Gil Yoon[1,*]

[1]Department of Materials Science and Engineering, Chungnam National University, Daeduk Science Town, 34134, Daejeon, Rep. of Korea

[2]Advanced Nano-Surface Group, Korea Basic Science Institute (KBSI) 169-148 Gwahangno, Yuseong-gu, Daejeon 34133, Rep. of Korea

[3]Advanced Materials Division, Korea Research Institute of Chemical Technology, Daejeon, 34114, Rep. of Korea

Abstract

Graphene is attractive for conventional semiconductor applications because of its flexibility, transparency, and high mobility. However, pristine graphene does not have a bandgap, which makes it a challenge to take advantage of its extraordinary electronic properties in practical thin film transistors (TFTs). Many studies have been focused on engineering an appropriate graphene bandgap for many semiconductor applications, which includes transistors. To enable predominant electrical performance of graphene-based TFTs; herein, we report the fabrication of transparent, flexible, stretchable TFTs using nitrogen-doped graphene films. Large-scale, high-quality, monolayer graphene was synthesized directly on flexible and stretchable polydimethylsiloxane (PDMS) substrates at 100 °C. The nitrogen-doped graphene TFTs with a channel width (100 μm) and length (60 μm) recorded an on/off current ratio of ~ 3.2×10^9, field-effect mobility of ~ 332 cm^2 $(V \cdot s)^{-1}$, threshold voltage (V_{TH}) of ~ 0.3 V, and a subthreshold swing (*S.S.*) of ~ 0.08 V dec^{-1} at room temperature with a high optical transparency of ~ 90% and a high thermal stability that reached an operation temperature of 130 °C. Furthermore, 4 inch-scale TFTs revealed a predominant flexibility for 5,000 cycles under 7% tensile strain and a high stretchability for 3,000 cycles under 140% strain perpendicular to the direction of current. These results could pave the way for the development of flexible, stretchable, and transparent electronics for next-generation TFTs.

Keywords: Direct monolayer graphene synthesis at low temperatures, Transfer-free, Low sheet resistance, Flexibility, High field-effect mobility.

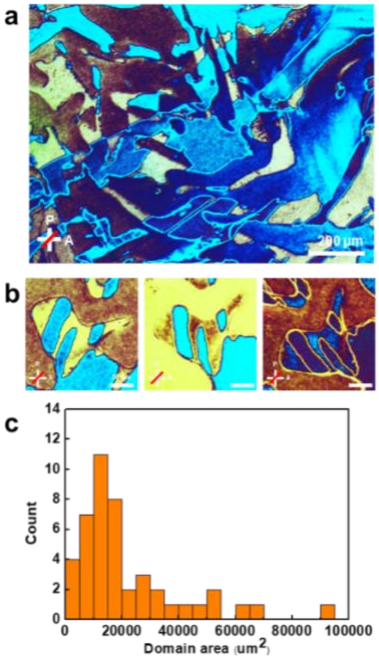

Figure 1 a, POM image of liquid crystal coated-graphene films synthesized on Ti (10 nm)/Si (001). The POM image shows graphene grains and the boundaries of graphene grains. **b,** Magnified POM images of liquid-crystal coated graphene films synthesized on Ti (10 nm)/Si (001). The orientation of liquid-crystals on the graphene film changes depending on the graphene grain (left image, 0° rotation; center image, anticlockwise rotation by + 30°; right image; anticlockwise rotation by + 60° rotation). **c,** Distribution of graphene grain size synthesized on Ti (10 nm)/Si (001). Average grain size of graphene is approximately 130 μm.

References

1. Anthopoulos, T. D. *et al.* Solution processible organic transistors and circuits based on a C70 methanofullerence. *Appl. Phys*. **98**, 54503 (2005).
2. Hummelen, J. C., Yu, G., Gao, J., Wudl, F. & Heeger, A. J. Polymer photovoltaic cells: Enhanced efficiencies via a network of internal donor-acceptor heterojunctions. *Science* **270**, 1789-1791 (1995).

Natural Graphite and Solvent Processed Bulk Graphene Nanoplatelets For Clean Energy Harvesting

D. Mohapatra [1,2,*], J.-J. Shim[1], and S. S. Nemala [1,2]

[1] School of Chemical Engineering, Yeungnam University, Gyeongsan, Gyeongbuk 38541, Republic of Korea.
[2] Department of Metallurgical Engineering & Materials Science, Indian Institute of Technology Bombay, Mumbai 400076, India.
[*]E-mail: debanandaiitb@gmail.com; debanandam@yu.ac.kr

Abstract:
Dye-sensitized solar cells (DSSCs) have provoked an intense research interest in recent years to improve the efficiency and stability of DSSCs. It has shown its potential to be the next generation of photovoltaic devices due to its low cost, environmental friendliness, and easy fabrication procedure. In this work, we discuss the first-ever successful attempt to prepare graphene nanoplatelets (GN) in bulk scale using water as a natural solvent instead of conventional harsh chemical treatment methods and multistage post-synthesis purifications, resulting in low yield. GN facilitated counter electrode (CE)-based DSSC device demonstrated as good as photovoltaic efficiency (η) of 7.6% compared to the standard Pt-CE, η=6.95%, proving the high-quality graphene and its true potential to be an excellent alternative to Pt-free low-cost DSSC. The demonstrated GN CE-based DSSCs are exceptionally stable for more than 3000 hours under continuous illumination, with almost no efficiency fading. We will also introduce you for the first-time application of multi-shelled fullerene, i.e., carbon nano-onion (CNO), as an alternative efficient and optically transparent CE for economical DSSCs (**Fig. 1**). The CNO-powered DSSC demonstrated optical transparency of >55% with a significant solar energy conversion efficiency of 5.17%.

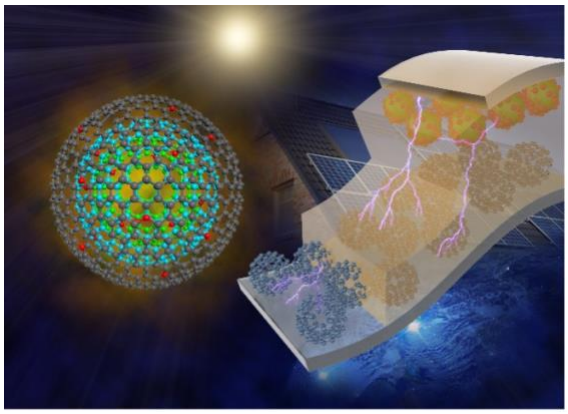

Figure 1: Demonstrating optically semi-transparent carbon nano-onion-powered dye-sensitized solar cell for building-integrated photovoltaics.

Engineering Qubits in 2D Semiconductors

Kuan Eng Johnson Goh[1,2*]

[1] Institute of Materials Research and Engineering, Agency for Science Technology and Research (A*STAR), 2 Fusionopolis Way, Innovis, #08-03, Singapore 138634

[2] Department of Physics, National University of Singapore, 2 Science Drive 3, Singapore 117551

[*] E-mail: gohj@imre.a-star.edu.sg; phygkej@nus.edu.sg; kejgoh@yahoo.com

Abstract:
Quantum computing with few to tens of qubits is now available, but the scale-up to a universally programmable quantum computer for real world application remains significant challenge. Amongst various priorities, increasing the number of qubits whilst maintaining a manageable error rate is paramount. This a multidisciplinary problem requiring scientific and engineering breakthroughs in materials, processes, multi-qubit architectures, and quantum measurement techniques in the least. In this talk, I will introduce our recent efforts to establish the capabilities for building spin-valley qubits based on monolayer 2D semiconductors [1]. The unique spin-valley coupling in such materials is expected to suppress decoherence since a spin flip requires the concomitant change of valley. In addition, the inherent spin-orbit interaction provides for fast gate operations, and the compatibility with electrostatically gated planar qubit architectures can be advantageous for reducing system complexity and hence scalability. I shall present our recent progress [2] in materials engineering and quantum dot devices toward this goal.

Keywords: 2D Semiconductors, qubits, spin-valley, valleytronics, quantum materials, quantum dot, quantum computing.

References:

1. Bussolotti F., Kawai H., Ooi, Z. E., Chellappan V., Thian D., Pang A. L. C., Goh K. E. J. (2018) Roadmap on finding chiral valleys: screening 2D Materials for Valleytronics, *Nano Futures*, 2, 032001 https://doi.org/10.1088/2399-1984/aac9d7.
2. Goh K. E. J., Bussolotti F., Lau C. S., Kotekar-Patil D., Ooi Z. E., Chee J. Y. (2020) Toward Valley-Coupled Spin Qubits, *Advanced Quantum Technologies*, 3, 1900123. https://doi.org/10.1002/qute.201900123

Mass production of soluble graphite that shows ultra-high exfoliation efficiency in liquid

Y. Arao[1], M. Kubouchi[1]

[1]Tokyo Institute of Technology, School of Materilas and Chemical Technology, Tokyo, Japan

Abstract:
Constructing mass production method of graphene is essential for practical usage of this remarkable material. Direct exfoliation of graphite in liquid is the promising approach for production of high quality graphene[1]. However, this technique has three huge obstacles to be solved; limitation of solvent, low yield and low exfoliation degree.
Here, we found that soluble graphite produced by mechanochemical reaction with salts overcomes above three drawbacks. The schematic process is shown in Fig. 1. Graphite is milled with weak acid salts. During the process, the salts were adsorbed at the edge of graphite. These salts imrove the exfoliation efficiency of graphite in liquid due to the enhanced electrical repulusion cansed by desocciation of cations. We called the edge-functionalized graphite as solubule graphite.
The soluble graphite was exfoliated into 100% monolayer graphene with more than 10 % yield in five min. of sonication. Surprisingly, the modified graphite was easily exfoliated in low-boiling point solvent such as acetone, alcohol and water without an aid of surfactant. Molecular simulation revealed that the salt is adsorbed to the active carbon at the graphite edge. In the case of weak acid salts, the original bonding nature between alkali atom ion and the base molecule is kept after the reaction. Thus, the alkali metals are easily dissociated in polar solvent, leading to negative charging of graphene. This phenomenon enables the exfoliation of graphite in low boiling point solvents. The approach proposed here opens up a practical usage of the attractive 2D materials.

Keywords: Graphene, Mechanochemical reaction, Liquid phase exfoliation

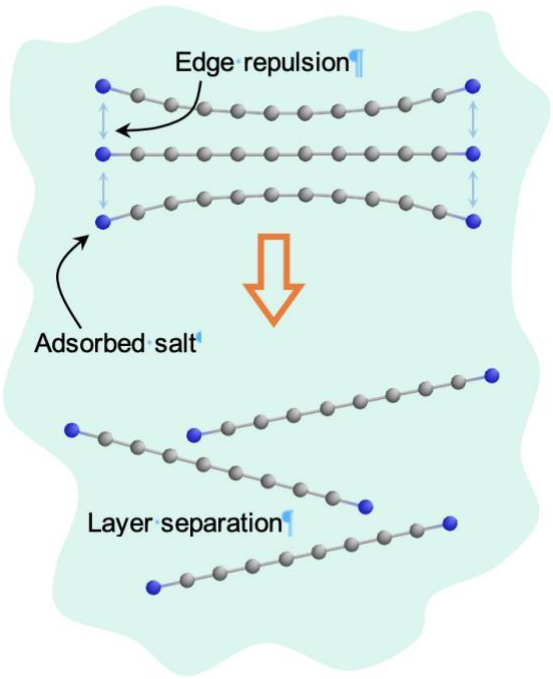

Fig. 1. Salts are adsorbed at the edge of graphite during ball milling. The salts at the graphite edge can be dissociated in polar solvent. This induces the electrical repusibe force, and facilitates the exfoliation of graphite in liquid.

Reference

1. K. Paton et al. Scalable production of large quantities of defect-free few-layer graphene by shear exfoliation in liquids *Nature Materials*, Vol. 13, 624-630, 2014.

Roll-to-roll process-based fabrication of large-area wrinkled graphene on flexible substrates

Prashant Narute[1,2,*], Chang Jun Lee[2], Rakesh Sadanand Sharbidre[2], Seong-Gu Hong[1,2]

[1] Department of Nano Science, University of Science and Technology, Daejeon 34054, Rep. of Korea
[2]Division of Industrial Metrology, Korea Research Institute of Standards and Science, Daejeon 34113, Rep. of Korea

Abstract

Wrinkle engineering of graphene is demonstrated as an effective tool to alter physical properties, and exhibits potential applications in flexible and stretchable electronics, surface modifications, tunable optical transmittance, and energy storages. Therefore, efforts have been made to construct controlled and ordered wrinkled graphene (WGr) corrugations. In previously reported studies, however, deformed substrate was used as target substrate. Which curb the scalability, as the fabrication technique offers limited feature dimensions and substrate material choice. Wrinkle transferable methods, on other hand, consist removal of deformed substrate by harsh post chemical or mechanical treatment which inevitably impairs intrinsic material properties. What is more important, as far as practical applications are concerned, the substrate-independent subsequent transferability of employed wrinkled patterns from deformed substrate to commercially available flexible polymeric target substrate, without sacrificing intrinsic material properties. Here, we report a roll-to-roll technique, offers transfer of large-area (>cm^2) wrinkled graphene pattern, formed on thermally shrinkable polystyrene substrate, onto ethylene vinyl acetate/Polyethylene terephthalate (EVA/PET) and poly(dimethyl siloxane) PDMS substrates. Our technique uses poly(4-styrenesulfonic acid) (PSS) as a sacrificial skin layer between graphene and deformable (i.e. polystyrene) substrate. Here, the PSS skin layer enables contamination free transfer of wrinkled graphene pattern from deformed substrate to flexible target substrates by simply dissolving in water. Most importantly, morphology and structural integrity of wrinkled graphene was retained even after transfer operation. Highly transparent (optical transmittance >90%) wrinkled graphene was extensively investigated for electromechanical response. Transferred wrinkled graphene exhibited high stretchability (~80%) with excellent stability tested for hundred cycles.

Keywords: wrinkled graphene, flexible electronics, stretchability, EVA/PET, thermally shrinkable polystyrene

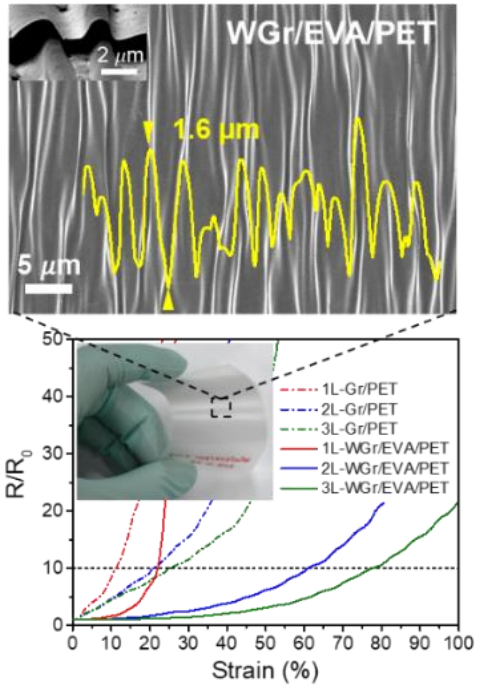

References:

1. Wenjun C., Xuchun G., Leilei Y., Hai Z., Zikang T. (2019), Wrinkling of two-dimensional materials: methods, properties and applications, *Nanoscale Horiz.* 4, 291-320

XUV-laser induced detachment of multi-layer graphene from silicon carbide substrate

V. Vozda[a,b,1], T Burian[b,c], J. Chalupský[b], J. Čechal[d,e], V. Hájková[b], L. Juha[b], M. Krůs[c], J. Kunc[a], N. Medvedev[b,c]

[a] Charles University, Faculty of Mathematics and Physics, Institute of Physics,Ke Karlovu 5, CZ-121 16, Prague 2, Czech Republic
[b] Institute of Physics, Czech Academy of Sciences, Na Slovance 2, 182 21 Prague 8,Czech Republic
[c] Institute of Plasma Physics, Czech Academy of Sciences, Za Slovankou 3, 182 00Prague 8, Czech Republic
[d] Central European Institute of Technology–CEITEC, Purkyňova 123, 616 69 Brno,Czech Republic
[e] Institute of Physical Engineering, Faculty of Mechanical Engineering, Brno Universityof Technology, Technická 2, 616 69 Brno, Czech Republic

Abstract:
Widely used and most reliable growing technique for fabrication of large-scale graphene grains, a thermal decomposition on silicon carbide (SiC), significantly reduces the carrier mobility partially due to crystal imperfections and partially due to substrate phonons which collide with the charge carriers. Elimination of the substrate influence is therefore essential to keep the carrier mobility at a very high level. In our experiment, samples of multi-layer epitaxial graphene grown on SiC were exposed to intense 21.2-nm radiation provided by Ne-like Zn XUV laser driven by the Prague Asterix Laser System (PALS). A sub-nanosecond pulse of energetic (58.5 eV) photons is used to break relatively weak bonds between the SiC substrate and graphene while keeping the graphene layer almost unaffected. An irradiated area was inspected by micro-Raman spectroscopy, white-light interferometry (WLI), atomic force microscopy (AFM) and scanning electron microscopy (SEM). Data show clear evidence of detachment of the multi-layer graphene which is elevated by 5 nm. Decrease of the mechanical strain and increase of number of defects in the irradiated area observed from Raman spectra is discussed.

Keywords: graphene, carrier mobility, conductivity, silicon carbide, laser irradiation, PALS, ablation imprint, strain, micro-Raman spectroscopy, WLI, AFM, XPS.

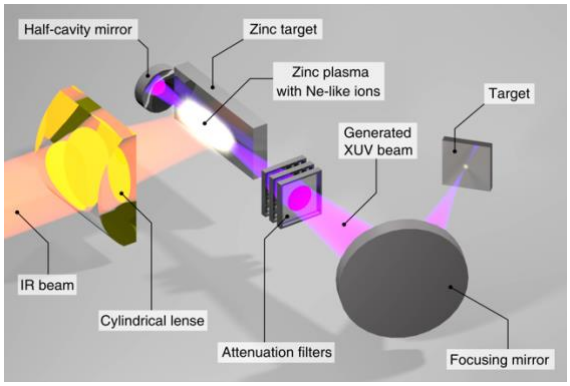

Figure 1: Illustration of the experimental settings at PALS.

[1] Corresponding author. E-mail: vozda@fzu.cz

Chloride Migration in Grpahene Oxide Concrete

B. Kim,[1,*] M. Ambrose,[1]

[1] University of Plymouth, School of Engineering, Computung and Mathematics, Plymouth, UK

Abstract:
Concrete used in marine environments faces severe challenges. Traditional concrete is very brittle, which can lead to micro-cracks and void gaps. Cracks can cause serious damage to concrete structures, in particular, those exposed to coastal environments since sea salt can induce chloride ingress and allow penetration into the concrete. This chloride infiltration corrodes the steel reinforcements in the concrete. The corrosion can damage the strength, aesthetics and serviceability of structures. The utilisation of high performance concrete is hence required. Ever since its discovery in 2004 [1], graphene has provided a new way to solve the issues that concrete faces in harsh environments due to graphene's exceptional mechanical, thermal, optical and electrical properties, and electrical conductivity. It is an ideal nano-filler that can modify the cementitious material, although it is hard to synthesize and very expensive at present. It can be synthesized to Graphene Oxide (GO): layered graphite interspersed with oxygen molecules around its plane and edges called functional groups and then exfoliated into single-layer and few-layer GO sheets. Addition of a small amount of graphene into a concrete mix can improve significantly the strength of concrete [2]. Here, we report our experimental work on the chloride penetration resistance of concrete, incorporating 0%, 2% and 3% GO by weight of cement, along with water absorption tests, Field Emission Scanning Electron Microscope and Energy Dispersive X-ray Spectrometry analyses. The test results show that the inclusion of GO into a cementitious mix does have a noticeable effect on the increase of chloride resistance.

Keywords: Graphene Oxide; rapid chloride migration test; chloride penetration; permeability; water absorption, cement mortar; concrete

Figure 1: Figure illustrating measuring the chloride penetration depth in a concrete disk as part of the rapid chloride migration test.

References:

1. Novoselov, K., Geim, A., Morozov, S., Jiang, D., Zhang, Y., Dubonos, S., Gregorieva, I. and Firsov, A. (2004). Electric Field Effect in Atomically Thin Carbon Films. *Science*, 306(5696), pp.666-669.
2. Dimov D., Amit, I., Gorrie, O., Barnes, M., Townsend, N., Neves, A., Withers, F., Russo, S. and Craciun, M. (2018). Ultrahigh Performance Nanoengineered Graphene-Concrete Composites for Multifunctional Applications. *Advanced Functional Materials*, 28(23), 1705183.

Graphene as a standard material for accurate dimensional measurement of the focal volumes of Raman microscopes

A. Sacco [1], C. Portesi [1], A. M. Giovannozzi [1], A. M. Rossi [1*]

[1] Quantum Metrology and Nanotechnology Department, Istituto Nazionale di Ricerca Metrologica (INRiM), Turin, Italy

Abstract:
Raman microscopy is a versatile vibrational spectroscopy technique that allows fast, non-destructive chemical identification and characterization of materials at the microscopic scale. Nowadays, it is used in a wide range of research and industrial fields, spanning from fundamental studies and materials characterization to biological and pharmaceutical applications. As of now, Raman is mainly employed as a qualitative characterization tool, and sometimes for relative quantification; however, absolute quantification traceable to the International System of Units (SI) is still unfeasible. One of the reasons is that the community currently lacks standard procedures and reference materials for the accurate measurement of the dimensions of the focal volumes of Raman microscopes.
In this work, a graphene flake with a straight edge (tolerance within 10 nm) is proposed as a standard material to quantify the three dimensions of confocal volumes of three Raman microscopy setups. Graphene has a high Raman cross section, is chemically and mechanically stable in ambient conditions, and has a very low thickness. These properties make it an ideal candidate as a Raman probe. By scanning the surface of the graphene layer and its straight edge in different directions, Raman intensity profiles can be acquired and analyzed to reconstruct the geometry of the focal volume and focused beam waist. Furthermore, with this concept a technique to obtain actual projections of the focal volume on planes parallel to the optical axis ("side views" of the volume) is applied. These data, combined with theoretical knowledge and precise definitions of the profiles and their boundaries, allow the metrological dimensional characterization of the focal volumes and beam waists of Raman microscopes and the estimation of measurement uncertainties, which is a fundamental step towards traceable Raman microspectroscopy quantification in all its fields of application.

Keywords: Raman spectroscopy, metrology, Raman quantification, focal volume, dimensional analysis, vibrational spectroscopy.

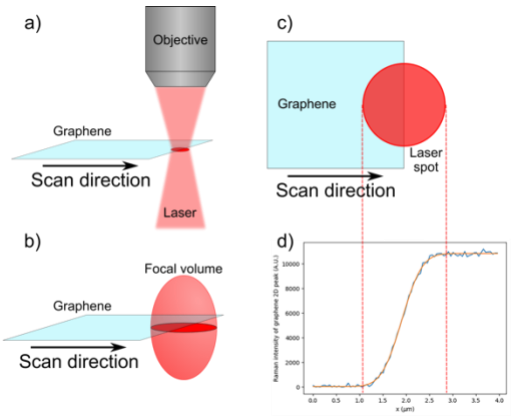

Figure 1: Schematization of the graphene method for the Raman microscope lateral profile measurement of the beam waist. a) Perspective side view of the system (the focused spot is shown in dark red). b) Same view with the focal volume explicitly shown. c) Top view of the system. d) Actual measurement of a profile (blue line) and least-squares functional regression (orange line). Note that this is a cumulative function of the intensity at each position. The vertical dashed lines indicate a profile delimited by an intensity threshold of $1/e^2$ of the maximum.

References:

1. Kim, Y., Lee, E. J., Roy, S., Sharbirin, A. S., Ranz, L. G., Dieing, T., & Kim, J. (2020). Measurement of lateral and axial resolution of confocal Raman microscope using dispersed carbon nanotubes and suspended graphene. *Current Applied Physics*, 20(1), 71-77.

SurfCoat Korea 2021 Session II.B:

Surface treatments and coatings deposition, functionalization, modelling and characterization

Plasma engineering of graphene nanowalls and other 2D structures beyond graphene

U. Cvelbar[1]

[1] Jožef Stefan Institute, Ljubljana, Slovenia, EU

Abstract:
Plasma engineering finds its applications in various fields of materials science including the building of 2D carbon nanostructures like graphene nanowalls (GNW), which is an emerging field of material synthesis with some challenges related to its processing. Synthesis of GNW in a controlled manner with plasma-enhanced techniques opened future pathways for the large-scale, rapid functionalization of graphene for advanced applications. Plasma-supported methods enhance the possibility of processing (synthesis and functionalization) during the surface interactions between substrate and GNW offer the possibility for surface post-treatment. Among the important plasma-assisted methods for GNW synthesis, the most frequently used method is plasma-enhanced chemical vapour deposition (microwave-assisted, inductively coupled, capacitively coupled PECVD), which can enable the grow GNW on the substrate even in the absence of the metal catalyst. This talk addresses the most important challenges associated with plasma-assisted mechanisms of GNWs dealing with the growth and doping of GNWs or further materials beyond graphene. From this point of view, it's clear the importance of gas mixtures and plasma's properties. In these systems, plasma parameters, including the densities of ions and radicals, are regulated by the discharge parameters, including power, gas mixture ratio, gas flow, and pressure. However, the main challenge is connected to understanding the role of plasma species in growth and their efficient control for improving the quality and selectively modifying properties of the synthesised GNW. Another challenge is material doping and understanding the mechanism of plasma doping. Nitrogen functionalization and doping are one of the potential directions on how to alter the electronic properties, the oxygen plasma treatment, for example, helps to enhance surface morphological properties and band gaps widening, etc. In this perspective, the talk will highlight the recent progress in the field of plasma building GNW, including the processing, functionalization, and future challenges that we have to address in GNW synthesis. Here the top-end simulations with our developed full-scale models will be used for predictions of material plasma growth or synthesis, whereas the simulations are supported by experimental evidence.

Keywords: plasma growth, plasma synthesis, plasma functionalization, graphene nanowalls, 2D structures, 2D beyond graphene, plasma modelling, structure formation.

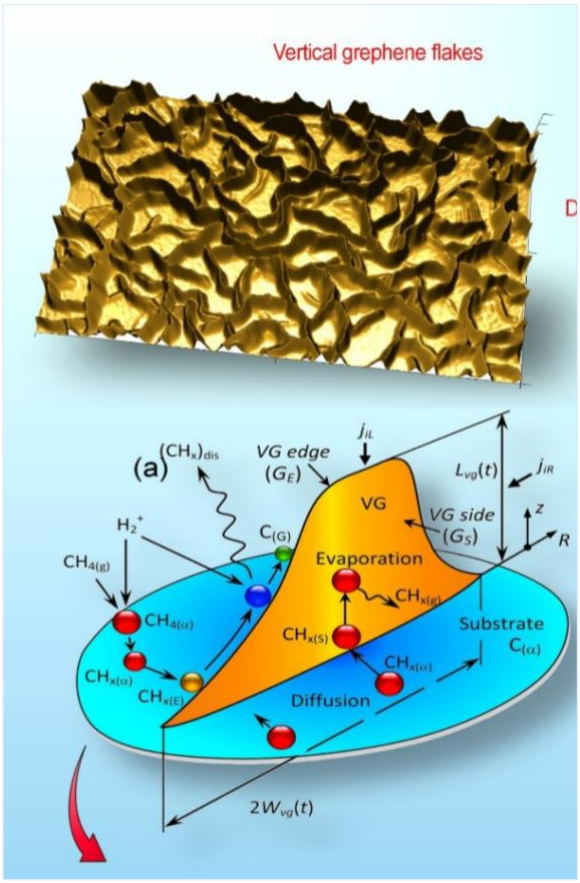

Figure 1: Figure illustrating the as-grown versicall graphene flakes and major plasma processes ond the surface simulated during the growth.

Insights into oxidation processes of protective coatings from AIMD modelling

Fangyu Guo[1,2], Thomas Glechner[3], Nikola Koutná[3], Yong Du[2], Helmut Riedl[3], Paul H. Mayrhofer[3] and David Holec[1]

[1] Department of Materials Science, Montanuniversität Leoben, A-8700, Leoben, Austria
[2] State Key Laboratory of Powder Metallurgy, Central South University, Changsha, China
[3] Institute of Materials Science and Technology, TU Wien, A-1060 Vienna, Austria

Abstract:
Increasing requirements on hard coatings in high-performance machining processes such as high speed and dry cutting, demand further developments of the already well-established coatings (such as Ti-Al-N) or identification of novel systems. The aim of this work is to review recent advances in bottom-up approach focusing on modelling of elemental oxidation processes when the coating surface is exposed to oxidizing environment. The method of choice is *ab initio* molecular dynamics (AIMD) due to its versatility (chemistry) and accuracy.
Firstly, we will focus on establishing the method by reproducing temperature- and composition-dependent trends in Ti-Al-N model system. AIMD is able to pick improved oxidation resistance for Al-rich systems (with respect to Al-poor compositions) as demonstrated by a more intact surface in the former case, as well as oxide-scale stratification similar to that observed experimentally [1]. Next, we study the impact of alloying in Ti-Al-X-N with X (X = V, Hf, Si) in the surface layer. The additions of Hf and Si facilitate the formation of layered oxides with Ti-rich and Al-rich oxides, respectively, which improves the antioxidant performance at high temperatures. Contrarily, the Al-rich layer is absent during oxidation of V-containing coating [2]. Furthermore, later oxidation stages are accounted for by over-saturating simulation box with O and considering also diffusion barriers both in bulk as well as along grain boundaries [3].
Encouraged by this qualitative success, we will discuss our most recent results of applying the same methodology for understanding the impact of Si on oxidation performance of TaC.

Keywords: protective coatings, ab initio molecular dynamics, DFT, oxidation, nitrides, carbides

References:

1. Guo, Fangyu, Jianchuan Wang, Yong Du, David Holec, Pengfei Ou, Hao Zhou, Li Chen, and Yi Kong. 2019. "Structural Evolution of Oxygen on the Surface of TiAlN: Ab Initio Molecular Dynamics Simulations." *Applied Surface Science* 470:520–25.
2. Guo, Fangyu, David Holec, Jianchuan Wang, Songlin Li, and Yong Du. 2020. "Impact of V, Hf and Si on Oxidation Processes in Ti–Al–N: Insights from Ab Initio Molecular Dynamics." *Surface and Coatings Technology* 381:125125.
3. Cottom, Jonathon, Anton Bochkarev, Emilia Olsson, Kamal Patel, Manveer Munde, Jürgen Spitaler, Maxim N. Popov, Michel Bosman, and Alexander L. Shluger. 2019. "Modeling of Diffusion and Incorporation of Interstitial Oxygen Ions at the TiN/SiO2 Interface." *ACS Applied Materials & Interfaces* 11 (39):36232–43.

Plasmas in Additive and Subtractive Surface Manufacturing of Functional Surfaces

J.L. Endrino,[1,2]

1Basque Center for Materials, Applications & Nanostructures, UPV/EHU Science Park, Barrio Sarriena s/n, 48940 Leioa, Spain.
2 IKERBASQUE, Basque Foundation for Science, Maria Diaz de Haro 3, 48013 Bilbao, Spain.

Abstract:
Subtractive and additive manufacturing methods are at the heart of 21st century manufacturing. Nowadays, there is a wide variety of surface process techniques based on these two methods which are being used in the fabrication at micro, meso and macro level. Among them, plasma-based processes bring the possibility of manufacturing precision surfaces using novel chemistries and simple in-process metrology technologies. This contribution will present different case studies for additive and subtractive manufacturing using plasmas. The first case study will deal with the deposition of hard TiB2 coating surfaces by cathodic vacuum arcing of specialised ceramic cathodes. The subtractive manufacturing case study is an example of the use of reactive plasma jets capable of removing material from optical materials. Finally, the combination of both subtractive and additive manufacturing processes in the preparation of deterministic metallic surfaces inspired on snake skins will be also be discussed.

Keywords: deterministic surface, photochemical machining, pin-on-disc tests, rapid atmosferic plasma torch, coefficient of friction, biomedical applications.

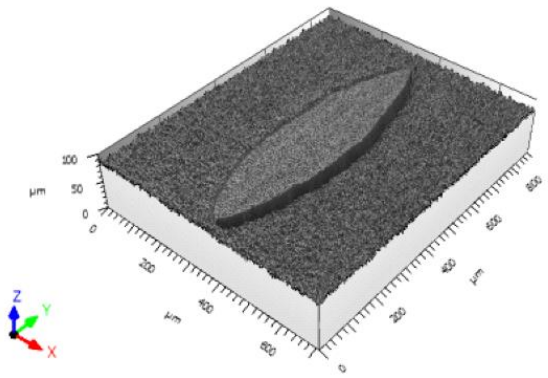

Figure 1: Figure illustrating the size and shape of surface texture elements with the chemical etching time inspired by the characteristics of the shed skin of Vipera Ammodytes snake.

References:

1. T. L. Brzezinka, J. Rao,… Jose L. Endrino (2020), Facilitating TiB2 for filtered vacuum cathodic arc evaporation. Coatings Submitted
2. AD Lantada, JL Endrino (2016), Nanomanufacturing Technologies for Biomedical Microsystems Interacting at a Molecular Scale. Microsystems for Enhanced Control of Cell Behavior, 147-162

A route to complexity : sputter deposition using target powders

D. Depla[1]

[1] Ghent University, Department of Solid State Sciences, Krijgslaan 281 (S1), 9000 Gent, Belgium

Abstract:
Magnetron sputter deposition has two major advantages : its scalability and its flexibility to modify the chemical composition of the thin films. Several options are possible to achieve thin films with different chemical composition. The use of multiple sources is one option [1-3], but it also possible to grow the complex films starting from a multi-element target. Examples are the deposition from ceramic targets [4-5], and targets with inserts [6]. In this contribution, another method is discussed i.e. thue use of uni-axial pressed powder targets. Some fundamental differenes with solid targets will be highlighted [7-9]. The paper will then focus on the deposition of multicomponent alloys (also known as high entropy alloys) [10-11]. The addition of a reactive gas such as oxygen or nitrogen permits to deposit not only multicompenent alloys, but also oxides or nitrides. The influence of reactive gas addition on the growth of these alloys will be reviewed [12]. Powder targets also enables to think out of the traditional box regarding the target composition. This will be illustrated with the growth of porous thin films based on powder targets with salt as one of the constituents [13].

References:

1. M. Saraiva, V. Georgieva, S. Mahieu, K. Van Aeken, A. Bogaerts, D. Depla, *J. Appl. Physics 107 (2010) 034902*
2. J.S. Lamas, W.P. Leroy, Y.-G. Lu, J. Verbeeck, G. Van Tendeloo, D. Depla, *Surface Coat. Techn 238 (2014)*
3. S. Van Steenberge, D. Depla *J. Phys. D: Appl. Phys. 49 (2016) 245302*
4. T. Kubart, D. Depla, D. Martin, T. Nyberg, S. Berg Appl. Phys. Lett. 92 (2008) 221501
5. T. Kubart , J. Jensen, T. Nyberg, L. Liljeholm, D. Depla, S. Berg, Vacuum 83 (2009) 1295
6. B.R. Braeckman, F. Boydens, D. Depla, D. Poelman, J.Alloys Comp. 578 (2013) 44
7. F. Boydens, W.P. Leroy, R. Persoons, D. Depla, Physica Status Solidi A 209 (2012) 524-530
8. B.R. Braeckman, F. Boydens, H. Hidalgo, P. Dutheil, M. Jullien, A.-L. Thomann, D. Depla, Thin Solid Films 2015 (580) 71-76
9. D. Depla Vacuum 184 (2021) 1879-2715
10. B.R. Braeckman, F. Misják, G. Radnóczi, D. Depla, Thin Solid Films 616 (2016) 703–710
11. B.R. Braeckman, F. Misják, G. Radnóczi, M. Caplovicová, Ph. Djemia, F. Tétard, L. Belliard, D. Depla, Scripta Materialia 139 (2017) 155–158
12. R.Dedoncker,Ph.Djemia,G.Radnóczi,F.Tétard,L.Belliard,G.Abadias,N.Martin,D.Depla, .Alloys Comp 769 (2018) 881-888
13. R. Dedoncker, H. Ryckaert, D. Depla, Appl. Phys. Lett. 115(2019) 041601

Keywords: sputter deposition, powder targets, multicomponent alloys and compounds, porous thin films

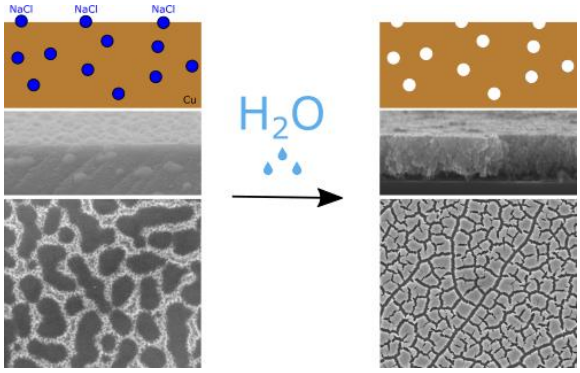

Figure 1: Principle of the growth of porous thin films from a powder target.

Formation of multiphase synthesized coatings on TiNi substrate

G. Baigonakova, S. Gunther, A.Shishelova

Tomsk State University, Tomsk, Russia

Abstract:
With the long-term functioning of implants made of TiNi alloys in the human body under aggressive corrosion-dynamic conditions, there is a serious problem associated with the biochemical compatibility of their surface [1, 2]. Therefore, a surface modification for biomaterials based on TiNi alloy is a promising way to increase their biochemical compatibility. There are many works to improve surface characteristics by creating oxide, nitride, oxynitride, inter-metallic and multiphase gradient coatings [3]. However, each of the surface modification methods does not fully meet the requirements for superelastic TiNi alloys.
This study presents a new method for creating a multiphase nanocoating on the surface of a NiTi alloy, combining the method of magnetron deposition of Ti-Ni-Ti nanolaminate of different thicknesses with subsequent reaction synthesis in a nitrogen atmosphere in order to provide a multifunctional set of properties.
The total thickness of the consequently deposited Ti / Ni / Ti layers by magnetron sputtering is 150 nm and 75 nm. In what follows, we will designate them as NL150 and NL75. After reaction annealing in an argon atmosphere at a temperature of 900 °C, both coatings have a crystalline gradient-layered structure: a three-layer coating of (layers I, II, III) bound to the substrate by a diffusion zone has been formed. However, studies have shown that the thicknesses of the deposited nanolaminates NL150 and NL75 affect the structure, morphology of the synthesized coating and reaction products.
The interfaces between the layers of the synthesized coatings are clearly visible, but their morphology is visually different. The map of the distribution of elements Ti, Ni, N, O of the cross-section of the samples has shown that their content periodically changes from layer to layer (Fig.1). During reaction annealing of deposited nanolaminates NL150 and NL75, different dynamics of the formation of diffusion reaction products with the participation of Ti and Ni elements and interstitial impurities O and N are observed.

This research was supported by Russian Science Foundation (grant #19-72-10105)

Keywords: nanolaminate, coating, Ti-N-Ti, magnetron sputtering, reaction synthesis

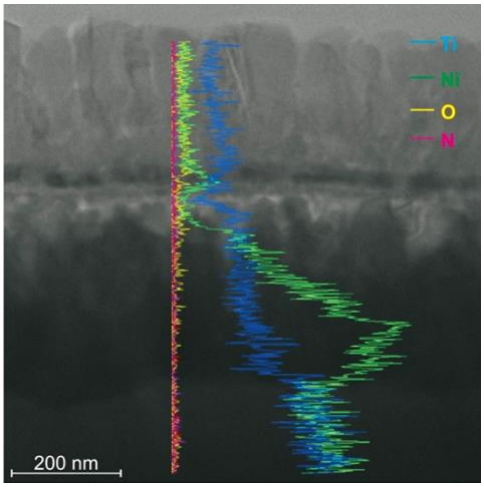

Figure 1: The cross-sectional EDS line scan analysis of the synthesized coating from NL 75

References:

1. Jani, J., Leary, M., Subic, A., Gibson, M. (2014) A review of shape memory alloy research, applications and opportunities. *Mater*. 56. 1078–1113.
2. Marchenko, E., Baigonakova, G., Yasenchuk, Y. (2020) Gradient crystalline coating on a biomedical TiNi alloy prepared by magnetron sputtering and annealing, *Vacuum*, 181, 109652.
3. Ryhänen, J., Niemi E., Serlo W., et.al. (1997) Biocompatibility of nickel titanium shape memory metal and its corrosion behavior in human cell cultures. *Journal of Biomedical Materials Research*, 6. 451-457.

Ultra-Thin Topological Insulator Films for Thermoelectrical Applications: Deposition and Properties.

J. Andzane,[1*], K. Niherysh,[1] E. Kauranens,[1] U. Malinovskis,[1], A. Felsharuk,[1] D. Erts[1,2]

University of Latvia, [1] Institute of Chemical Physics and [2]Department of Chemistry, Riga, Latvia

Abstract:
One of the world's biggest challenges is increase of energy efficiency of domestic and industrial processes by waste heat conversion to electrical energy. This can be done by thermoelectric (TE) devices, however, the efficiency of existing TE devices is fundamentally limited by combination of electrical and thermal properties of TE material – figure of merit , which is the main obstacle for commercial applications of TE devices.
Recent discovery that the best TE materials are topological insulators (TI) have opened new perspectives in the field of increasing their TE figure of merit. TI are a class of materials characterized by an insulating bulk state and conducting surface states. These surface states are protected by time-reversal symmetry and immune to surface disorders. Theoretical calculations performed for TI bismuth chalcogenide nanostructures [1] predict that downscaling (reduction of the thickness of TE material below 10 nm) together with specific doping will result in noticeable quantum tunnelling between the top and bottom surfaces and inducing of hybridization band gap near Dirac point. This should result in significant – by an order of magnitude – increase of existing ZT of the material. The hybridization gap can be tuned by variation of thickness of nanostructures. This allows to achieve maximal TE efficiency of bismuth chalcogenides for every target temperature range.
This work is focused at development of simple cost-effective method for deposition of ultra-thin TI films and on the experimental verification of the theoretical predictions related to the enhancement of the TE properties of such films. Pure and specifically doped ultra-thin (<10 nm, Figure 1) bismuth and antimony chalcogenide films were deposited using modified physical vapour deposition (PVD) technique [2]. Morphology, chemical composition and thickness of the obtained ultra-thin films were determined by scanning electron (SEM), energy-dispersive X-ray spectroscopy and
atomic force (AFM) microscopy methods.

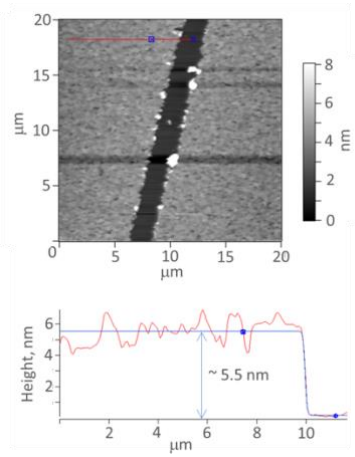

Figure 1. AFM image and height profile of a PVD-deposited 5.5 nm thin bismuth selenide film.

Electron transport and thermoelectric properties of the obtained ultra-thin films were determined for the temperature range 2-350 K, analysed and compared with the reported in literature properties of high-quality ultra-thin films deposited by expensive molecular beam epitaxy method. Effect of the down-scaling and specific doping on the TE properties of ultra-thin films is discussed.

Keywords: ultra-thin films, thermoelectrical applications, topological insulators, nanolaminates, physical vapour deposition, bismuth chalcogenides, antimony chalcogenides

References:

1. Tahir, M., Manchon, A., Schwingenschlol, U. (2014), Enhanced thermoelectric power in ultrathin topological insulators with magnetic doping, *J. Appl. Phys*., 116, 093708.
2. Andzane, J., Kunakova, G., Charpentier, S., Hrkac, V., Kienle, L., Baitimirova, M., Bauch, T., Lombardi, F., Erts, D. (2015), Catalyst-free vapour–solid technique for deposition of Bi_2Te_3 and Bi_2Se_3 nanowires/nanobelts with topological insulator properties, *Nanoscale*, 7, 15935.

Sol-Gel Surface Coating of 3D Printed Parts

Hugh G Manning,[1,2,3*] Joseph Mohan,[2,3] Mark Culleton,[1] Brendan Duffy,[2] James Kennedy.[3]

[1] Advanced Materials and Bioengineering Research (AMBER) Centre, Trinity College Dublin, Ireland
[2] Centre for Research in Engineering Surface Technology (CREST), Technical University (TU) Dublin, Ireland
[3] Kastus Technologies, Ireland

Abstract:
Additive manufacturing (AM), the 3 dimensional (3D) printing of materials is a revolutionary manufacturing technique that can produce a 3D object via layer-by-layer deposition. This bottom-up approach enables the fabrication of objects from digital models without the need for casting moulds, forming templates or wasteful subtractive shaping. Moreover, layer-by-layer manufacturing allows for unprecedented freedom in manufacturing complex structures that cannot be made through traditional methods.
The simultaneous creation of the part's material and shape enables the fabrication of features which can improve performance within specific applications e.g. tailoring the pore size, orientation, shape and interconnectedness within catalyst supports or optimized fuel distribution in combustion engines to enhance flow.[1] However, many challenges still remain for 3D printed metal and ceramic pieces, including; decreasing surface roughness, improving scratch resistance, reducing the anisotropy in mechanical properties, and increasing the corrosion resistance of certain materials. These challenges have fueled significant research and development within AM over recent years,[2] but reports on surface coating strategies for the resulting AM parts have lagged behind.
Organosilane sol-gel coatings have previously been shown to improve the corrosion protection of the surfaces of aluminium and steel.[3] Sol-gel infiltration and surface coating is a straightforward method to fix the poor mechanical properties caused by the residual porosities and surface roughness errors of 3D printed parts.[4] The sol-gel coating can be uniformly applied by a simple dip-coating method. Once cured it provides a hard, durable, protective coating. The coating thickness is controlled by the formulation viscosity and the withdrawl speed of the part from the sol-gel solution. In this work we investigate the sol-gel infiltration and surface coating of 3D printed Ti6Al4V metal and alumina ceramic pieces.

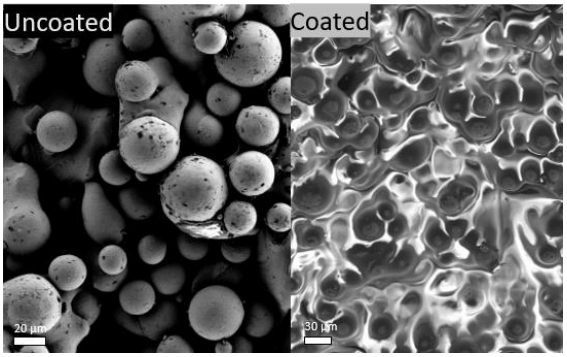

Figure 1: Scanning electron micrograph of a 3D printed part, as-printed (left) and sol-gel coated (right).

Keywords: Additive manufacturing, 3D printing, sol-gel, anti-corrosion, coatings, dip-coat, anti-fouling coating.

References:

1. Schlier, Lorenz, et al. "Macro-cellular silicon carbide reactors for nonstationary combustion under piston engine-like conditions." International Journal of Applied Ceramic Technology 8.5 (2011): 1237-1245.
2. Global Additive Manufacturing Market, Forecast to 2025. Frost & Sullivan's Global 360° Research Team 2016. Available from: https://store.frost.com/concept-to-production-future-of-additive-manufacturing-19900.html
3. Varma, R. et al.: Corrosion Protection Properties of Various Ligand Modified Organic Inorganic Hybrid Coating on AA 2024-T3.ECSTransactions,vol. 24 (1), 2010,pp. 231-246. doi:10.1149/1.345361
4. Stumpf, Martin, et al. "Sol-gel infiltration of complex cellular indirect 3D printed alumina." Journal of the European Ceramic Society 38.10 (2018): 3603-3609.

Investigation of Electroless Copper Plating on Textiles using Different Catalysts

G. Taghavi Pourian Azar,[1*] D. Fox,[1], L. Krishnan[1], A.J. Cobley[1]

[1] Coventry University, Faculty of Engineering Computing and Environment, Coventry, UK

Abstract:
The MATUROLIFE project utilises two disciplines of materials science and design to meet the needs of older adults to lead independent lives through design-driven Assistive Technology (AT). Metallised conductive textiles are potentially an enabling technology for AT allowing better and more discreet integration of electronics into clothing, footwear and furniture.
Electroless copper plating is a versatile method for the metallisation of insulating materials such as textiles, owing to its capability for uniform deposition with consistent thickness, simplicity and relatively low cost. This procedure is a useful approach to produce electrically and thermally conductive textiles which are flexible to be utilised in smart textiles. In the case of non-conducting materials, a catalyst is required to activate the surface and generate nucleation sites for the copper ions to deposit on. The most widely used catalyst is a palladium/tin colloid, however, the use of palladium makes the process expensive. Therefore, alternative and inexpensive metals such as silver and copper have been recently investigated to catalyse the electroless copper plating reactions.
In this study, different catalysts such as Pd, Ag and Cu nanoparticles (functionalised by various organic molecules) have been utilised for electroless copper plating of textiles. Catalysts and metallised textiles were characterized using various techniques including X-ray Photoelectron Spectroscopy (XPS), Transmission Electron Microscopy (TEM), Scanning Electron Microscopy (SEM), sheet resistance measurements and adhesion tests.
It was found that the degree of coverage of fibres by copper coatings and the resulted conductivities are strongly dependent on the applied catalyst. Using the best-performing organic molecule in functionalisation of Cu nanoparticle catalyst resulted in coatings with complete coverage and consequently high electrical conductivity being favourably comparable to the coatings catalysed with a Pd catalyst.
Keywords: Electroless copper plating, catalysts, copper nanoparticles, functionalization, textiles, polyester.

Acknowlegments
The authors would like to thank the European Union for funding this work via the H2020 NMBP project ‘MATUROLIFE’ (Grant No. 760789).

Characterization of solid devices using quadrupole SIMS

N. Wehbe

[1] Imaging and Characterization Core lab, King Abdullah University of Science & Technology (KAUST), Thuwal 23955-6900, Saudi Arabia.

Abstract:
Dynamic Secondary Ion Mass Spectrometry (D-SIMS) is a very powerful tool for the characterization of solid surfaces and is a requisite technique for researchers developing devices in the field of semiconductors, photovoltaics and energy storage technologies. Dynamic SIMS instruments equipped with quadrupole analyzer are simple and easy to use although they don't allow the best performance in term of mass resolution and sensitivity compared to SIMS instruments equipped with analyzers of magnetic sector type.
Throughout this contribution, I will be showing several examples obtained in our lab and illustrating the information that can be derived from the quad-SIMS data. The presentation will cover the most common topics requested by the researchers including the in-depth analysis of solar and photovoltaic cells, the in-depth quantification of elements incorporated either as dopant (SIMS) or as high content (SNMS). The presentation will be also focused on the characterization of multilayer devices[1] and the limitation or artifacts that may be occurring during the sputtering process.

Keywords: Surface Characterization, Secondary Ion Mass Spectrometry, SIMS, Depth Profiling.

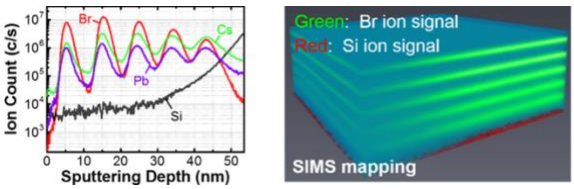

Figure 1 (a) SIMS depth profiling of perovskite-based artificial MQW. The ion signals, ascribed to Br, Cs, Pb, and Si, are plotted versus the sputtering depth.SIMS. **(b)** SIMS Three-dimensional mapping of Br and Si signals.

Reference:

1. Kwang Jae Lee, Bekir Turedi, Lutfan Sinatra, Ayan A. Zhumekenov, Partha Maity, Ibrahim Dursun, Rounak Naphade, Noor Merdad, Abdullah Alsalloum, Semi Oh, Nimer Wehbe, Mohamed N. Hedhili, Chun Hong Kang, Ram Chandra Subedi, Namchul Cho, Boon S. Ooi, Omar F. Mohammed, Osman M. Bakr. (2019) Perovskite-Based Artificial Multiple Quantum Wells, *Nano. Lett.*, 19, 3535-3542.

Finite element simulation of residual stresses and failure mechanism of plasma sprayed thermal barrier coating considering real interface.

Ahmed Abdelgawad[1], Khaled Al-Athel[2]

[1]King Fahd University of Petroleum and Minerals, Dhahran, Saudi Arabia, g201705510@kfupm.edu.sa
[2]King Fahd University of Petroleum and Minerals, Dhahran, Saudi Arabia kathel@ kfupm.edu.sa

Abstract

In order to increase the efficiency of gas turbine engines, which are used for propulsion and electricity generation, the turbine inlet temperature (TIT) has to be as high as possible. Using Thermal Barrier Coatings (TBC) allows the metallic internal components to operate at elevated temperature near to its melting temperature. Thermally growing oxide induces cracks formation in the top coat that may lead to complete failure TBC due to spallation. This research aims at investigating the development of the stresses and critical cites that have possibility of crack nucleation due to thermal mismatch during operating cycle of a typical plasma sprayed TBC. A true finite element model was developed based on a scanning electron microscope image taking the advantage of a commercial finite element package (ABAQUS) and image processing techniques. The model including the effect of creep on all layers and plastic deformation of BC, TGO and substrate. The results show that unlike common unit cell models in literature, a better understanding can be achieved by having a model based in an SEM image that represents the real geometry.

Keywords: Micromechanics, Thermal barrier coatings, Residual stresses, Finite element modelling (FEM).

One Structure – Three functionalizations: Laser based microstructures on aluminium with superhydrophobic, ice-repellent and self-cleaning properties

S. Milles,[1,*] M. Soldera,[1,2] A.F. Lasagni,[1,3]

[1] Technische Universität Dresden, Institute of Manufacturing Science and Engineering, Dresden, Germany
[2] PROBIEN-CONICET, Universidad Nacional del Comahue, Department of Electrical Engineering, Neuquén, Argentina
[3] Fraunhofer Institut for Material and Beam Technology IWS Dresden, Dresden, Germany

Abstract:
Technical surfaces are increasingly subject to major challenges so that a single functionalization is not sufficient anymore. A nature inspired template for these multifunctional surfaces can be found on the leaves of several plants, such as nelumbo nucifera which is also known as the lotus flower [1]. The microscopic surface topography consisting of a hierarchical structure with nano and microscaled features is the reason for its superhydrophobic and self-cleaning functions. Transferring this ability to technical applications is a great challenge for the scientific community. For instance, using laser radiation as a structuring tool, it is possible to create such hierarchical topographies on metals to enhance their wettability and self-cleaning properties. Furthermore these structures also have an ice-repellent function which is important for wind turbines, the food industry or the energy and cooling sector. In the present work, laser-based methods are used to produce functional structures on aluminum using pulsed laser radiation with a wavelength of 1064 nm. In particular, the nanosecond pulsed Direct Laser Writing (DLW) was successfully used to pattern mesh-like textures with lateral sizes of 50 µm, while picosecond pulsed Direct Laser Interference Patterning (DLIP) was used to structure periodic micropillars with a spatial period of 7.0 µm. Moreover, these methods are combined to create hierarchical structures (Figure 1). The topography of the resulting functional surfaces were characterized by optical confocal microscopy and scanning electron microscopy. Additionally, the structured samples were investigated with respect to their wetting, self-cleaning and ice repellency properties. The ice formation on these structures was investigated under constant conditions of -20°C and a humidity of 12 % [2]. The self-cleaning function was investigated with respect to organic and inorganic micrometer-sized contaminations with various particle size. The laserstructured surfaces showed a constant superhydrophobic characteristic after several days and the ice-forming was delayed up to 150% on these substrates.

Keywords: Surface treatment, superhydrophobic, ice-repellent, self-cleaning, multifunctional surfaces, laser structuring, direct laser interference patterning, direct laser writing.

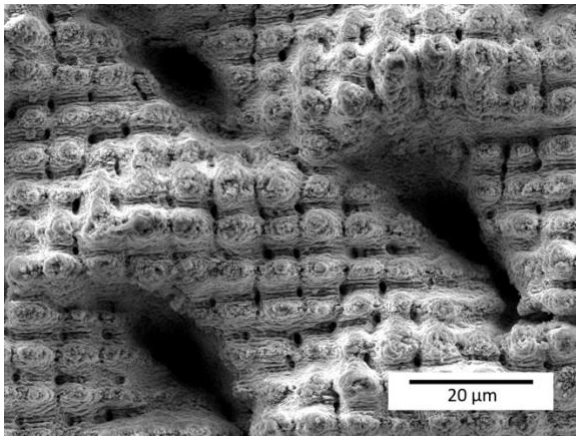

Figure 1: SEM image of a hierarchical microstructure fabricated on pure aluminium using DLW for the mesh-like structure with a lateral feature size of 50 µm and DLIP for pillar-like structure with a spatial period of 7 µm.

References:

1. Bhushan, B., Jung, Y. C., Koch, K. (2009), Self-Cleaning Efficiency of Artificial Superhydrophobic Surfaces, *Langmuir*, 25, 3240-3248.
2. Milles, S., Soldera, M., Voisiat, B., Lasagni, A. F. (2019) Fabrication of superhydrophobic and ice-repellent surfaces on pure aluminium using single and multiscaled periodic texture, *Scientific Reports*, 9, 13944.

Durable polymeric nanocomposite coatings with remarkable icephobic performance

H. Memon,[1] J. Liu,[1] D. Focatiis, [1] K. Choi, [1] X. Hou[1]

[1] University Of Nottingham, Faculty of Engineering, Nottingham, UK

Abstract:
Durability or capability of a material to maintain icephobic performance under repetitive de-icing tests and/or continued abrasive damage has been a detrimental challenge to the deployment of polymeric icephobic coatings in engineering applications. Generally a material is considered icephobic if it can maintain ice adhesion strength (IDS) of <10 KPa even after it is damaged to a considerable level. We have developed several icephobic coatings with different filler types to understand and study the durability of the low IDS polymeric coatings. IDS on our polymeric coatings were maintained under 1 KPa even after 90 minutes of silicon carbide suspension impingement tests. The results indicated high adhesion reduction factor as compared to as-received aluminium substrates. The coatings delayed the ice formation by ~6 minutes and virtually no or negliable ice was formed under static and dynamic anti-icing tests. The coatings also demonstrated good stability in IDS before and after the silicon carbide suspension impingement test and durability was significantly increase after the incorporation of fillers.

Keywords: Icephobic, anti-icing, coatings, ice adhesion strength, nanocomposites

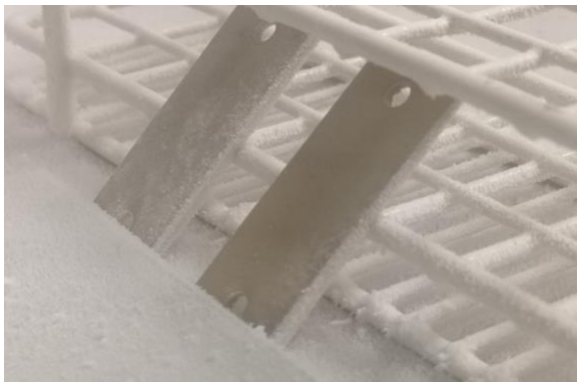

Figure 1: Figure illustrating the static anti-icing tests on the pristine (left) and icephobic (right) polymeric coatings.

Friction level control of pneumatic rod seals by surface texturing

M. Brase,[1] M. Wangenheim,[1]

[1] Leibniz University Hannover, Institute of Dynamics and Vibration Research, Hannover, Germany

Abstract:
The friction behaviour is an important property of tribological systems. While in some applications, low friction is desired to increase energy efficiency, high friction is favoured in other applications to improve the force transmission between contacting surfaces. Surface texturing is one method to reduce or increase friction without the need to change materials or the lubricant. At this, the friction level can be controlled by modifying the area of contact, the contact pressure distribution and the lubrication gap. In this study, the friction force between pneumatic rod seals with different surface textures and a translational moving rod is measured. The texture is applied to the seal surface in the form of deterministic dimples and a microscopic surface roughness. The geometry of the round dimples is defined by the diameter, distance and depth, the surface roughness by its mean roughness Ra. The seals are manufactured in an innovative production process, in which the texture is directly transferred from the mould to the seal surface during vulcanization. The prevention of a subsequent laser surface treatment of the rubber seals has both advantages for the producibility, since the seals are convenient for mass production, and for the experimental test procedure, because the material behaviour of the elastomer seals remains unchanged. During these investigations, we had the chance to test a large number of 19 surface textures allowing a targeted control of friction, since some of the surface textures analysed reduce friction between the pneumatic rod seal and the metallic rod, whereas other textures increase friction. The objective of this study is the identification of optimal surface textures under various operating conditions such as contact pressures and rod velocities, which either decrease or increase the friction level depending on the desired case of application.

Keywords: Friction control, surface texturing, rod seals, friction measurement.

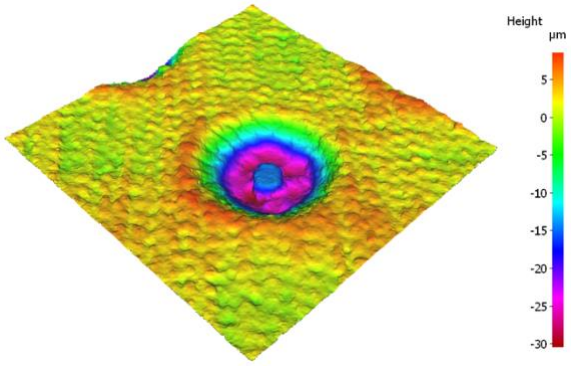

Figure 1: Figure illustrating an exemplary scan of the rod seal surface including the microscopic surface roughness and one single dimple, that functionalize the seal surface to control the friction level (Surface area: 400x400 µm).

Mechanical and tribological characteristics of carbon- and nitrogen-based thin films prepared by bottom-up approach

L. Kolodziejczyk [1,*], W. Szymanski [1], D. Martínez-Martínez [2], R. Parkhomenko [3], O. De Luca [4], M. Knez [3], P. Rudolf [4], L. Cunha [2]

[1] Institute of Materials Science and Engineering, Lodz University of Technology, Lodz, Poland
[2] Physics Department – Centre of Physics, University of Minho, Braga, Portugal
[3] CIC nanoGUNE, Donostia-San Sebastian, Spain
[4] Zernike Institute for Advanced Materials, University of Groningen, Groningen, Netherlands

Abstract:
The evaluation of the mechanical and tribological properties is one of the important issues related to the manufacturing of smart materials, implants and nanomaterials.
The aim of our work is to compare the nanoscale tribological properties of materials synthesized using different bottom-up techniques, including graphene structures, Ag and Si doped carbon-based coatings as well as Ti and Al nitrides thin films. The latter group of analyzed materials was synthesized by the atomic layer deposition (ALD) and served as the base material for tailored bottom-up deposition of MAX and MXene in form of thin films. These novel materials combine many of the best features of metals and ceramics, and their applications range is very broad, from heating elements in corrosive environments or neutron irradiation resistant parts to biological interface systems, e.g. by providing sites for many bio-factors including drugs and enzymes.
A comparative study was focused mainly on nanotribology methods including lateral force microscopy and depth-sensing techniques with the use of nanoindenter. The results were supplemented with surface geometry structure analysis and selected mechanical properties testing and their impact on friction and wear at the nanoscale.
A significant decrease in the friction coefficient (CoF) in comparison with the substrate material was found for both types of graphene structures, what is in full compliance with the current literature reports. A higher CoF of metallurgical graphene as compared to chemically vapor deposited one can be attributed to large amount of defects arising at manufacturing and transfer stages of the former.
As a result of the study on tribological properties of doped DLC coatings an increase in wear for Si-DLC coatings with respect to DLC was obtained, which, however, does not eliminate them in application for low-loaded friction couples. Another conclusion regarding wear of Si-DLC coatings is the lack of correlation between elastic strain to failure (which is related to H/E) and resistance to the plastic deformation (often associated with H^3/E^2). In the case of Ag doped DLC coating negative influence of silver admixture on tribological properties was observed.
On the basis of the obtained results for ALD-derived coatings, it was found that for the TiN film, the CoF value is almost 2 times lower compared to the magnetron sputtered reference sample. It was also shown that the wear rate of the AlN coating obtained by the ALD method is similar as for the magnetron sputtered AlN.
The obtained results constitute the basis for research on the mechanical and tribological properties of the MAX and MXene phases based on nitrides and carbides - novel materials synthesized by the bottom-up growth using the atomic layer deposition or similar methods.

Keywords: nanotribology, wear, friction, lateral force microscopy, nanoindentation, atomic layer deposition.

Acknowledgement

This study was partially supported by funding from EU and National Science Centre, Poland under Grant No. 2016/22/Z/ST5/00693.

References:

1. Anasori B., Gogotsi Y. (2019), 2D Metal Carbides and Nitrides (MXenes), Springer.
2. Kolodziejczyk L., Szymanski W., Batory D., et al. (2016), Nanotribology of silver and silicon doped carbon coatings, *Diam. Relat. Mater.*, 67, 8–15.
3. Kolodziejczyk L., Kula P., Szymanski W., et al. (2016), Frictional behaviour of polycrystalline graphene grown on liquid metallic matrix, *Tribol. Int.*, 93, 628–639.

SurfCoat Korea 2021 Session III.A:

Surface engineering / coatings for environment, energy, electric, photovoltaic and magnetic applications

Development of ceramic coatings with hydrogen, corrosion, irradiation, and electrical resistance

T. Chikada *

College of Science, Academic Institute, Shizuoka University, Shizuoka, Japan

Abstract:
Appropriate control of tritium in a fuel system is a critical issue for the establishment of a fusion reactor. Tritium permeates fast through metal walls at elevated temperature, resulting in a crucial fuel loss and radiological hazard for the environment. Moreover, hydrogen dissolves in most metals with forming metal hydrides, leading to a degradation of mechanical properties of metal structural materials, as it is called hydrogen embrittlement. Corrosion and erosion of structural materials by high-temperature tritium breeders such as solid lithium ceramic pebbles, liquid lithium, lithium-lead alloys and molten salts are also serious concerns. A promising solution to reduce tritium permeation and corrosion/erosion to an acceptable level is to coat a thin film as a multi-functional coating with tritium permeation barrier performance and corrosion protection property. However, no appropriate coating materials or fabrication methods for practical applications have been determined since 1970s. Our efforts have been dedicated to investigating hydrogen permeation mechanism in ceramic coatings for more than fifteen years, resulting in the achievement of the world's highest permeation reduction factor at elevated temperatures [1]. The development of coating process toward plant-scale fabrication has also progressed using liquid phase methods. A multi-layer structure has been investigated to make the coatings have sufficient tritium permeation barrier performance and compatibility with tritium breeders. Irradiation effects on tritium permeation in the coating have been also studied using heavy-ions and gamma-ray sources. The latest progress is to elucidate the combination effects of hydrogen, corrosion, and irradiation for a further understanding of physical and chemical phenomena in fusion reactors (Figure 1). In this presentation, recent advances and future challenges for the research and development of multi-functional coatings are overviewed.

Keywords: ceramic coating, hydrogen, deuterium, tritium, permeation, corrosion, irradiation, electrical insulation, fusion reactor, lithium-lead, neutron, γ-ray, diffusivity, solubility.

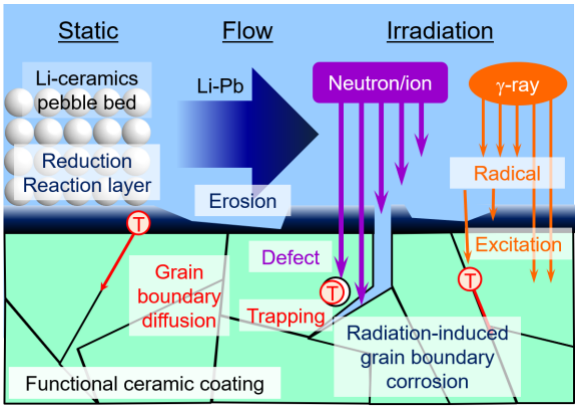

Figure 1: Physical and chemical phenomena of hydrogen, corrosion, irradiation, and electrical interactions in fusion reactor blanket functional ceramic coating.

References:

1. Chikada, T. (2020), Ceramic coatings for fusion reactors, In: Konings, R. and Stoller, R. (Eds.) *Comprehensive Nuclear Materials 2nd Edition*, Elsevier, 274-283.

Tribological performance of novel water-based nanolubricants used for hot steel rolling

Hui Wu[1], Sihai Jiao[2], Han Huang[3], Zhengyi Jiang[1*]

[1] School of Mechanical, Materials, Mechatronic and Biomedical Engineering, University of Wollongong, Wollongong, NSW 2522, Australia
[2] Baosteel Research Institute (R&D Centre), Baoshan Iron & Steel Co., Ltd., Shanghai 200431, China
[3] School of Mechanical and Mining Engineering, The University of Queensland, Brisbane, QLD 4072, Australia

Abstract:
The green manufacturing and its sustainable development are becoming increasingly important in the field of manufacturing engineering, such as hot steel rolling [1]. Although the traditional oil-in-water emulsions and other oil-based lubricants exhibit superior lubricating properties, they inevitably generate contamination to the environment when discharged. Therefore, it is desirable to develop high-performance green lubricants to substitute the traditional ones. In this regard, water-based nanolubricants are expected to serve as potential candidates [2-6]. In this study, novel water-based nanolubricants with excellent dispersion stability and wettability were synthesised using TiO_2 nanoparticles (NPs) and additives including sodium dodecyl benzene sulfonate (SDBS) and glycerol. The tribological performance of synthesised water-based nanolubricants with and without SDBS was investigated using a ball-on-disk tribometer, in which the ball represented the work roll material, and the disk represented the strip steel. The application of water-based nanolubricants in hot steel rolling was evaluated on a 2-high Hille 100 experimental rolling mill. The results showed that the water-based nanolubricant containing 4 wt% TiO_2 and 0.4 wt% SDBS exhibited superior tribological performance by decreasing coefficient of friction and ball wear up to 70.5% and 84.3%, respectively, compared to those of pure water. Additionally, the use of water-based nanolubricant containing 4 wt% TiO_2 and 0.4 wt% SDBS had significant effect on polishing the work roll surface, and thus reduced the rolling force up to 8% at a rolling temperature of 850 °C with a reduction of 30%. The lubrication mechanisms during hot steel rolling were primarily due to the formation of lubricating film and ball-bearing effect of the TiO_2 NPs, as shown in Figure 1.

Keywords: water-based, nanolubricant, TiO_2 nanoparticle, hot rolling, steel.

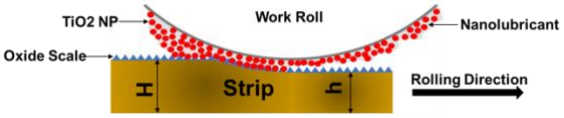

Figure 1: Figure illustrating the lubrication mechanisms during hot steel rolling, including the formation of lubricating film and ball-bearing effect of TiO_2 NPs.

References:

1. Wu, H., *A study of novel nano-additive water-based lubrication in hot rolling of steels.* Ph.D. Thesis, 2017.
2. Wu, H., et al., *Analysis of TiO_2 nano-additive water-based lubricants in hot rolling of microalloyed steel.* Journal of Manufacturing Processes, 2017. **27**: p. 26-36.
3. Wu, H., et al., *A study of the tribological behaviour of TiO_2 nano-additive water-based lubricants.* Tribology International, 2017. **109**: p. 398-408.
4. Wu, H., et al., *Friction and wear characteristics of TiO_2 nano-additive water-based lubricant on ferritic stainless steel.* Tribology International, 2018. **117**: p. 24-38.
5. Wu, H., et al., *Oxidation Behaviour of Steel During hot Rolling by Using TiO_2-Containing Water-Based Nanolubricant.* Oxidation of Metals, 2019. **92**(3-4): p. 315-335.
6. Wu, H., et al., *Effect of water-based nanolubricant containing nano-TiO_2 on friction and wear behaviour of chrome steel at ambient and elevated temperatures.* Wear, 2019. **426**: p. 792-804.

Adsorption Study on The Porphyrin Aggregates Formed at The Toluene/Water Interface

T.A. Gusman,[1,2,*] S. Tsukahara,[1]

[1] Osaka University, Department of Chemistry, Osaka, Japan
[2] University of Muhammadiyah Cirebon, Cirebon, Indonesia

Abstract:
Ordered porphyrin aggregates are expected to show specific optical characteristics, such as photovoltaic and/or photoelectric properties. This study focuses on the formation of microscopic porphyrin aggregates at the oil/water interface. We employed 5-(4-carboxyphenyl)-10,15,20-triphenylporphine (TPPCOOH), and have investigated the effects of pH of the aqueous phase, porphyrin concentration, and inorganic salt concentration on the aggregate formation in the toluene/water system. A toluene solution of TPPCOOH (5.0×10^{-5} mol L^{-1}, 1.0 mL) was settled on aqueous solutions (1.0 mL, pH 10 – 13) for 1 hours until the equilibrium reached. UV-Vis spectroscopy indicated that the absorption maximum (λ_{max}) of TPPCOOH in toluene was 420 nm. The TPPCOOH concentration in the toluene phase decreased with an increase in pH (10 – 13) of the aqueous solution. On the other hand, a quite small absorption at 449 nm (λ_{max}) was observed in the aqueous solutions at higher pH, meaning the existence of small amounts of dissociated $TPPCOO^-$ in the aqueous phase. These facts suggested that large amounts of TPPCOOH moved to the toluene/water interface at the higher pH. Microspectrophotometry under an optical microscope showed that the absorption maximum of the interfacial $TPPCOO^-K^+$ was 451 nm. The red-shift of the Soret band from 445 nm to 451 nm indicated the formation of J-type aggregates of $TPPCOO^-K^+$ at the interface. Further measurements using the optical microscope revealed that needle-shaped microdomains of $TPPCOO^-K^+$ aggregates were formed as shown in Figure 1. The shape and size of the aggregates are independent of K^+ as counterions. The dependency of absorbance of the aggregates on the polarization direction of polarized light indicates the ordered assembling of $TPPCOO^-K^+$ in the aggregates.

Keywords: Toluene/water interface, Microspectrophotometry, Polarized light, Porphyrin aggregates, 5-(4-carboxyphenyl)-10,15,20-triphenylporphine, adsorption

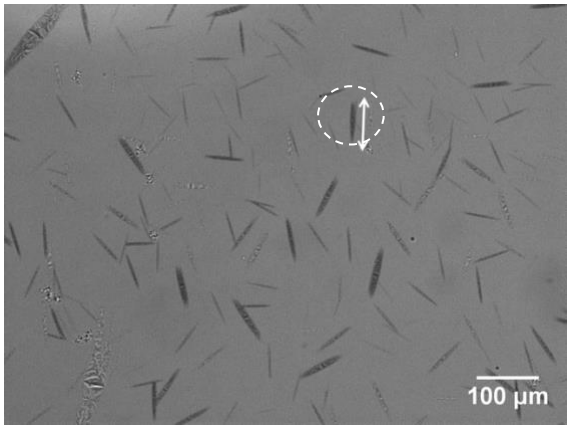

Figure 1: A microscopic picture of $TPPCOO^-K^+$ aggregates at the toluene/water interface after 60 min with a polarized light at 451 nm, which was supplied with a xenon lamp and a monochromator. The polarization direction of the incidence light is shown with a white arrow.

References:

1. Kamiya, Y., Tsukahara, S., Fujiwara T., (2007) Ordered Microdomain of Diprotonated Tetraphenylporphine Aggregate Formed at Dodecane/ Aqueous H_2SO_4 Interface Measured by Microspectrophtometry, *Chem. Lett.*, 36, 344-345
2. Zhou, M., Ouyang, S., Liu, Z., Lu, G., Gao, S., Li, Z., (2009) Orientation Change of Porphyrin in Aggregates Caused by Counterion, *Vib. Spectrosc.*, 49, 7-13.

Fundamental Analysis of Lignin Molecular Binding Mechanism using Surface Forces Apparatus (SFA)

D. Lee [1,*], Y. Song [1], S. Lee [1], J. Park [1], H. Kwon [1], J. Lee [1], C. Lim [1]

[1] School of Energy and Chemical Engineering, Ulsan National Institute of Science and Technology, Ulsan, Republic of Korea

Abstract:
Lignin has been spotlighted as an abundant biorenewable resource in various industries. Consequently, studies on the molecular binding mechanism of lignin became essential to develop optimal design of lignin into higher-valued products. In this study, interaction forces between lignin nanofilms were directly measured using a surface forces apparatus (SFA) at various concentrations of electrolyte solution.[1] The obtained results were analyzed by DLVO and hydrophobic theories. Additional measurements between CH_3-SAM and lignin film confirmed that hydrophobic interaction dominated overall interaction of lignin film. Furthermore, lignin incorporated hydrophobic composites showed enhanced compressive strength, which validated lignin as a reinforcing binder without the addition of other polymeric materials. As the salt concentration increased, the compressive strength of the composite decreased, which corresponds to adhesion force decrease with increasing salt concentration, measured with SFA.

Keywords: lignin, surface force apparatus, DLVO theory, hydrophobic interaction, composite

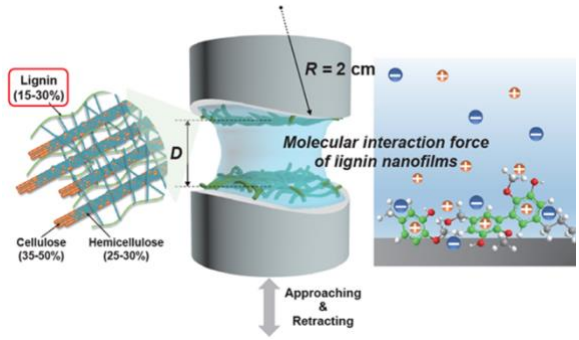

Figure 1: Figure illustrating the schematic of Surface Forces Apparatus set-up for measuring interaction forces between lignin nanofilms

References:

1. Song, Y., Park, J., Lim, C., Lee, D. (2020) In-depth study of the interaction mechanism between the lignin nanofilms: Toward a renewable and organic solvent-free binder, *ACS Sustain. Chem. Eng.*, 8, 362-371.

General Trends in Core-shell Preferences of Bimetallic Nanoparticles

N. Eom, M. E. Messing, J. Johansson and K. Deppert

Solid State Physics and NanoLund, Lund University, Box 118, 22100 Lund, Sweden

Abstract:
Bimetallic nanoparticles have gathered considerable attention in various thin film surface coating applications related to optical sensing, photocatalysis, photovoltaics, and biomedical research.[1, 2] Different types of structure of bimetallic nanoparticles (e.g., core-shell, mixed) can be advantageous or undesirable depending on the applications. However, the fundamental understanding of the equilibrium structure of such particles is still not complete, and hence development of new bimetallic nanoparticles is normally built on a trial-and-error approach. Here we present general trends and governing factors of morphology preference for 45 bimetallic nanoparticle systems studied by molecular dynamics (MD) and Monte Carlo (MC) simulations.[3]
Simulations were performed using LAMMPS code and the embedded-atom method (EAM) potentials were employed for simulating the interactions between atoms in the bimetallic nanoparticle systems composed of 10 metals; Ag, Cu, Au, Pd, Fe, Co, Ni, Pt, Al, and Mo. In order to quantify the core-shell preference, the MD/MC results were analysed to identify surface atoms using the alpha-shapes method. The core and shell compositions of the preferred equilibrium structures of the bimetallic combinations were then used to categorize each combination into one of four different types depending on the level of core-shell tendency: mixed, core-shell, highly segregated core-shell, or Janus-like (Figure 1).
The categorized MD/MC results were analysed using principal component analysis (PCA) and linear discriminant analysis (LDA) to determine the primary factors that dictate core-shell tendency. Eight possible factors were considered, and cohesive energy and atomic radius are found to be the two primary factors that have an 'additive' effect on the core-shell preference in the bimetallic nanoparticles studied. In the majority of the investigated combinations, the element with higher cohesive energy has smaller atomic radius and tend to occupy the core. Highly segregated structures (highly segregated core-shell or Janus-like) are expected to form when both the relative cohesive energy difference is greater than ~ 20 % and the relative atomic radius difference is greater than ~ 4 %. However, when the element with higher cohesive energy has larger atomic radius, the core-shell tendency decreases. The general trend observed in the current study can be used as a guide in nanoparticle synthesis methods[4] and in predicting the equilibrium structures of bimetallic nanoparticles to optimize the properties of thin films made of such particles.

Keywords: bimetallic nanoparticles, core-shell nanoparticles, molecular dynamics, principal component analysis, linear discriminant analysis

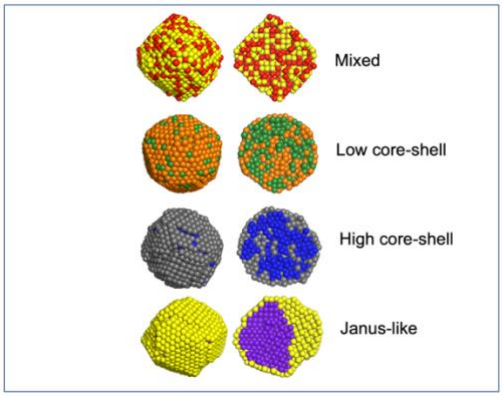

Figure 1: Four different types of bimetallic nanoparticle structures found in the combined molecular dynamics (MD) and Monte Carlo (MC) simulations for 1 : 1 composition; mixed, low level of core-shell, high level of core-shell, and Janus-like. The cross-sectional view is placed on the right side.

References:

1. C. Zhang, B. Q. Chen, Z. Y. Li, Y. N. Xia and Y. G. Chen, *J. Phys. Chem. C*, 2015, **119**, 16836-16845.
2. M. K. Sharma, R. D. Buchner, W. J. Scharmach, V. Papavassiliou and M. T. Swihart, *Aerosol Sci. Technol.*, 2013, **47**, 858-866.
3. N. Eom, M. E. Messing, J. Johansson and K. Deppert, *ACS Nano* 2021, Accepted
4. M. Snellman, N. Eom, M. Ek, M. E. Messing and K. Deppert, *Nanoscale Advances* 2021, Accepted

Zr alloy protection against high-temperature oxidation: coating by a double-layered structure with active and passive functional properties

I.Kratochvílová,[1,2,*] J. Škarohlíd,, R. Škoda, P. Ashcheulov[1,2]

[1]Institute of Physics of the Czech Academy of Sciences, Na Slovance 2, CZ-182 21, Prague 8, Czech Republic
[2]Czech Technical University in Prague, Czech Institute of Informatics, Robotics and Cybernetics, Jugoslávských partyzánů 1580/3, Prague 6, CZ-160 00, Czech Republic
*corresponding author: krat@fzu.cz, +420 723 814 810

Abstract:
In this work, a new strategy for protecting metal surfaces against degradation caused by high-temperature oxidation is presented. We were the first to prepare a double-layered coating consisting of an active and passive part as a protective element for Zr alloy surface against high-temperature oxidation in a hot water environment. ZIRLO nuclear fuel cladding was protected against oxidation in water-cooled nuclear reactors by coating with a double layer consisting of an active 500 nm thin nanocrystalline diamond (NCD) layer (bottom) and a passive 2 μm thin CrAlSiN (upper) layer [1-3].
Double-layer coatings reduce ZIRLO nuclear fuel tube oxidation by more than 88% compared to that of uncoated ZIRLO tubes treated for 4 days in 400 °C hot steam. This result also confirms good adhesion of CrAlSiN coating both to ZIRLO surface and to NCD coated ZIRLO surface [3].
At the initial oxidation stage (<10 minutes) in the 1000°C hot steam furnace, CrAlSiN acted as a barrier against surface oxidation. The corrosion of bare ZIRLO and NCD coated ZIRLO was similar as carbon diffusion from NCD coating just begins and does not significantly affect oxidation kinetics of zirconium alloy. On the contrary, CrAlSiN and double layer coating at this initial stage importantly affect the typical oxidation kinetics of zirconium –mainly due to small amount of defects in CrAlSiN coating However, for longer oxidation times (>10 minutes) in the 1000°C hot steam furnace the oxidation of CrAlSiN-coated ZIRLO was higher than the oxidation of ZIRLO coated with a double layer as the CrAlSiN coating was typically more cracked. At this stage carbon from NCD coating diffuse into growing ZrO_2 layer and by changing its electrical properties decrease ZIRLO corrosion.
In our case, the bottom NCD water-permeable coating served as the active antioxidation element. During high-temperature treatment, carbon incorporation into Zr alloy nuclear fuel cladding tubes changed the physical, chemical and structural properties, which worsened the conditions for the Zr alloy oxidation process. The water-impermeable top CrAlSiN coating passively prevents physical contact of the Zr cladding tube surface with hot steam.

Keywords: zirconium alloys high temperature corrosion, nanocrystalline diamond protective coating, CrAlSiN protective coating

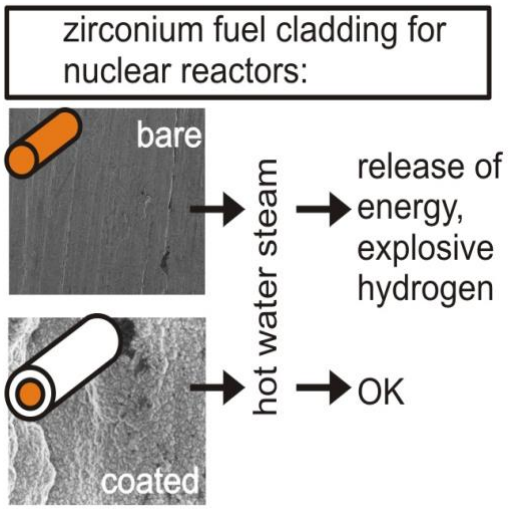

Figure 1: Nuclear fuel protection against corrosion: nanocrystalline diamond coating combined with CrAlSiN coating

References:

1. J. Skarohlid et al: Scientific Reports, 7 (2017) 14.
2. P. Ashcheulov, Applied Surface Science, 359 (2015) 621-628.
3. I. Kratochvilova et al.: Corrosion Science, https://doi.org/10.1016/j.corsci.2019.108270

Penetration behaviour of different blasting particles at composite peening

M. Seitz[1*] ,K. A. Weidenmann[2]

[1] Karlruhe Institute of Technology (KIT), IAM-WK, Karlsruhe, Germany
[2] Augsburg University, Institute of Materials Resource Management, Augsburg, Germany

Abstract:
Composite peening is a new peening process designed to introduce ceramic particles into a metal matrix close to the surface layer [1]. The reinforcement rate decreases with increasing surface distance. This graded layer can be locally embedded by the process.
Due to the high particle velocity and high process temperatures, penetration depths of up to 40 µm have been achieved. In addition to process parameters such as pressure, feed rate and temperature, the shape and size of the beam particles influence the thickness of the ceramic layer. Another important factor is the material of the particles. The differences are illustrated in Fig. 1.: the highest penetration depth can be achieved with tungsten carbide as blasting particles (c). While aluminium oxide (a) also forms a ceramic layer, silicon carbide (b) is hardly introduced into the aluminium matrix.
It can also be observed that a high percentage of the particles are significantly smaller than their initial size of 10 µm after the process. This fragmentation is most likely due to the repeated impact of the blasting particles.
This study quantifies the penetration depth of different blasting materials with equal process parameters.

Keywords: composite peening, penetration behavior, particle fracturing.

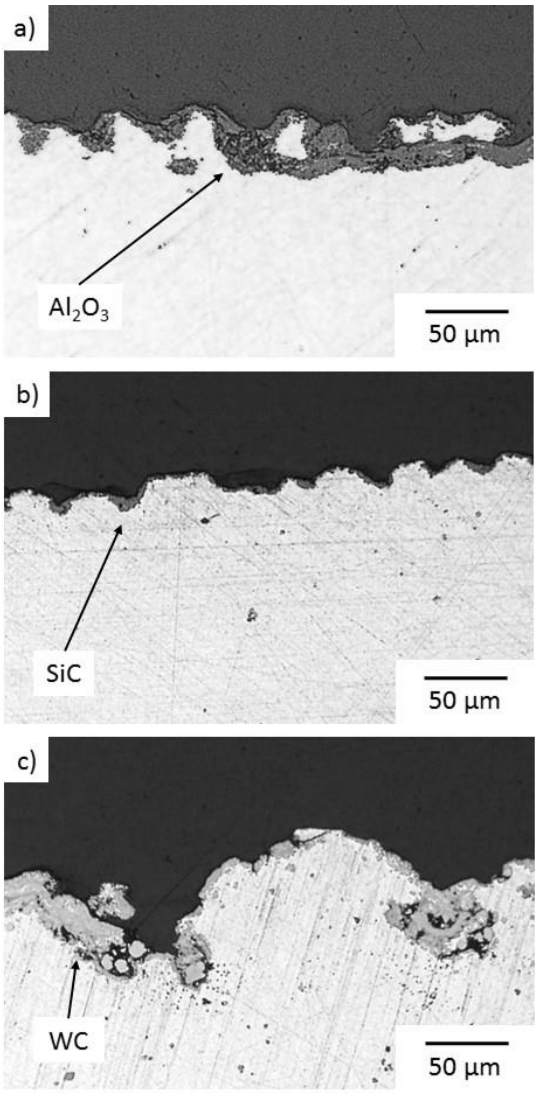

Figure 1: Surface layer after composite peening with different blasting material. (a) Aluminiumoxid, (b) Siliciumcarbid, (c) Wolframcarbid [2].

References:

1. Seitz, M., Reeb, A., Klumpp, A., Weidenmann, K. A. (2017) Composite Peening – A Novel Processing Technology for Graded Reinforced Aluminium Matrix Composites, *Key Engineering Materials*, 742, 137-144.
2. Seitz, M., Weidenmann, K. A. (2019) Mechanical Investigations on Composite Peened Aluminium, *International Conference on Advanced Surface Enhancement*, Springer, 10-18.

A new method for testing the abrasive wear of cementitious materials loaded with a spinning wheel

S. Czarnecki [1], K. Krzywiński[1,*], M. Moj[1], A. Chowaniec[1], Ł. Sadowski[1]

[1] Department of Building Engineering, Wroclaw University of Science and Technology, Wroclaw, Poland

Abstract:
Currently, commonly used and standardized methods of investigating the absrasive wear are: the Böhme abrasion test, the British Cement Association standard test, and the Rolling Wheel Abrasion method [1]. The paper describes a new method for determining the abrasive wear of cementitious materials. The novelty of the paper is to describe the wear mechanism occurred due to a loaded spinning wheel that is not moving in any direction during the test (Figure 1).

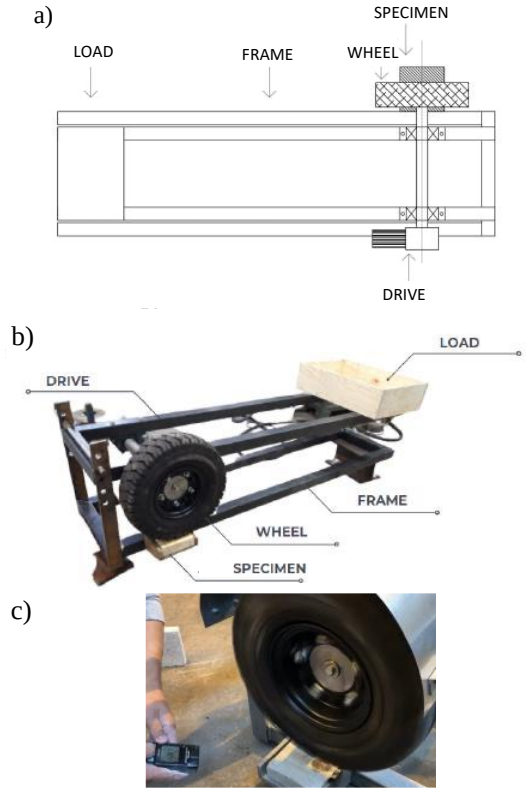

Figure 1: The method for testing the abrasion resistance of the cementitious materials loaded with a spinning wheel: a) top view scheme of the device; b) prototype of the device; c) measurement of the temperature on the specimen's surface after the spinning of the wheel.

The device can also be used to analyze the changes in the surface morphology and the temperature of cementitious materials caused by the loaded spinning wheel [2]. Therefore, a temperature changes during measurements after the spinning of the wheel on the cementitious surfaces together with the surface morphology measurements were presented. The changes of the temperature and the values of surface morphological parameters are presented in Figure 2.

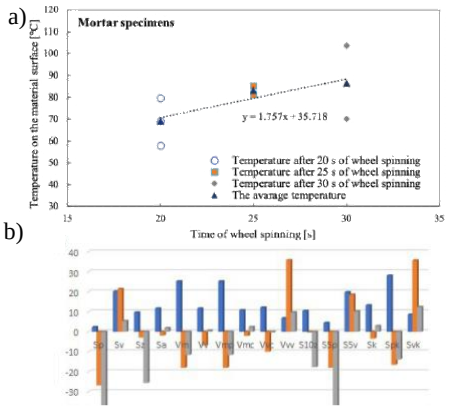

Figure 2: Changes of: a) the temperature and b) the morphological parameters during the test

Acknowledgement
The authors received funding from the project supported by the National Centre of Science, Poland [grant no. 2019/35/O/ST8/01546

Keywords: abrasion resistance test; cementitious materials; thermal analysis; floor.

References:

1. Hulett, T. (2013), Abrasion resistance of warehouse floors, *Concrete*, 47, 53-54,
2. Torres, H. et al. (2016), Experimental simulation of high temperature sliding contact of hot rolled steel, *Tribology International*, 93, 745-754.

The effect of the addition of granite powder to the primer on the pull-off strength of epoxy resin coatings

Ł. Kampa[1], Ł. Sadowski[1]

[1] Wroclaw University of Science and Technology, Wybrzeże Wyspiańskiego 27, 50-370 Wroclaw, Poland

Abstract:
Currently, there are many attempts to increase the pull-off strength of epoxy coatings. This can be, for example, achieved by appropriate treatment of the surface of a concrete substrates, such as surface mechanical treatment or texturing [1]. In the authors opinion, a simpler method is the modification of the composition of the resin. There are some examples in this regard. These examples include the addition of SiO2, graphene, natural fibers, and granite powder [2, 3]. However, mostly this modification is related to the epoxy resin used as the final finishing layer of coatings, while the primer seems to be the layer more directly related to the adhesive properties of epoxy resin coatings. Moreover, there is currently no research related to the modification of the primer by granite powder and its effect on the pull-off strength of epoxy resin coatings. The place of its application in this study is shown in Figure 1.
In this research, the primer was modified using the granite powder in the amount ranging from 10% to 60% in relation to the mass of the resin. A reference sample was also made to compare the obtained results. For each configuration, the pull-off strength tests of the epoxy resin coating were assessed and the obtained results were compared with the reference sample. The highest pull-off strength of the coating was observed for the primer with the addition of 20% of granite powder (increase by 18% compared to the reference sample) and 10% of granite powder (increase by 11%). The addition of 30% of granite powder caused a slight increase, while the rest of the results reduced the adhesion. Finally, an economical analysis will be presented to show the benefits of the developed technology.

Keywords: resin floors, pull-off strength, granite flour.

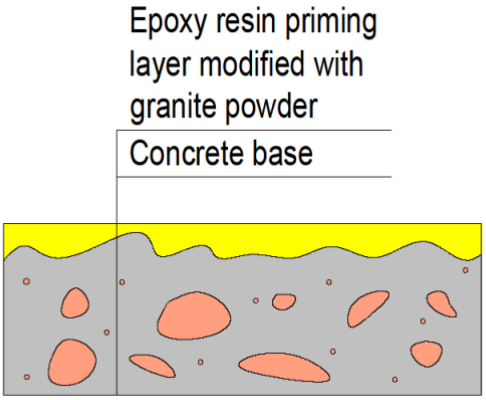

Figure 1: A cross-section of a typical resin coating that was modified during the test

References:

1. Krzywiński, K., Sadowski, Ł. (2019), The effect of texturing of the surface of concrete substrate on the pull-off strength of epoxy resin coating. *Coatings*, 9, 143.
2. Pourhashema, S., Vaezia, M., Rashidib, A. (2017), Investigating the effect of SiO2-graphene oxide hybrid as inorganic nanofiller on corrosion protection properties of epoxy coatings. *Surf. Coat. Technol*., 311, 282–294.
3. Madhusudhan, B., Meenakshi, R., Madhu Sudan, D., Ananthakrishna, N., Venkateshwar, P., (2017), Development and characterisation of Cordia Dichotoma Fibre / Granite filler reinforced polymer blended (Epoxy/Polyester) hybrid composites*Advances in Materials and Processing Technologies*,

Self-protective Paste Nitriding Process of AISI 304 SS for Sea Water Applications

G. Vargas,* L. López

Center for Research and Advanced Studies (Cinvestav), Saltillo, México

Abstract:
Seawater is a complex mixture containing different salts, dissolved gases, trace elements, suspended solids, decomposed organic matter, and living organisms. As such, seawater can be an aggressive medium. For most metal alloys, it can cause wear and corrosion. Furthermore, the wear and corrosion behavior of metals in seawater is largely influenced by the oxygen content, seawater currents velocity, temperature, pollution, and marine organisms. Stainless steels in seawater, require then, high resistance to wear without their corrosion deterioration. Most research looking for stainless steels with high erosion-corrosion resistance have been oriented to develop the surface formation of expanded austenite (a nitrogen- or carbon-supersaturated stainless steel) without the precipitation of chromium carbides at the grain boundaries. This aim has been achieved via low-temperature (<450 ºC) plasma nitriding [1,2]. However, their initial investment, the degree of control required, their maintenance and operation expenses and their limitations for treatment of big size parts and the skill level required from operators difficult the widespread dissemination of this technology. Conventional liquid nitriding (above 580 ºC) can improve the surface hardness and tribological properties of stainless steels. However, corrosion resistance is significantly decreased due to the precipitation of chromium nitrides or chromium carbides. This process is therefore not applicable for the improvement of the erosion-corrosion resistance of stainless steels under sea water [3]. The main objective of the present work is to propose and evaluate a new nitriding process by a self-protective paste to simultaneously increase the erosion-corrosion resistance of stainless steels.

The nitriding of AISI 304 stainless steel was studied using a mixture of sodium cyanate and sodium carbonate salts. This self-protective paste was applied on previously polished steel substrates to increase simultaneously their hardness and their pitting corrosion resistance. Nitriding treatments (540 °C for 3 to 20 minutes and 450 ºC for 2 to 5 hours) were studied to evaluate the formation of the expanded austenite and the precipitation of chromium nitrides and carbides. Characterization of the materials was carried out using XRD and SEM/EDS. The corrosion resistant was evaluated in a solution of synthetic seawater using potentiodynamic polarization and electrochemical impedance spectroscopy. The hardness was evaluated in cross section by Vickers indentation and the wear resistance of the surface by Pin-on-Disc testing.

Both, nitriding time and temperature played an important role in the surface modification of the stainless steel, in terms of the nature of phases formed, thickness of layers, hardness and corrosion properties of treated samples. Treatment times longer than 10 minutes at 540ºC was detrimental for the stabilization of the expanded austenite and to avoid the precipitation of chromium nitrides and carbides. The nitriding at 540 ºC for 10 minutes and the nitriding at 450 ºC for 5 hours, both improved 3 times the hardness of the AISI 304 SS samples without treatment. Under these conditions, the use of self-protective pastes of sodium cyanate and sodium carbonate also allowed the development of a surface microstructure of the samples based on expanded austenite without precipitation of chromium nitrides and carbides, improving then their pitting corrosion.

Keywords: Self-protective paste, nitriding, 304 and 316L stainless steels, corrosion and wear, sea water.

References

1. Zhang Z. L., Bell T. (1985), Structure and corrosion resistance of plasma nitride stainless steel, *Surface Engineering*, 1:2, 131-136.
2. Bell T. (2002), Surface engineering of austenitic stainless steel, *Surface Engineering* 18:6, 415-422.
3. Jianj L., Luo H. and Zhao C. (2018) Nitrocarburising of AISI 316 stainless steel at low temperature, *Surface Engineering* 34:3, 205-210.

Amorphous carbon nitrogen-modified layers for light emitting diodes

K. Dyndał [1,*], G. Lewińska, J. Sanetra [2], S. Kluska, K.W. Marszalek [1]

[1] Institute of Electronics, AGH University of Science and Technology, Al. Mickiewicza 30, 30-059 Kraków, Poland
[2] The author Jerzy Sanetra is retired.
[3] Faculty of Materials Science and Ceramics, AGH University of Science and Technology, Al. Mickiewicza 30, 30-059 Kraków, Poland
*Corresponding author: kkoper@agh.edu.pl

Abstract:
The rapid development of organic light-emitting diode technology begin after 2000 and still is in progress. Now, organic light-emitting diodes are a major technology in the manufacture of flat panel displays and for lighting. Screens based on OLED technology are characterized by unique properties such as energy savings, wide viewing angle, fast response, high contrast and high color purity. Unfortunately, OLEDs are not without disadvantages. The main problem with OLEDs is their aging, which can be caused by many factors such as atmospheric and operating conditions. The most important cause of OLED aging is the influence of moisture and oxygen. In the world literature one can find many publications describing the influence of aging processes on OLEDs and the degradation mechanisms, however, despite this fact, the scientific area has not been sufficiently understood yet. Currently, the best option to prevent aging seems to be encapsulation or the use of materials with low water vapour and air penetration. Layered technologies are highly promising for materials and devices exposed to environmental factors such as water vapour and oxygen. In this work prompted us to investigate the possibility of using hydrogenated amorphous carbon nitrogen-modified (a-C:N:H) leyer as protective passive coatings for organic LEDs. The layers were deposited on the active polymer layer and as a stand-alone active layer in the devices by plasma-assisted chemical vapour deposition, with 13.56 MHz. As previously reported, the lifetime of the diodes is more stable by obtaining them in a plasma-purged vacuum chamber due to the absence of impurities in the reaction atmosphere. In the present study different types of the OLEDs architectures were prepared and subjected to further studies of the current-voltage and electroluminescent-voltage characteristics: glass/ITO/PVK /Ca/Al, diodes with glass/ITO/PVK/a-C:N:H layers/Ca/Al and glass/ITO/a-C:N:H layers/Ca/Al layers. The UV and VIS spectroscopy studies have been carried out for the investigated hydrogenated amorphous carbon nitrogen-modified leyer. The absorption bands and maxima were determined. Photoluminescence was confirmed and the fluorescence spectra of the layers obtained. The optical properties and stability of the layers were measured using spectroscopic ellipsometry. The influence on the gradient structure of the layers by spin-coated polymer film was analysed. The influence of organic solvents and water on the dispersion dependence of the refractive index and extinction coefficient were also determined. The investigated layers turned out to be resistant to solvents and water, which is a promising result in the context of the layers application in OLEDs technology.

Keywords: a-C:N:H leyer, RF PACVD, light emitting diodes, electroluminescence, UV-Vis spectroscopy

Acknowledgements: This research was supported by the Polish National Science Center project No. UMO-2017/27/N/ST8/01611.

References:

1. Low, J.Y., Aljunid Merican, Z.M., Hamza, M.F. (2019) Polymer light emitting diodes (PLEDs): An update review on current inovation and performance of material properties, in: *Mater. Today Proc., Elsevier Ltd.*, 1909-1918.
2. Scholz, S., Kondakov, D., Lüssem, B., Leo K. (2015), Degradation mechanisms and reactions in organic light-emitting devices, *Chem. Rev*. 115, 8449-8503.
3. Jaglarz, J., Dyndał, K., Tkacz-Śmiech, K. (2019), Thermo-optical properties of hydrogenated amorphous carbon and nitrogen-modified carbon layers from in situ ellipsometric studies, *J. Mater. Res. Technol.*, 9, 1698-1707.

Electrostatic discharge behaviors of Diamond-like Carbon on Alumite

S.Yamamoto[1], H.Ezaki[2)]

[1)]Japan Coating Center Co., LTD., Kanagawa, Japan
[2)]TOEI Denka Kogyo Co.,LTD. Kanagawa, Japan

Abstract:
Electrostatic Discharge (ESD) and tribrogical behaviors of Diamond-like Carbon (DLC) on an alumite were investigated. The electrostatic is accumulated on insulators such as an alumina or plastics during sliding motion and a spike ESD at a few nsec, which induces high voltage or high current, causes a fatal damage on semiconductor devices when they are close to touch[1)]. The ESD causes not only yield drop of semiconductor production but also malfunction due to the electromagnetic interference. A DLC coating is one of excellent solutions for the semiconductor equipment struggled with ESD problems because the DLC has slow discharge properties[2)] as well as excellent tribological properties such as low coefficient of friction (COF), high hardness and good corrosion resistance. An alumite is an important surface treatment for an aluminum to enhance hardness and anticorrosion properties. A serious amount of aluminum members with alumite treatment are used to build the semiconductor equipment. Because alumites would be considered to accumulate electrostatic due to the Al_2O_3 matrix there could be fraught with ESD risks. It was investigated how DLC coatings can improve the ESD protection for alumites as well as tribological properties.
Two types of alumite at 15 μm thickness were anodized on A5052 aluminum substrates in sulphate and oxalic acid baths. The DLCs at 2 μm were deposited on alumites by Plasma-Immersion Ion Implantation (PIII) using C_2H_2 gas. The sheet resistances of alumites and the DLC on the alumites measured by a high resistance meter (Trek Model 152) were approximately $10^{10}\Omega$ for both alumites and $10^{9}\Omega$ for the DLC on alumites. The ESD behavioures of the specimens were measured by a static honest-meter (Shishido Electrostatic H0110). After exposed corona discharge at -10 kV in 30 secs the surface voltage decay was monitored.
Electrostatic on both alumites were disappeared instantly in spite of the high sheet resistance. For the DLC on alumites slow charge and discharge was observed as shown in Fig.1. The DLC coatings on the alumites improved COF at 0.2 compared with the alumite itself at 0.85 against SUJ2(E52100) as shown in Fig.2 as well as the breakdown voltage and hardness.

Keywords:Diamond-like carbon (DLC), alumite, electrostatic discharge (ESD), slow discharge,

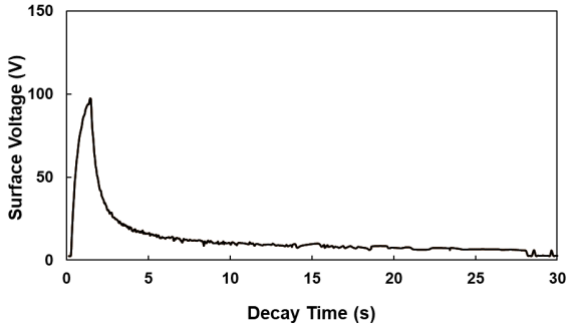

Figure 1: Discharge decay curves of the electrostatic for a DLC on sulphate alumite.

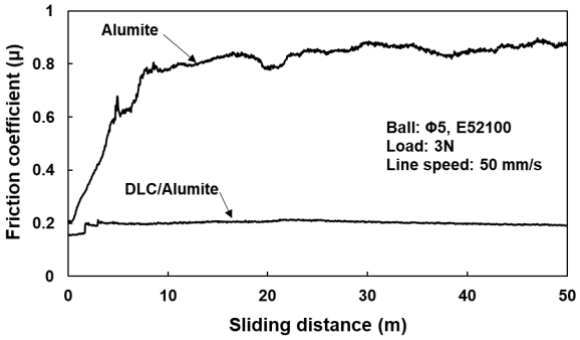

Figure 2: COF of alumite and DLC on alumite against SUJ2(E52100)

References:

1. IEC IS 61340-5-1: Protection of electronic devices from electrostatic phenomena-General Requirements.
2. S.Yamamoto, T.Nonaka, Protective properties of DLC coatings against electrostatic discharge damage, Thin Solid Films in press

Abnormal Aging and Recovery Processes in Perovskite Solar Cells with Metal Electrodes

Dong Geon Lee,[1*] Min-cheol Kim,[2] Shen Wang,[2] Byeong Jo Kim,[1,3] Ying Shirley Meng,[2,4] Hyun Suk Jung,[1]

[1] School of Advanced Materials Science & Engineering, Sungkyunkwan University, Rep. of Korea
[2] Department of NanoEngineering, University of California, California 92093, USA
[3] Department of Chemistry, Ångström Laboratory, Uppsala University, Uppsala, Sweden
[4] Materials Science and Engineering Program, University of California,, California 92093, USA

Abstract:
Perovskite solar cells (PSCs) have been rapidly improved in their energy converging performances, currently exhibiting up to 25.2 % of power conversion efficiencies (PCEs). Despite their great performances, they still suffer from various issues such as stabilities and scaling-up problems. PSCs struggle to maintain their performance owing to fast chemical decomposition or performing instability caused by hysteretic behavior or ion migration. Large-area perovskite film fabrication and cost problems of electrodes should be resolved for practical photovoltaic application. Among present problems, electrode selection is one of most important assignments in solving both hurdles for commercialization because the most popular metal electrodes, Au or Ag, are instable chemically and it is too much expensive to be used in mass production system, especially Au electrode. PSCs with Ag electrode performs low PCEs with low open circuit voltage and fill factor showing an s-shape kink in current density-voltage (J-V) curves at first (Figure 1). However, with aging time, the performance of PSCs recovers to the normal level and such abnormal performing instability can be a huge obstacle for commercial application of Ag electrode. The s-shape J-V curves are mainly attributed to inferior majority charge carrier extraction from the photo-absorbing area to the cathode or anode, however, the underlying reason for these phenomena, especially for the abnormal aging and recovery mechanism in PSCs with Ag electrode has not been elucidated at all. It is important to understand the origin of the s-shape J-V curves of PSCs with Ag electrode at early stage and the mechanism of aging and recovery phenomena with elimination of s-shape for securing the possible use of Ag electrode in commercialized PSCs.
Here in this work, we present the different time-dependent performance change trends of PSCs with regard to metal electrodes (Au and Ag). PSCs with Ag electrode exhibit a clear s-shape J-V curves in early stage, however they recover to their best performance with 12 h of aging time. On the other hands, PSCs with Au electrode exhibit their best performance from the beginning. In order to clarify this abnormal aging and recovery process in PSCs with Ag electrode, we also investigate the time-dependent carrier dynamics alteration by photo-luminescence behaviors which proves the performance changes with aging time. By the measurement and simulation results, we are able to verify that the work function difference between Ag electrode and hole transport materials, Spiro-MeOTAD, induces a significant injection barrier for holes, and it clearly cause the formation and alleviation of the s-shape J-V curves in PSCs with Ag electrode. We finally address the potential of Ag electrodes for commercial use by demonstrating highly stable PSCs with Ag electrode for durations exceeding 350 h under light-illumination, which is close to the results of PSCs with Au electrode.

Keywords: perovskite solar cells, hole injection, work function, interfacial reaction, metal electrodes.

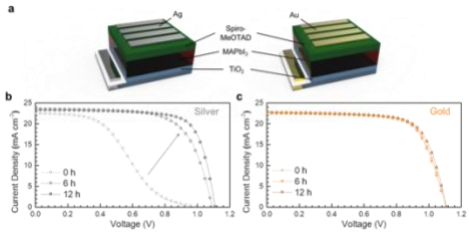

Figure 1: Different aging behavior of Perovskite solar cells depending on metal counter electrode (a) Perovskite solar cell device structure ($FTO/TiO_2/MAPbI_3$/Spiro-MeOTAD/Ag or Au) and time evolution plot of J-V curves for perovskite solar cells with (b) Ag and (c) Au for their metal counter electrode for different aging time (0, 6, 12 h).

References:

1. Best Research-Cell Efficiencies. https://www.nrel.gov/pv/assets/pdfs/best-

research-cell-efficiencies.20191106.pdf
(accessed 01/12).

Mechanisms for electron emission in ion surface interactions

P. Riccardi

Dipartimento di Fisica, Università della Calabria and INFN- Gruppo collegato di Cosenza
Via P. Bucci cubo 33C, 87036 Arcavacata di Rende, Cosenza, Italy
e-mail: Pierfrancesco.riccardi@fis.unical.it

Abstract:
Electron emission from surfaces by slow ions is of crucial importance in determining the properties of electrical discharges. Ion-induced electron emission from solids is generally attributed to the two main processes [1] of In kinetic electron emission (KEE) and potential electron emission (PEE), depending on the source of excitation energy.
Studies of KEE are often performed under sufficiently selective experimental conditions to isolate the effect under consideration or focus on individual processes revealed by the experiments. Although this clarifies the basic physics of each emission mechanism, it leaves open the question of the interplay between different electron excitation and emission phenomena.
In this work, we deal with the complexity of the interactions leading to electron emission induced by atomic particles by studying electron emission in the interaction of Ne^+, Ne^+, Na^+, Ar^+, Kr^+ ions with Al surfaces at impact energies below a few keV. For this projectile-target systems, several emission processes are known to occur [2,4], including electron promotion and inner shell excitation of projectiles and target atoms, bulk plasmon excitation, and emission below the promotion threshold (fig.1). Our goal is to clarify the role of the observed emission mechanisms, when they concur in determining the behaviour of electron emission yields with incoming ion velocity.

Keywords: Plasma Surface Interactions, Secondary Electron Emissions, Auger Electron Emissions, Ion Scattering, Noble Gases, Aluminum

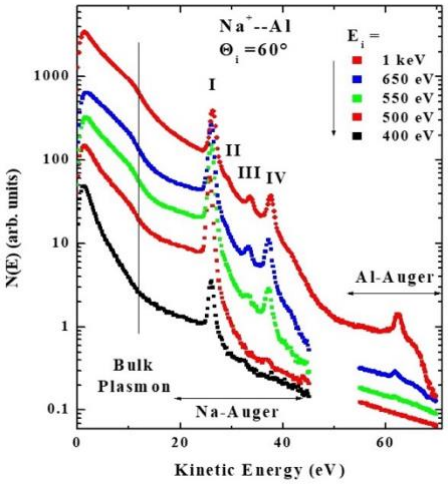

Figure 1: Energy spectra of electrons emitted from the Al surfaces under the impact of Na^+ ions at varying incident ion energy for fixed incidence angle $\Theta_i = 60°$. The spectra have been arbitrarily displaced on the vertical scale for clarity.

References:

1. R.A. Baragiola and P. Riccardi in Reactive Sputter Deposition – edited by D. Depla and S. Mahieu - Springer Series in Material Science – Vol. 109 – 2008 – Chap.2
2. P Riccardi, RA Baragiola, CA Dukes Phys. Rev. B 92, 045425 (2015)
3. P. Riccardi, F. Cosimo, A. Sindona Phys. Rev. A 97 032703 (2018)
4. M. Minniti et al. Phys. Rev. B 75, 045424 (2007)

SurfCoatKorea 2021 Session III.B:

Bio-interfaces/ Biomedical/ Bioactive surfaces and coatings

Atomic Layer Deposition of Noble Metals with Low Concentration Ozone

Abstract

Noble metal thin films have several potential applications in electronics, protective coating, and catalyst industries. The atomic layer deposition (ALD) of noble metal films are currently achieved using either oxygen or hydrogen as precursors or annealing agents, requiring high temperatures leading to increased risks of explosion and fire. ALD methods not using oxygen or hydrogen as precursors or annealing agents have so far resulted in noble metal oxides instead of pure metal films. An ALD process has been developed for noble metal thin films preparation utilizing low concentration ozone (1.22 g/m^3) as a reactant, without the need for any oxygen or hydrogen. This process has been successfully demonstrated for the fabrication of Rhodium (Rh) and Palladium (Pd) thin films. Both metal films exhibited extremely uniform surface with the root mean square (RMS) surface roughness below 0.2 nm. The 20 nm thick metal films had very low resistivity of 12μΩ cm for rhodium and 63 μΩ cm for palladium, showing the deposited metal films had a high purity. The reaction mechanism of palladium ALD from $Pd(hfac)_2$ and low concentration ozone was also studied by density functional theory (DFT). The simulation results show that $Pd(hfac)_2$ dissociative chemisorbed on Si (100) surfaces. Subsequently, ozone reacted with Pd(hfac)* by cleaving its C-C bond to produce gaseous oxygen and adsorbed CF_3-OC and CF_3-CO-CHO with a relatively low activation barrier. Hence, the reaction was kinetically favourable. The adsorbed complex carbide was then depleted by the excess ozone. The calculated results reveal that pure palladium can be prepared by $Pd(hfac)_2$ and ozone in low concentration without oxygen or hydrogen. All the results indicate that this low concentration ozone based ALD process could yield high quality noble metal films in low temperature and safer way.

Development of Electrically Activable Phosphonium Self-Assembled Monolayers to Efficiently Kill and Tackle Bacterial Infections

S. Auditto[1*], S. Carrara[1], F. Rouvier[2], F. Brunel[1], C. Janneau[3], M. Camplo[1], M. Sergent[4], I. About[3], J.-M. Bolla[2], J.-M. Raimundo[1*]

[1] Aix-Marseille Univ, CNRS, CINAM, Marseille, France.
[2] Aix-Marseille Univ, INSERM, SSA, IRBA, MCT, Marseille, France.
[3] Aix-Marseille Univ, CNRS, ISM, Inst Movement Sci, Marseille, France.
[4] Aix-Marseille Université, Avignon Université, CNRS, IRD, IMBE, Marseille, France.

Abstract:
Bacterial infections are one of the major threats to public health, food safety and development today which makes it urgent to combat by developing materials or strategies limiting or preventing these bacterial proliferations and biofilm infections.[1] Although, medical implants have led to dramatic improvement in patient's health and well-being, there are often drawbacks that include surgical risks during placement or removal, implant failure and more specifically microbial infections. These implant-associated infections are mainly caused by the bacterial biofilm formation in which bacteria are more recalcitrant towards treatments. Indeed, implant surfaces are non-vascularized abiotic materials rendering the common strategies inappropriate and ineffective.[2]
In this context we have designed and developed innovative and smart interfaces based on phosphonium SAMs[1] that can be electrically activated on-demand for eradicating bacterial infections on solid surfaces. Hence, upon electroactivation, using a low potential of 0.2V for 1 hour, a successful stamping out of Gram-positive and Gram-negative bacteria strains has been clearly highlighted on SAM-modified titanium surfaces. Subsequently, using these conditions, *Staphylococcus aureus* and *Klebsiella pneumoniae* were killed up to 95% and 90% respectively and full eradication if time is prolongated (Fig. **1**). More importantly, no harmful activity has been observed towards eukaryotic cells which clearly demonstrates the biocompatible character of these novel surfaces for further implementation.

Keywords: responsive surfaces, self-assembled monolayers, phosphoniums, electroactivation, biocidal effect.

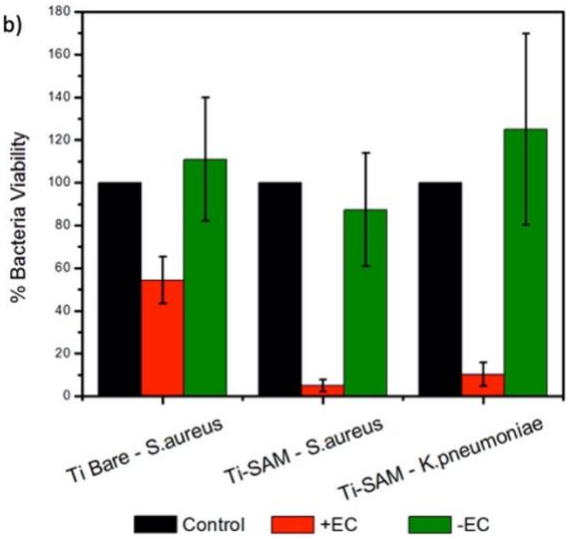

Figure 1: Percentage of viability of bacteria on Ti surface and SAM-modified Ti, upon contact with *Staphylococcus aureus* and/or *Klebsiella pneumoniae* with (+EC) and without electrical activation (-EC).

References:

1. Tacconelli, E.; Carrara, E.; Savoldi, A.; Harbarth, S.; Mendelson, M.; Monnet, D. L.; Pulcini, C.; Kahlmeter, G.; Kluytmans, J.; Carmeli, Y.; Ouellette, M.; Outterson, K.; Patel, J.; Cavaleri, M.; Cox, E. M.; Houchens, C. R.; Grayson, M. L.; Hansen, P.; Singh, N.; Theuretzbacher, U.; Magrini, N. (2018) *Lancet Infect. Dis.*18, 318-327.
2. a) Brunel, F.; Lautard, C.; Giorgio, S.; Garzino, F.; Raimundo, J. M.; Bolla, J. M.; Camplo, M. (2018) *Bioorg. Med. Chem. Lett.* 28, 926-929; b) Brunel, F.; Lautard, C.; Garzino, F.; Raimundo, J. M.; Bolla, J. M.; Camplo, M. (2020) *Bioorg. Med. Chem. Lett.* 30, 127389; c) Raimundo, J.-M.; Camplo, M.; Bolla, J.-M.; Brunel, F.; Lautard, C.; PCT Int. Appl. (2020) WO 2020008000 A1 20200109; d) Carrara, S.;

Rouvier, F.; Auditto, S.; Brunel, F.; Janneau, C.; Camplo, M.; Sergent, M.; About, I.; Bolla, J.-M.; Raimundo, J.-M. (2021) *ACS Appl. Mater. Interfaces* submitted.

Synthesis of 5,15-A_2BC-Type Porphyrins to modify a Field-Effect Transistor for Detection of Gram-Negative Bacteria

L. Neumann[1], L. Könemund[1], F. Hirschberg[1], R. Biedendieck[2], D. Jahn[2], H.-H. Johannes[1,*], W. Kowalsky[1]

[1]TU Braunschweig, Institut für Hochfrequenztechnik, Braunschweig, Germany
[2]TU Braunschweig, Institute of Microbiology and Braunschweig Integrated Centre of System Biology (BRICS), Braunschweig, Germany
[*] Corresponding author. E-mail: h2.johannes@ihf.tu-bs.de

Abstract:
Current biological sensing technologies of bacteria are time consuming, labor intensive and thus expensive. Also their accuracy and reproducibility should be improved. Conventional electrical measurement methods might connect high sensitive sensing systems with biological requirements. One conception is the trapping of bacteria on the gate-electrode surface of a modified field-effect transistor (FET) using porphyin based self-assemled monolayers (SAMs).
Porphyrins as a modifier for these sensing systems are of interest due to their biological compatibility, their fluorescence in visible range, and their chemical stability under ambient conditions. Another advantage is their easy accessibility *via* chemical synthesis.
In this work 5,15-A_2BC-type porphyrins were synthesized originating from a 5,15-diphenylporphyrin with the possibility to connect on a gold surface by linker I (Figure 1). This porphyrin linker showed its ability of SAM formation on the gold electrode surface and proved by well-established methods like UV/Vis spectroscopy, Drop-Shape-Analysis (DSA) or Cyclic Voltammetry (CV). In a second synthesis route linker II (Figure 1) was attached with a peptide or cysteine functionality for trapping of Gram-negative bacteria. It was already shown that this peptide can bind to the outer membrane of Gram-negative *Escherichia coli*.[1] For a verification of the ability of linker II with a peptide or cysteine group to connect to *E. coli*, FLIM (Fluorescence Lifetime Imaging Microscopy) measurements of bacteria stained with the porphyrin were performed.
Conclusively, 5,15-A_2BC-type porphyrins (Figure 1) with the peptide or cysteine group as linker II were applied to a gold electrode surface. In this work DAPI stained *E. coli* were successful immobilized on these porphyrin SAM modified surfaces which was analyzed by FLIM measurements.

Keywords: porphyrin, self-assembled monolayer (SAM), Gram-negative bacteria detection, sensing technologies.

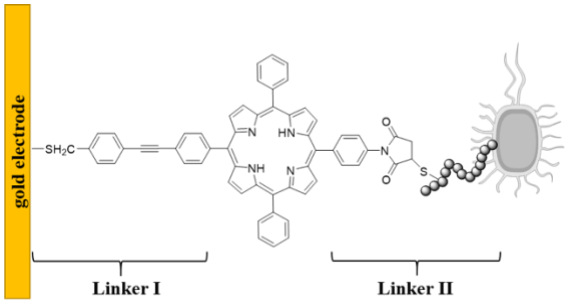

Figure 1: Schematic of the 5,15-A_2BC-type porphyrin attached to a gold electrode surface. Linker I is connected to the gold electrode surface through the sulfur group and linker II acts as a trapper for Gram-negative bacteria through a peptide or cysteine functionality shown here as small beads.

References:

1. Liu, F., Soh Yan Ni, A., Lim, Y., Mohanram, H. Bhattacharjya, S., Xing, B. (2012), Lipopolysaccharide Neutralizing Peptide–Porphyrin Conjugates for Effective Photoinactivation and Intracellular Imaging of Gram-Negative Bacteria Strains, *Bioconjugate Chemistry*, 23, 1639-1647.
2. Sathyapalan A., Lohani A., Santra A., Goyal A., Ravikanth M., Mukherji S., Rao V. R., (2005), Preparation, Characterization, and Electrical Properties of a Self-Assembled meso-Pyridyl Porphyrin Monolayer on Gold Surfaces, *Aust. J. Chem*., 58, 810-816.

Modification of a Field-Effect Transistor for Gram-negative Bacteria Detection Using Porphyrin SAMs

L. Könemund[1], L. Neumann[1], F. Hirschberg[1], R. Biedendieck[2], D. Jahn[2], H.-H. Johannes[1,*], W. Kowalsky[1]

[1]TU Braunschweig, Institut für Hochfrequenztechnik, Braunschweig, Germany
[2]TU Braunschweig, Institute of Microbiology and Braunschweig Integrated Centre of System Biology (BRICS), Braunschweig, Germany
[*] Corresponding author. E-mail: h2.johannes@ihf.tu-bs.de

Abstract:
Bioelectronics as interface between well-established electrical measurement methods and biological systems have the potential to open up new opportunities for biological research. Besides a fast response and improvements in the sensitivity the sample volume can be reduced drastically compared to traditional sensing technologies which leads to a miniaturization of the biosensor.[1,2] One approach might be the linkage of bacteria on a functionalized gate-electrode of a modified field-effect transistor (Figure 1). Trapped bacteria shift the potential at the gate-solution interface measureable due to changes of the current between source and drain.[2] The use of an extended-gate field-effect transistor (EGFET) is necessary for physical separation but electronical connection of the liquid based sensing area from the measuring unit.[2,3] It prevents the contact between the water based bacteria suspension and the organic semiconductor which degrades by exposure to water. The sensing area is functionalized with a porphyrin self-assembled monolayer (SAM) containing two different linkers. One linker connects the porphyrin with the gate-electrode's surface. The other linker acts as trap for Gram-negative bacteria.[4] The formation of a porphyrin monolayer on gold surfaces has been first verified by well-established methods as UV/ Vis spectroscopy and cyclic voltammetry (CV). The linkage of *Escherichia coli* (*E. coli*) on the functionalized electrode surface were further analyzed by fluorescence lifetime imaging microscopy (FLIM). Beyond these results changes in the output characteristic of the developed field-effect transistor can clearly be related to the attendance of *E. coli*. The results indicate a possible reaction of the bacterial metabolism caused by the applied potential.

Keywords: extended-gate field-effect transistor (EGFET), porphyrin self-assembled monolayer (SAM), Gram-negative bacteria detection.

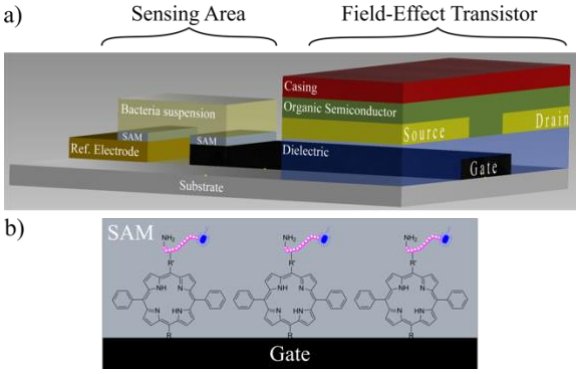

Figure 1: Schematic of the developed field-effect transistor (a) with an adapted self-assembled monolayer (SAM) in larger scale (b) composed of functionalized porphyrins for trapping of Gram-negative bacteria.

References:

1. Zhang, A., Lieber, C. M. (2016), Nano-Bioelectronics, *Chem. Rev.*, 116, 215-257.
2. Gutiérrez-Sanz, Ó., Andoy, N. M., Filipiak, M. S., Haustein, N., Tarasov, A. (2017), Direct, Label-Free, and Rapid Transistor-Based Immunodetection in Whole Serum, *ACS Sens.*, 2, 1278-1286.
3. Thomas, M. S., White, S. P., Dorfman, K. D., Frisbie, C. D. (2018), Interfacial Charge Contributions to Chemical Sensing by Electrolyte-Gated Transistors with Floating Gate, *J. Phys. Chem. Lett.*, 9, 1335-1339.
4. Liu, F., Soh Yan Ni, A., Lim, Y., Mohanram, H. Bhattacharjya, S., Xing, B. (2012), Lipopolysaccharide Neutralizing Peptide–Porphyrin Conjugates for Effective Photoinactivation and Intracellular Imaging of Gram-Negative Bacteria Strains, *Bioconjugate Chem.*, 23, 1639-1647.

Graphene Korea 2021 Session III:

Graphene for electronic, photovoltaic and magnetic applications

Ink formulations of 2D materials for 3D printed energy devices

Abstract

The 3D printing of 2D materials, such as graphene, transition metal dichalcogenides and M-Xenes, offers a cost-efficient and sustainable route for the fabrication of integrated electronics and advanced energy devices with arbitrarily complex architectures. In particular, the assembly of 2D materials into rationally designed three-dimensional electrodes can enhance the charge transport kinetic and increase the electrochemically active surface area, resulting in superior electrochemical performance. In this talk I will discuss new classes of 3D printed supercapacitors obtained from aqueous inks of pristine graphene, one type and TMDS, the second type, without the need of functional additives or high-temperature processing. We discuss performance in the context of the state- of the art of microsupercapacitors. With an electrical conductivity of ~1370 S m^{-1} and rationally designed architectures, the symmetric supercapacitors can achieve an exceptional areal capacitance of 1.57 F cm^{-2} at 2 mA cm^{-2} which is retained over 72% after repeated voltage holding test. The areal power density (0.968 mW cm^{-2}) and areal energy density (51.2 μWh cm^{-2}) outperform many carbon-based supercapacitors previously reported, indicating the feasibility of this approach for the fabrication of efficient energy storage devices.

Research of graphene in 200 mm pilot line: from theory to devices

M. Lukosius[1*], M. Lisker[1,2], R. Lukose[1], J. Dabrowski[1], M. Elviretti[1], F. Akhtar[1], G. Luongo[1]
G. Dziallas[1], C. Alvarado[1], G. Lippert[1], A. Mai[1,2], Ch. Wenger[1,3]

[1]IHP– Leibniz-Institut für innovative Mikroelektronik , Im Technologiepark 25, 15236 Frankfurt (Oder), Germany
[2]Technical University of Applied Science Wildau, Hochschulring 1, 15745, Wildau, Germany
[3] BTU Cottbus Senftenberg, 03046 Cottbus, Germany
* lukosius@ihp-microelectronics.com

Abstract:
Due to the unique electronic band structure, graphene has opened great potential to extend the functionality of a large variety of graphene-based devices. Despite the significant progress in the fabrication of various graphene based microelectronic devices, the integration of graphene devices still lack the stability and compatibility with Si-technology processes. Therefore, the investigation and preparation of graphene devices in conditions resembling as close as possible the Si technology environment is of highest importance [1,2].
Towards these goals, this work focuses on the full spectra of graphene research aspects in 200mm pilot line. We investigated different process module developments such as CMOS compatible growth of high quality graphene on germanium and its growth mechanisms (Fig.1), transfer related challenges on target subtrates, patterning, passivation and various concepts of contacting of graphene on a full 200 mm wafers. Finally, the attempts to fabricated simple proof-of-concept test structures e.g. TLM, Hall bars (Fig. 2), as well as complex modulator devices will be presented.

Keywords: Graphene, Chemical Vapour Deposition, Transfer, Integration, CMOS, DFT, Simulations.

Acknowledgements:
This project has received funding from the European Union's Horizon 2020 research and innovation programme under Graphene Flagship grant agreement No 952792.

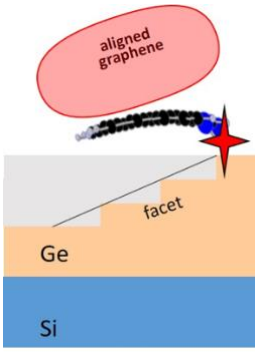

Figure 1: Schematic representation of the Ge faceting phenomena based on DFT simulations.

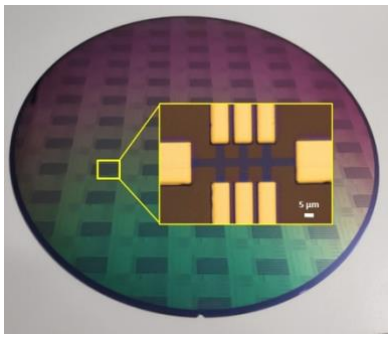

Figure 2: Optical image of the 200 mm wafer with patterned graphene proof-of-concept-devices. The inset shows the example of Hall bar structure.

References:

1. Neumaier, D., Pindl, S., Lemme, M., (2019), Integrating graphene into semiconductor fabrication lines, *Natur. Mater.*, 8, 525-528.
2. Lisker, M., Lukosius, M., et. al., (2019) Processing and integration of graphene in a 200 mm wafer Si technology enviroment, *Micro. Eng.*, 205, 44-52.

Atom-by-atom design of graphene-like structures

C. Morais Smith [1]

[1] Institute for Theoretical Physics, Utrecht University, Utrecht, The Netherlands

Abstract:
Feynman's original idea of using one quantum system that can be manipulated at will to simulate the behavior of another more complex one has flourished during the last decades in the field of cold atoms. More recently, this concept started to be developed in nanophotonics and in condensed matter. In this talk, I will discuss a few recent experiments, in which 2D electron lattices were engineered on the nanoscale. The first is the Lieb lattice [1,2], and the second is a Sierpinski gasket [3], which has dimension D = 1.58. The realization of fractal lattices opens up the path to electronics in fractional dimensions. Then, I will show how to realize topological states of matter using the same procedure. We investigate the robustness of the zero modes in a breathing Kagome lattice, which is the first experimental realization of a designed *electronic* higher-order topological insulator [4], and the fate of the edge modes in a Kekule structure, upon varying the sample termination [5]. Finally, I will discuss how to realize *p*-orbital Dirac cones and flat bands in designed honeycomb lattices [6].

Keywords: graphene, electronic quantum simulators, topological states, Kekule structure, designed lattices

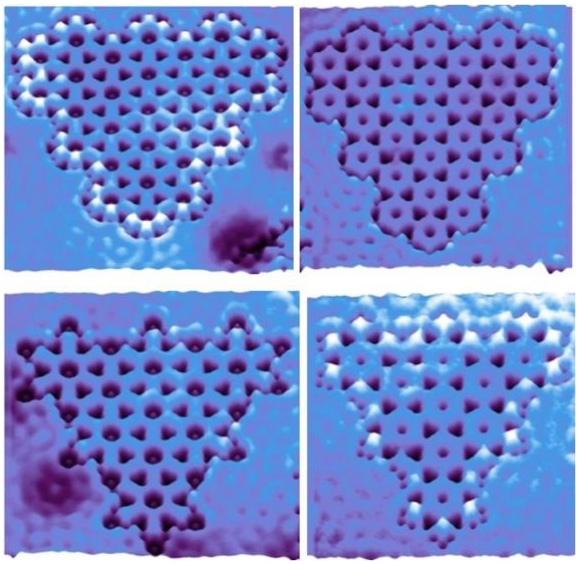

Figure 1: Kekule lattices with different ratio of weak and strong bonds and different termination. The existence or not of topological states depends on both, the sample termination and the position of strong bonds [5].

References:

1. M.R. Slot et al., Nature Physics 13, 672 (2017)
2. M.R. Slot et al., Phys. Rev. X 9, 011009 (2019)
3. S.N. Kempkes, M.R. Slot, S.E. Freeney, S.J.M. Zevenhuizen, D. Vanmaekelbergh, I. Swart, C. Morais Smith, Nature Physics 15, 127 (2019)
4. S.N. Kempkes, M.R. Slot, J.J. van den Broeke, P. Capiod, W.A. Benalcazar, D. Vanmaekelbergh, D. Bercioux, I. Swart, C. Morais Smith, Nature Materials 18, 1292 (2019)
5. S.E. Freeney, J.J. van den Broeke, A.J.J. Harsveld van der Veen, I. Swart, C. Morais Smith, Phys. Rev. Letters 124, 236404 (2020)
6. T.S. Gardenier, J.J. van den Broeke, et al., ACS Nano 14, 13638 (2020)

Graphene, chemistry and single molecule devices

G. Schneider

Leiden Univ., The Netherlands

Abstract:
DNA sequencing and biomolecular sensing are among the most envisioned applications of graphene, nonetheless each step towards these targets faces important challenges. Our research exploits chemistry: from the synthesis of graphene and porous 2D membranes, to handling, functionalization and application for 2D sensing devices. We recently introduced an innovative mixed cold/hot walls synthesis for CVD graphene and developed bottom-up 2D organic films from polycyclic aromatic hydrocarbons structured by self- assembly as a network of molecularly precise nanopore arrays. Furthermore, we implemented polymer free transfer methods based either on the biphasic caging of graphene using cyclohexane or lipid clamps, ensuring graphene films free of polymer residuals allowing the formation of novel graphene heterostructures made from graphene-lipid superstructures. Interestingly, the chemical functionalization of graphene via the hydrogenation of the basal plane and through the electrografting of diazonium salts at the edge, brings us to better understand the interplays between electrochemistry and quantum transport, both in terms of molecular selectivity and sensitivity of next generations of graphene field effect transistor sensors. In sensing devices based on free-standing graphene, we discovered that graphene is hydrophilic in water, aiming now to understand the impact of water – conferring hydrophilic characteristics to graphene when suspended in water – on how graphene sensors in water operate in the presence of biomolecules (most particularly for nanopore and nanogap sensors).

In the last part of my talk, I will present how we achieved the first dynamic tunneling graphene nanogap at the intersection of two single carbon atoms. In the coming years, I believe that chemistry will play an increasingly larger role in the design of the next generation of graphene technologies.

Large-dimensional MoS_2 Transistors Array Fabricated by RF Sputtering and Its Applications

Heekyeong Park[1], Na Liu[1], Bong Ho Kim[2], Young Joon Yoon[2,*] and Sunkook Kim[1,*]

[1] Sungkyunkwan University, School of Advanced Materials Science & Engineering, Suwon-si, Gyeonggi-do, Republic of Korea
[2] Korea Institute of Ceramic Engineering and Technology, Nanomaterials and Nanotechnology Center, Jinju-si, Gyeongsangnam-do, Republic of Korea

Abstract:
Two-dimensional molybdenum disulfide (MoS_2) has been recognized as a promising material for various sensing applications such as optoelectronic and chemical sensors because of its great optical and electrical properties. However, a large-scale synthesis of MoS_2 films still reminds a big challenge for uniform and reproducible sensor fabrication and performance. In semiconductor and display industries, physical vapor deposition (PVD), especially sputtering, is a major technique and widespread commercialization technology to deposit uniform semiconducting thin-films, such as amorphous silicon (α-Si), polycrystalline silicon (poly-Si), and indium gallium zinc oxide (IGZO), having large-area. A continuous MoS_2 films can be directly synthesized on a substrate using a radio-frequency (RF) magnetron sputtering system, which offers great advantage for high compatibility with conventional thin-film fabrication processes.
In this study, we fabricated large-scale continuous and high quality MoS_2 films based on RF sputtering and post-treatments of electron-beam treatment and sulfurization. As-deposited MoS_2 film having amorphous structure was changed to polycrystalline through the post-treatments, which was confirmed by transmission electron microscopy (TEM) analysis. In addition, we demonstrated that an atomic rearrangement during post-treatments results in variation of chemical and electrical structure of the films to 2H stacking n-type semiconductor using X-ray photoelectron spectroscopy (XPS) analysis and photosmission spectroscopy (PES) analysis in secondary cut-off regions.
Based on large-area uniformity of the films, we fabricated MoS_2 thin-film transistors (TFTs) array on the substrate and confirmed no deviation of electrical performances in more than 20 MoS_2 TFTs. The MoS_2 TFTs array can be utilized for two different sensing applications, a photodetector and gas sensor.
As photodetector, our MoS_2 TFTs exhibited high photoresponsitivy (3.7 AW^{-1}) and photosensitivity (1.4×10^4 %), which is a dramatic improvement over previously reported properties of flake MoS_2 TFTs. In addition, the device showed superior detection properties for nitrogen dioxide (NO_2) gas with low detection limit of 8 ppm.
These excellent sensing properties were attributed to abundant grain boundaries in polycrystalline sputter-grown MoS_2 films. The grain boundaries form trap states in the bandgap, which was confirmed by PES spectra near valence band. Under illumination of the light, the trap states capture the excess holes generated by light absorption, resulting in a photogating effect and high photoresponsitivity. For gas sensor, adsorptions of NO_2 gas molecules on grain boundaries increase the potential barriers of the trap states, inhibiting the carrier flow and inducing drain current variations.
This work represents the great potential of sputter-grown two-dimensional materials for highly responsive and ultra-sensitive sensor array systems.

Keywords: RF sputtering, MoS_2 growth, MoS_2 TFTs array, TFT-based photodetector, TFT-based NO_2 gas sensor.

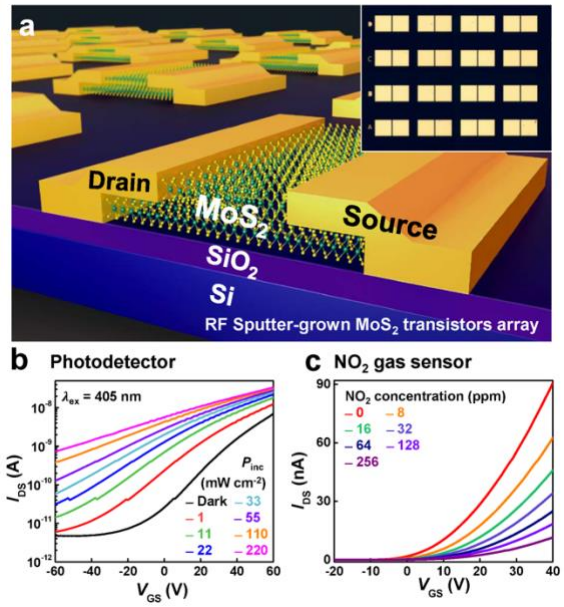

Figure 1: sputter-grown MoS_2 transistors array and its sensing properties. (a) Schematic and optical images (inset) of MoS_2 transistors array and transfer characteristics of MoS_2 transistor (b) under illumination of various incident power densities (P_{inc}) from 1 to 220 Mw cm^{-2} at an excitation wavelength (λ_{ex}) of 405 nm, and (c) under NO_2 gas exposure with the concentration range from 8 to 256 ppm.

Enhanced sensitivity of humidity and soil moisture sensor using liquid exfoliated MoS_2 nanosheets

Mohd Salman Siddiqui[1], Vinay S. Palaparthy[2], Hemen kalita[1,3], Maryam Shojaei Baghini[4] and M. Aslam[1]

[1]Department of Physics, Indian Institute of Technology, Bombay, India
[2]Centre for Research in Nanotechnology and Science, Indian Institute of Technology, Bombay, India
[3]Department of Physics, Gauhati University, India
[4]Department of Electrical Engineering, Indian Institute of Technology Bombay, India

Abstract:
In this work, an ultrasensitive humidity and soil moisture sensor has been developed using exfoliated MoS_2 nanosheets as a sensing film in combination with the interdigitated electrode configuration. The performance of the sensor was examined at room temperature with respect to different relative humidity levels (RH) and soil moisture content (θg). MoS_2 nanosheets were synthesized by ultra-sonication induced exfoliation from bulk MoS_2 using poly (sodium 4-styrenesulfonate) (PSS) as a surfactant. A variation from 34 pf to 14180 pf capacitance were obtained when RH levels changes between 11% and 96% at room temperature. The response and recovery times of the sensor were approximately 70 s and 60 s, respectively. Soil sensing properties were investigated in a detection range from dry soil (2.3% θg) to saturation level (53% θg). High plastic clay (Black soil) was selected as a testing mass to explore the soil sensing ability of MoS_2 nanosheets. The capacitance of the MoS_2 based sensor increases monotonically when the soil moisture content increased from 2.3% to 53% θg. The observed variation in capacitance corresponding to 53% and 42% θg is approximately 260 and 146 times of that observed for 2.3% θg. The soil sensing results shows unprecedented response, long-term stability and good reproducibility. Our results demonstrate the potential for applying MoS_2 nanosheets to the fabrication of highly sensitive humidity and soil moisture sensors.

Keywords: Micro-sensor, Humidity sensor, Soil moisture sensor, MoS_2 nanosheets, poly (sodium 4-styrenesulfonate) (PSS).

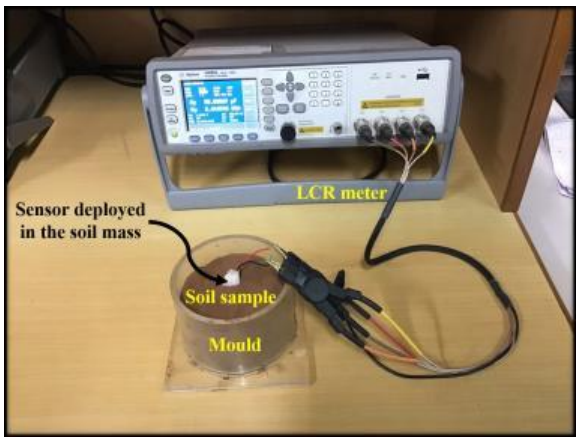

Figure 1 Digital photograph of the experimental set-up to study the soil moisture response of fabricated micro-sensor with MoS_2 nanosheets as a sensing film.

References:

1. M. Donarelli, S. Prezioso, F. Perrozzi, F. Bisti, M. Nardone, L. Giancaterini, C. Cantalini, L. Ottaviano, (2015) Response to NO_2 and other gases of resistive chemically exfoliated MoS_2-based gas sensors, Sensors and Actuators B: Chemical, Volume 207, 602-613.
2. F. K. Perkins, A. L. Friedman, E. Cobas, P. M. Campbell, G. G. Jernigan, B. T. Jonker, (2013) Chemical vapor sensing with monolayer MoS_2, Nano Letters 13 668–673.

Conductive cationized cotton yarns coated with graphene sheets: *in-situ* mechanical and electrical properties

Léa Maneval, Anatoli Serghei, Nathalie Sintes-Zydowicz, Emmanuel Beyou

UMR 5223, University of Lyon 1, Villeurbanne, France

Abstract:
Smart textiles are defined as textile products where fibers and/or filaments, woven or knitted, can interact with the environment and the user. They are usually based on electrical conductive textiles including metal-based fillers. Nevertheless, most of the metal-based fillers are toxic so the use of graphene sheets is preferred regarding their thermal and chemical stability as well as their high electrical conductivity (10^4 $S.cm^{-1}$). Aqueous suspensions of reduced graphene oxide (rGO) have been reported to interact with cotton fabric through Hydrogen bonds between remaining hydroxyl groups and cotton.[1] Graphene, dispersed in water in presence of an anionic surfactant, has also been deposited onto cotton fabric andit was demonstrated that at least 5 padding coating cycles were required to obtain a conductivity of 1.9 $S.cm^{-1}$.[2]
Herein, the elaboration of electrical conductive textiles was based on the adsorption of graphene sheets onto cotton yarns through the use aqueous suspensions of graphene stabilized with a cationic surfactant such as cetyltriamonium bromide (CTAB). Indeed, considering that graphene sheets and cotton yarns exhibit a negative zeta potential, CTAB was well adapted to favor electrostatic interactions. After an immersion of the cotton yarns for 1 hour in an ultrasonic bath fixed at 0 °C containing an aqueous graphene suspension of 5 g/L with CTAB, it was shown that the cotton yarns display improved electrical conductive properties under stretching. In particular, the electrical conductivity increased from ≈10^{-3} $S.cm^{-1}$ to 1.1 ± 0.4 $S.cm^{-1}$ for a strain of 13.7 ± 1.1 % (Figure 1).

Keywords: graphene, e-textiles, coating, cotton, graphene yarn, mechanical/electrical coupled characterization

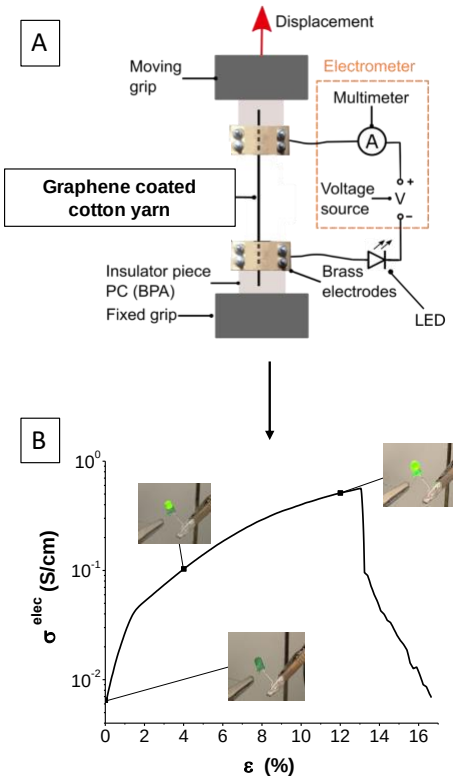

Figure 1: (A) Electrical and mechanical set–up used for simultaneous measurement of electrical and mechanical properties (adapted from C.Beutier and all)[3]. (B) Influence of strain onto the electrical conduction of cotton yarns coated with graphene sheets.

References:

1. Karim, N. et al. Scalable Production of Graphene-Based Wearable E-Textiles. ACS Nano 11, 12266–12275 (2017)
2. Afroj, S., Tan, S., Abdelkader, A. M., Novoselov, K. S. & Karim, N. Highly Conductive, Scalable, and Machine Washable Graphene-Based E-Textiles for Multifunctional Wearable Electronic Applications. Adv. Funct. Mater. 30, (2020).
3. C. Beutier, L.David, G. Sudre, P. Cassagnau, P. Heuillet, B. Cantaloupe, A. Serghei. In-situ coupled mechanical/electrical investigations of EPDM/CB composite materials: the electrical signature of the mechanical Mullins effect. Submitted in Composites Science and Technology (2021)

Superconducting Dirac point in proximetized graphene

Gopi Nath Daptary[1], Eyal Walach [1] , Efrat Shimshoni [1], Aviad Frydman[1]

[1] Department of Physics, Jack and Pearl Resnick Institute and the Institute of Nanotechnology and Advanced Materials, Bar-Ilan University, Ramat-Gan, Israel

Abstract:
Two-dimensional (2D) materials, composed of single atomic layers, have attracted vast research interest since the breakthrough discovery of graphene. One major benefit of such systems is the simple ability to tune the chemical potential by back-gating, in-principle enabling to vary the Fermi level through the charge neutrality point, thus tuning between electron and hole doping. For 2D Superconductors, this means that one may potentially achieve the regime described by Bose Einstein Condensation (BEC) physics of small bosonic tightly bound electron pairs. Furthermore, it should be possible to access both electron and hole based superconductivity in a single system. However, in most 2D materials, an insulating gap opens up around the charge neutrality point, thus preventing approach to this regime. Graphene is unique in this sense since it is a true semi-metal in which the un-gapped Dirac point (DP) is protected by the symmetries. In this work we show that single layer graphene, in which superconducting pairing is induced by proximity to regions of a low density superconductor, can be tuned from hole to electron superconductivity through an ultra-law carrier density regime where the BEC limit is effectively realized. We study, both experimentally and theoretically, the vicinity of this "Superconducting Dirac point" (SDP) (Figure 1(a)) and find an unusual situation where reflections at interfaces between normal and superconducting regions within the graphene, suppress the conductance (Figure 1(b)) and, at the same time, Andreev reflections maintain a large phase breaking length. In addition, the Fermi level can be adjusted so that the momentum in the normal and superconducting regions perfectly match, giving rise to ideal Andreev reflection processes.

Keywords: Graphene, Andreev reflection, Superconductor-insulator transition

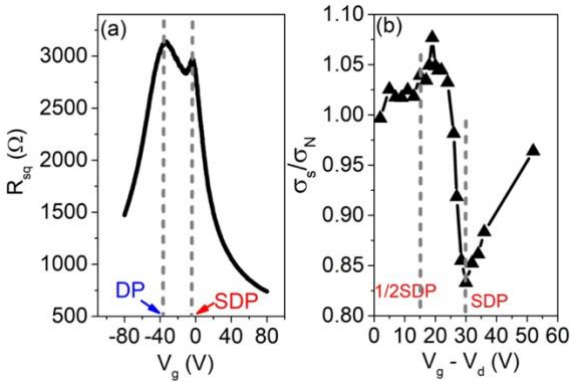

Figure 1: (a) Sheet resistance as a function of gate voltage of bilayer of single layer graphene and disordered indium oxide film (SLG/InO). (b) Relative conductivity σ_S/σ_N (σ_S is the differential conductivity of bilayer of SLG/InO and σ_N is the differential conductivity of bare SLG) as a function of bias voltage V_{DC}. Measurements were performed at T=0.33K and B=0T.

References:

1. Daptary, G., Walach, E., Shimshoni, E., Frydman, A., (2020) Superconducting Dirac point in proximetized graphene, *arxiv:2009.14603*.

Posters Session

Al_2O_3 and TiO_2 Atomic Layer Deposition on Die Casting Mold Steel for Surface Engineering

R.M. Silva,[1] F.Oliveira,[1] R.F. Silva[1]

[1] University of Aveiro, Department of Materials and Ceramic Engineering, CICECO, Aveiro, Portugal

Abstract:
Metal oxides such as, aluminium oxide (Al_2O_3) and titanium oxide (TiO_2) are versatile materials with a diverse range of existing applications. These two metal oxides can be fabricated in thin film form, by atomic layer deposition (ALD) allowing a controlled deposition of the thin films on a surface [1]. ALD is a powerful and versatile technique for the coating or decoration of different types of substrates, incluing substrates with 3D geometries. It permits a precise deposition of conformal and homogenous thin films, based on a reaction between precursor materials, which are separated into successive surface reactions. Accordingly, the reactants are kept separated reacting with surface species in a self-limiting process, *i.e.*, without the presence of gas phase reactions. The conformal growth of the ALD film is a direct consequence of self-limited surface reaction and the film thickness is determined by the number of cycles. ALD technique is widely used for metal oxide thin films deposition, which formation involves the reaction between a metal precursor and an oxygen source (water or ozone) [1]. ALD is, therefore, specifically suited for the deposition of Al_2O_3 and TiO_2 on die casting mold steel components. ALD of these two metal oxides was employed to develop an thin film barrier on the surface steel samples, in order to modify their surface in terms of wettability. It is expected that this surface modification improves the final quality of the injected part. Figure 1. shows a representative illustration of the die casting steel samples coated with TiO_2 (yellowish coloration).

Keywords: atomic layer deposition, metal oxides, surface energy, wettability.

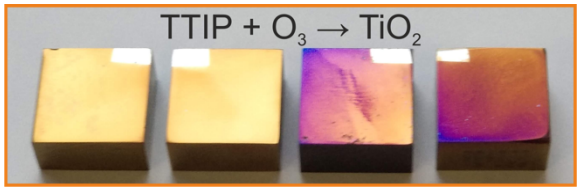

Figure 1: Figure illustrating different die casting mold steel samples, after ALD of TiO_2 for 400 cycles.

References:

1. Puurunen, R. L. (2005), Surface chemistry of atomic layer deposition: A case study for the trimethylaluminum/water process, *J. Appl. Phys*., 9, 121301-121357.

Fabrication of hierarchical TiO_2@NiO nanocomposite electrode with outstanding cycle durability for electrochromic application

Jung-Hoon Yu[1], Rak Hyun Jeong[1,2], Dong In Kim[1], Ji Won Lee[1,2], Ju Won Yang[1], Seong Park[1,2], Sang-Hun Nam[2], and Jin-Hyo Boo[1,2,*]

[1] Department of Chemistry, Sungkyunkwan University, 440-746 Suwon, Korea
[2] Institute of Basic Science, Sungkyunkwan University, 440-746 Suwon, Korea

Abstract:
Nickel oxide (NiO) is a well known transition metal oxide material for anodic electrochromic (EC) electrode due to its high EC efficiency, large optical modulation and low material cost [1]. The surface geometry of NiO closely related with EC properties such as response time, optical modulation, and cyclic durability. High surface area can enhance the above properties because it allows the electrolyte to penetrate and shorten the ions diffusion length within the hierarchical morphology. The chemical bath deposition (CBD) is effective method to form a porous NiO thin film with tow dimensionally networked nano wall structure [2]. In addition, CBD has several advantages such as low temperature processing, convenience for large-area deposition and cost-effective. Nevertheless, NiO films prepared by CBD shows poor cyclic durability because low adhesion between transparent conducting oxide and NiO films. Also, a couple of interwined redox reaction leads to gradual hydration of the thin film and resulted in isolation of NiOOH by intercalated water molecules which cause the degradation of bleaching process. This study report a solution-derived NiO nanoflake films covered with thin and uniform TiO_2 protective layers to improve the cycle durability against repetitive electrochemical reaction under aqueous electrolyte. Hierarchical TiO_2 protective layer covered NiO nanoflake films are prepared by CBD method in combination with a liquid phase deposition (LPD) method. The as-prepared NiO films have porous structure interconnected with 2-dimensionally networked nanoflake array. The Thickness of TiO_2 protective layers on the NiO films were controlled by varying the deposition time of LPD with 4 h to 8 h. The microstructure, crystalline quality and chemical composition of the films were characterized by scanning electron microscopy, X-ray-diffraction, Raman spectroscopy and X-ray photoelectron spectroscopy. The electrochemical and EC properties were also analyzed and compared with pure NiO films. Compared with the pure NiO film, the TiO_2 layer with deposition time of 4 h covered on NiO film showed a highly improved cycling durability with balanced optical modulation. This improved EC performance can be explained by the fact that the introduced TiO_2 has a high stability against alkaline electrolytes than NiO, thus acting as a protective layer.

Keywords: Nickel oxide, Electrochromic, Durability, Chemical bath deposition, Protective layer

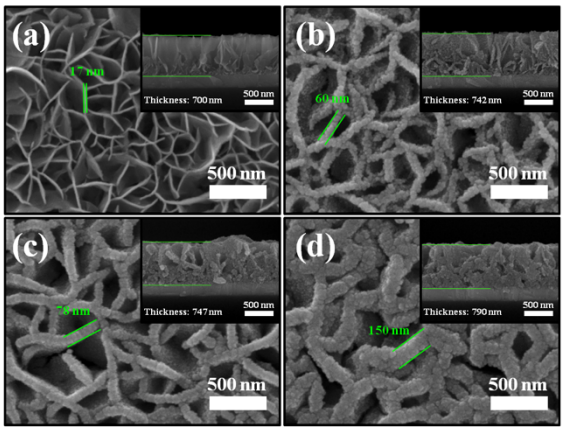

Figure 1: SEM photographs of the TiO_2 covered NiO films with different LPD time: (a) 0 h, (b) 4 h, (c) 6 h and (d) 8 h (corss-sectional view is presented in the inset).

References:

1. Cao F., Pan G. X., Xia X. H., Tang P. S., Chen H. F. (2013) Hydrothermal-synthesized mesoporous nickel oxide nanowall arrayswith enhanced electrochromic application, *Electrochim. Acta,* 111, 86-91.
2. Pawar S. M., Pawar B. S., Kim J. H., Joo O. S., Lokhande C. D. (2011), Recent status of chemical bath deposited metal chalcogenide and metal oxide thin films, *Curr. Appl. Phys*., 11, 117-161.

Effect of Heat Treatment Temperature on the Microstructure and Properties of Thermally Sprayed Ni-Cr-Mo-Al Alloy Coating

A. Srichen,[1] C. Banjongprasert,[1,*]

[1] Chiang Mai University, Department of Physics and Maerials Science, Chiang Mai, Thailand

Abstract:
At present, the damages caused by corrosion cost more than 3.4% of the global GDP (2013) in many countries around the world [1]. Thermal spray coating is one of the technologies to prevent corrosion and wear by creating a protection layers on the substrate. From previous research, the C276 alloy and Nicko-Shield 200 were sprayed on a low carbon steel substrate. The specimens were then heat treated at 1100°C for 60 min and 1200°C for 10 min. It was found that the corrosion rate of the Nicko-Shield 200 coating under 20% H_2SO_4 at 65°C for 200 hrs, decreased while C276 failed corrosion testing in all conditions [2]. However, the heat treatment at high temperatures was still limited to industrial applications. Therefore, this research will focus on studying microstructure and properties after heat treatment at appropriate temperatures and times. Workpieces were arc sprayed and heat treated at 300°C, 400°C, 500°C, 600°C, 700°C and then analyzed using Scanning Electron Microscopy by JEOL JSM-5910LV with Energy Dispersive X-ray Spectroscopy (EDS) techniques and Electron Back-Scattered Diffraction. Corrosion test of surface coating will be done by potentiodynamic technique under 20%H_2SO_4 and reference electrode is Ag/AgCl in KCl and a platinum is employed as the counter electrode. The working electrode exposed area is 1 cm^2. The potential is ranging from -0.05 to 1.6 V. The scan rate is 0.00016 V/s. Wear resistance will be tested by pin-on-disk technique with ball radius 6 mm, testing radius 3.1 mm, load 5 N, Sliding distance 150 m, line speed 7.5 cm/s and temperature 25°C which these methods we will use in testing.

Keywords: Microstructure, Heat Treatment, Ni-Cr-Mo-Al Alloys, Thermal Spray Coating, Corrosion.

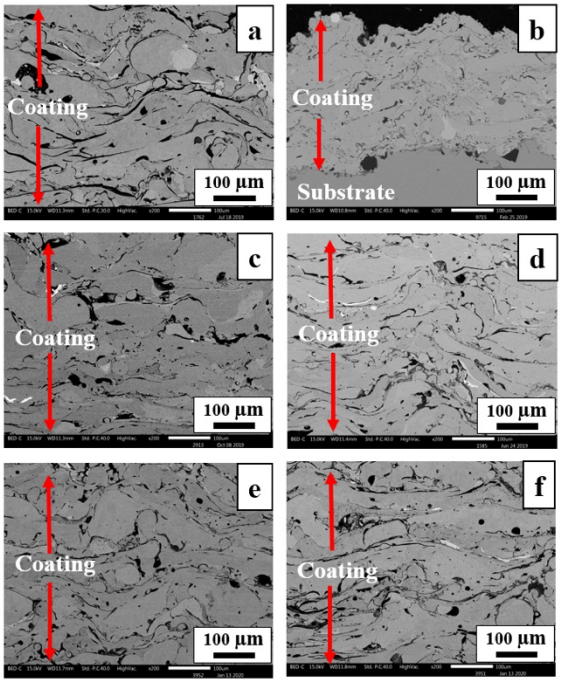

Figure 1: SEM images of NiCrMoAl alloy coating before and after heat treatments: (a) as-sprayed coating, heat-treated coating (b) at 300°C, (c) at 400°C, (d) at 500°C, (e) at 600°C and (f) at 700°C for 10 days

References:

1. Koch, G., Varney, J., Thompson, Neil.,Moghissi, O., Gould, M., Payer J. (2016), International measures of prevension, application, and economics of corrosion technologies study, NACE International.
2. Crowe, T., Guraydin, A. (2011), The Effect of Heat Treatment on Area Percent Porosity and Corrosion Behavior of High-nickel Thermal Spray Coatings, B. Eng. thesis Materials Engineering Department California Polytechnic State University, San Luis Obispo, USA.

Evaluation of self-cleaning efficiency of laser-structured aluminum surfaces contaminated with organic and inorganic particles

S. Milles,[1,*] M. Soldera,[1,2] A.F. Lasagni,[1,3]

[1] Technische Universität Dresden, Institute of Manufacturing Science and Engineering, Dresden, Germany
[2] PROBIEN-CONICET, Universidad Nacional del Comahue, Department of Electrical Engineering, Neuquén, Argentina
[3] Fraunhofer Institut für Werkstoff und Strahltechnik IWS Dresden, Dresden, Germany

Abstract:
The nature provides perfect templates for functional surfaces with many different properties such as superhydrophobicity or self-cleaning which can be found on the lotus and rice leaves. It is well known that a superhydrophobic and self-cleaning surface is able to wipe off water, dirt and contamination providing a clean and dry surface which slows down the process of corrosion and deterioration and extends the lifetime of a technical product or surface [1]. Due to its outstanding mechanical properties, aluminum is used in many different industrial sectors like aerospace, food industry, or automotive. In this work, laser-based methods are used to produce functional microstructures on aluminum using pulsed laser radiation with a wavelength of 1064 nm. Nanosecond pulsed Direct Laser Writing (DLW) method was used to pattern mesh-like textures with lateral feature sizes of 50 µm. Furthermore picosecond pulsed Direct Laser Interference Patterning (DLIP) was employed to structure periodic micropillars with a spatial period of 7.0 µm. In adition to that these methods are combined sequentially to generate hierarchical structures with superhydrophobic and ice-repellent properties [2]. In order to investigate the self-cleaning behavior of the laser treated surfaces, three sets of contamination particles were evenly distributed on the samples' surface, namely inorganic MnO_2 particles with a particle size of ~ 1 µm and ~ 100 µm, respectively, and organic polyamide particles with a particle size of ~ 100 µm. Then, 10 µl water droplets were released towards the samples. which are mounted on a tilted stage. Furthermore, the tilting angle was varied between 15° and 30° in order to inspect the influence of the rolling droplet velocity on the self-cleaning property. The remaining contamination on the surface after each released droplet was determined by optical analysis and the clean-to-dirty area ratio was calculated to quantitavely determine the sample self-cleaning behavior (Figure 1). As a result, DLIP treated surfaces were the most effective ones showing a self-cleaning ability capable to remove up to 85% of the inorganic contamination from the surface with a single droplet at a tilting angle of 30°.

Keywords: Surface treatment, superhydrophobic, self-cleaning, multifunctional surfaces, organic/inorganic contamination, microstructures

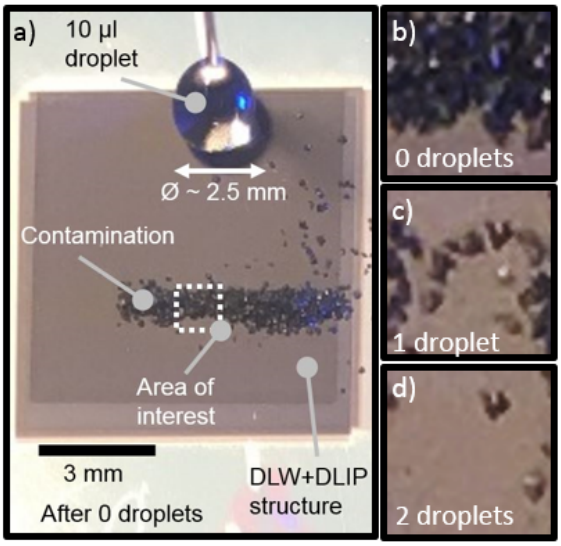

Figure 1: Self-cleaning characterization method using 10 µl droplets (a) and optical analysis after 0, 1 and 2 released droplets.

References:

1. Varshney, P., Mohapatra, S.S., Kumar, A. (2017) Fabrication of mechanically stable superhydrophobic aluminium surface with excellent self-Cleaning and anti-fogging properties, *Biomimetics,* 2,2.
2. Milles, S., Soldera, M., Voisiat, B., Lasagni, A. F. (2019) Fabrication of superhydrophobic and ice-repellent surfaces on pure aluminium using single and multiscaled periodic texture, *Scientific Reports*, 9, 13944.

GaN epitaxy on graphene/sapphire substrate

Chih-Yung Chiang, Yu-Ching Chang, Wen-Cheng Ke*

[1] National Taiwan University of Science and Technology, Department of Materials Science and Engineering, Taipei, Taiwan

Abstract:
This study presents a high quality of GaN thin films that can be grown on few-layer graphene (FLG)/sapphire substrate by embedding a hybrid AlN buffer layer. The hybrid AlN buffer layer is consisted with a high-temperature AlN (HT-AlN) grown by metal organic chemical vapor deposition (MOCVD) and low-temperature AlN (LT-AlN) grown by RF-sputtering. High material quality FLG layer was firstly grown on a 2 inch sapphire substrate by using copper catalyst technique. The 3.5-μm-thick GaN thin-film grown on FLG substrate using single traditional HT-AlN buffer layer exhibit a poor material quality. The high-resolution transmission electron microscopy (HRTEM) image indicated that the carbon atom of FLG layer diffuse out and generate a ~6-nm-thick amorphous layer. The high density of stacking faults and threading dislocations (TDs) were formed in the HT-AlN buffer layer and further extend to the GaN thin-film lead to two intense intensity of broad shoulder bands centered at 3.0 eV (blue-luminescence) and 2.2 eV (Yellow luminescence) in the 17 K photoluminescence (PL) spectrum. The high density of edge-type TD (1.2×10^{10} cm^{-2}) and high carbon concentration (1×10^{20} cm^{-3}) in GaN thin films provide current leakage paths, result in a linear and temperature independent of I-V-T characteristic curve for a Ni-based Schottky contact. The FLG dissociation during high-temperature MOCVD epitaxy can be effectively prevented by embedded a sputtering LT-AlN buffer layer on FLG/sapphire substrate. After optimized the growth temperature of LT-AlN buffer layer, a 20-nm-thick LT-AlN buffer layer grown at 550 ºC was deposited on FLG/sapphire substrate. The HRTEM image show that FLG layer still clearly found between the AlN buffer layer and sapphire substrate. The screw-type/edge-type TD density and carbon concentration of the GaN thin film grown on a hybrid AlN buffer layer/FLG substrate can be reduced to $3.1\times10^{8}/2.3\times10^{9}$ cm^{-2}, and 2×10^{18} cm^{-3} respectively. A narrower near-band edge emission peak at 3.508 eV with FWHM of 19 meV and no yellow luminescence was found in the 17K PL spectrum. In addition, Ni-based Schottky contact exhibits the barrier height of 0.78 eV and ideal factor of 1.6. The hybrid AlN buffer layer structure demonstrate a high-quality GaN thin-film can be grown on FLG substrate that is crucial for further GaN based devices application.

Keywords: GaN, Graphene, AlN, dislocation, Photoluminescence

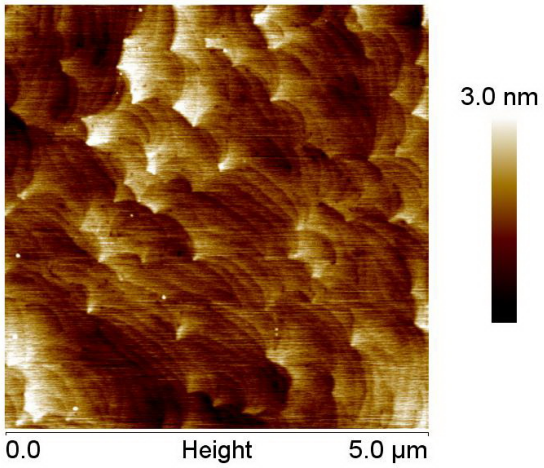

Figure 1: AFM image of GaN thjn-film grown on graphene/sapphire substrate.

References:

1. Wen-Cheng Ke* et al., (2019), Solid-State Carbon-Doped GaN Schottky Diodes by Controlling Dissociation of the Graphene Interlayer with a Sputtered AlN Capping Layer, *ACS Appl. Mater. Interfaces*, 11, 48086-48094.
2. Wen-Cheng Ke et al. (2019), Epitaxial growth and characterization of GaN thin films on graphene/sapphire substrate by embedding a hybrid-AlN buffer layer, *Applied Surface Science*, 456, 967-972.

Hydrogel Based Adsorption Particle Shuttling on Aqueous System while Removing Co Nuclides

Hyung-Ju Kim, Sung-Jun Kim, Chan Woo Park, Hee-Man Yang

Korea Atomic Energy Research Institute, Decommissioning Technology Research Division, Daejeon, Rep. of Korea

Abstract:
There are considerable amounts of radioactive wasteswater generated while decommissioning of nuclear power plant. Cobalt is one of the most problematic nuclides in nuclear wastewater. Since Co-60 emits gamma ray and 5.27 years of half-life, it shoud be treated before recycling or clearance of wastewater. For the treatment, it is supposed to be dealt with carefully, because there is possibility that radiation workers can be exposed to the gamma radiation while treatmenet of wasteswater. Therefore, there is interest to purify nuclear waste remotely.
Self-propelling particle is the particle uses energy from their environment for propulsion. There are some researches building smart systmes pre-programmed to perform specific tasks, such as separations and catalytic reactions. In this presentation, we demonstrate Co removing hydrogel based self-propelling particle shuttling on the surface of aqueous system. The propelling mechanism is based on the adjustment of surface tension by hydrogel. Also, zeolite adsorbing Co is incorporated in the hydrogel to specifically remove Co. The 1 ppm of Co aqueous solution is purified to 0.073 ppb using this particle within 25 min.

Keywords: hydrogel, zeolite, self-propelling particle, zeolite, adsorption, nuclides, separation application, cobalt.

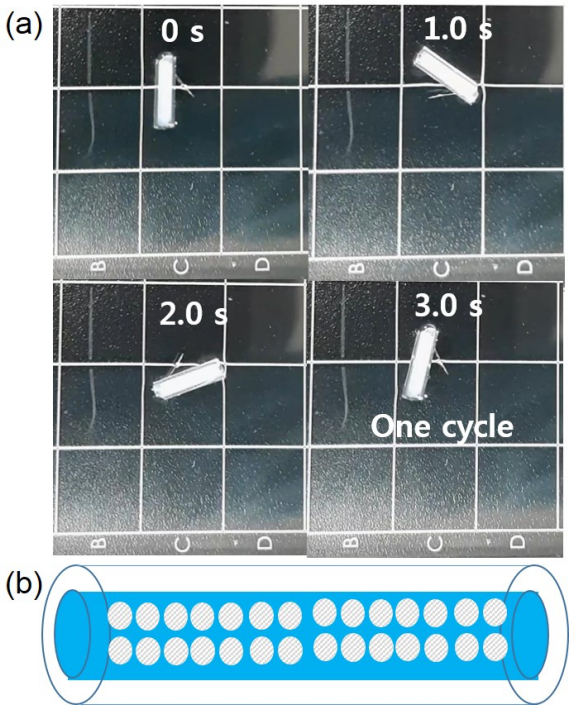

Figure 1: (a) Illustration of self-propelling particle (plastic tube, D=1.52mm) position with respect to time. (b) Scheme of zeolite incorporated hydrogel based self-propelling particle.

Figure 1(a) illustrating the self-propelling particle position with respect to time. Figure 1(b) shows scheme of zeolite incorporated hydrogel based self-propelling particle.

References:

1. Sharma, R., Chang S., Velev O.D. (2012) Gel-Based Self-Propelling Particles Get Programmed To Dance, *Langmuir,* 28, 10128−10135.
2. Kim, H.J., Sperling, M., Velev, O.D., Gradzielski, M. (2016), Active Steerable Catalytic Supraparticles Shuttling on Preprogrammed Vertical Trajectories, *Advanced Materials Interfaces*, 3, 1600095.

Surface protection of concrete surfaces with anti-graffiti systems

S. Jäntsch [1,2,*], C. von Laar [2], H. Bombeck[1]

[1] University of Rostock, Agricultural and Environmental Sciences, Rostock, Germany
[2] Hochschule Wismar, University of Applied Sciences Technology, Business and Design, Faculty of Engineering, Philipp-Müller-Straße 14, 23966 Wismar, Germany

Abstract:
Illegal graffiti and scribblings can be found all over the world. They constitute vandalism and may cause damage to the surface or substance of the objects concerned. With the increase of graffiti, the interest in proper removal and the possibilities of a high-quality protection system grew. Anti-graffiti systems (AGS) can be used to protect affected objects and buildings from damage caused by graffiti.
In this study, the influence of permanent anti-graffiti systems on different concrete surfaces is investigated and evaluated. The focus is on functionality (visual influences, cleaning performance), durability (surface properties of concrete and AGS) and polyfunctionality. In long-term tests over a period of 3 years, visual and physical characteristics and properties of concrete test pieces are determined and evaluated in regular weathering and cleaning cycles. The studies should show that it is necessary to assign the correct anti-graffiti system to each surface and that it is not possible to use a "Unitary product". A new view between the interaction of permanent AGS on different concrete substrates is intended to serve for the development of an evaluation system and thus enable and simplify a proper application of the materials. The test series comprises 180 concrete samples. 6 different concrete substrates are used, which differ in their concrete type and quality as well as their surface treatment. Among other things, the surface quality of concrete pavement slabs, high-strength ground facade slabs or fiber-reinforced concrete testers (angle supports, facade slabs with blasted surface) is investigated. Four different permanent anti-graffiti systems were used and applied according to the manufacturer's specifications. All systems differ in their composition and range from silane-siloxane compounds to polyurethane-polymer combinations. AGS1 and 2 are impregnations, AGS3 and 4 are 2-component coatings. The extent to which the material characteristics and the surface characteristics influence the functionality and durability of the AGS is to be determined and evaluated in 8 cycles. In each cycle, the samples are first exposed to natural weathering. Then the application of different graffiti sprays and a marker is carried out. After 24 hours the samples are cleaned. Figure 1 shows how the functionality (cleaning performance) decreases from the 6th cycle. Up to and including the 5th cycle, all 18 coated test specimens on substrates 1 to 6 show good to very good cleaning results per AGS. From the 6th cycle onwards, 39% of the test specimens can no longer achieve the required cleaning performance. Only 12 (AGS1) and 10 (AGS2) samples meet the requirements. While the first failures of the coatings are only apparent in the 7th cycle (8%). It is striking that the AGS in particular do not provide sufficient cleaning performance on the rougher surfaces. Strong graffiti residues remain on the surface. The smooth concrete surfaces (sanded, exposed concrete) have so far achieved good (pregnations) to very good (coatings) cleaning results.

Keywords: concrete, surface, protective coating, graffiti protection, anti-graffiti-systems, polyfunctionality, functionality, durability

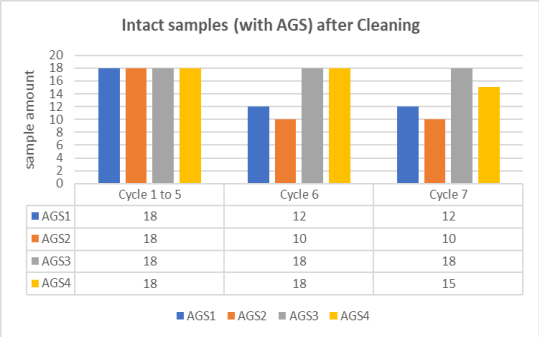

Figure 1: Representation of the intact samples of all 6 substrates with AGS1 to 4 after cleaning

References:

1. Jäntsch, S., von Laar, C., Bombeck, H. (2020) Anti-Graffiti-Systems for Con-crete Surfaces. Proceedings Binders 11/2019, ISBN 978-80-214-5816-1
2. Jäntsch, S., von Laar, C., Bombeck, H. (2020) Functionality and durability of anti-graffiti-systems on concrete. Scientific-Technical Conference MATBUD'2020, 10/2020, ISBN: 978-2-7598-9108-5

Comparison of wear and cavitation erosion resistance of the cermet coatings sprayed by HVOF

E. Jonda [1,*], L. Łatka [2], M. Szala [3], M. Walczak[3]

[1] Department of Engineering Materials and Biomaterials, Silesian University of Technology, Konarskiego St. 18a, 44-100 Gliwice, Poland; ewa.jonda@polsl.pl
[2] Faculty of Mechanical Engineering, Wroclaw University of Science and Technology, Łukasiewicza St. 5, 50-371 Wroclaw, Poland; leszek.latka@pwr.edu.pl
[3] Department of Materials Science and Engineering, Faculty of Mechanical Engineering, Lublin University of Technology, Nadbystrzycka St. 36D, 20-618 Lublin, Poland; m.szala@pollub.pl; m.walczak@pollub.pl

Abstract:
In this paper, the comparision of tribological properties such as wear and cavitation erosion resistance of High Velocity Oxy Fuel (HVOF) sprayed coatings onto AZ31 magnesium alloy were examined. As a coating material, three commercially available powders: WC-Co-Cr, WC-Co and WC-Cr_3C_2-Ni were used. The manufactured coatings were analyzed extensively using optical microscopy (OM), X - ray diffraction (XRD) and scanning electron microscopy (SEM), respectively. In the case of mechanical properties, the hardness, microhardness, elastic modulus and fracture toughness were measured. Cavitation erosion tests were conducted according to ASTM G32 with the stationary specimen method. Dry sliding wear tests were conducted using WC counter sample according to ASTM standard. In both tests, the results were compared with the AZ31 magnesium references sample. Cavitation tests indicate that in the initial stages of erosion the WC-Co-Cr sample has slightly higher resistance than WC-Cr_3C_2-Ni and far better cavitation resistance than WC-Co coatings. In further stages of erosion, the Ni-containing coating delaminates due to its lower fracture resistance and WC-Co-Cr sample stays solid until the end of test time. As-sprayed samples exhibit accelerated mass loss. The main wear mechanism resiles on the detachment of cermet material starting at microstructural and surface nonuniformities such as pores and ceramic-metallic phase interfaces. In the case of sliding wear, the results are strongly related to the mechanical properties. The WC-Co and WC-Co-Cr samples hardness, Young modulus exceed the WC-Cr_3C_2-Ni, therefore, presents lower values of wear factor, on the level of approximately $6 \cdot 10^{-7}$ $mm^3/N \cdot m$ and coefficient of friction related to 0.4. The wear mechanism is affected by abrasion, growing and transfer of the material between counterball and coatings. Deposition of the cermet coatings effectively prevents the magnesium substrate which is presented very poor resistance to cavitation and sliding wear.

Keywords: cermet coatings, HVOF, wear resistance, cavitation erosion resistance.

References:

1. Qiao, L., Wu, Y., Hong, S., Long, W. ,Cheng, J., (2021), Wet abrasive wear behavior of WC-based cermet coatings prepared by HVOF spraying, *Ceram. Int.*, 47, 1829–1836.
2. Sidhu, H.S., Sidhu, B.S., Prakash, S., (2006), Mechanical and microstructural properties of HVOF sprayed WC-Co and Cr_3C_2-NiCr coatings on the boiler tube steels using LPG as the fuel gas, *J. Mater. Process. Tech.*, 171, 77–82.

Optical sensing properties of citrate-reduced gold nanoparticle thin films

Geon Joon Lee[1*], Manesh A. Yewale[1], Linh Nhat Nguyen[1], Eun Ha Choi[1],
Dong Gyu Kim[2], Tae Young Kim[2], Chang Kwon Hwangbo[2]

[1] Department of Electrical and Biological Physics, Kwangwoon University, Seoul 01897, Korea.
[2] Department of Physics, Inha university, Incheon 22212, Korea

Abstract:
Nanostructured materials have unique physical and chemical properties as a result of their small size. Experimentally, there have been many research efforts devoted to the physicochemical properties of low-dimensional structures, such as quantum dots, nanoparticles, nanowires, and nanotubes.[1, 2] Among them, metallic nanostructures have drawn considerable attention because of selective photoabsorption and plasmon resonance effects. Nanostructures were prepared using different approaches like bottom up" and "top down" techniques but also many procedures were used to modify structural and optical properties of nanostructures. This research was focoused on optical sensing properties of gold nanoparticle synthesized by citrate reduction. Gold nanoparticles (AuNPs) were prepared by reduction of $HAuCl_4$ with the help of a reducing agent. The particle sizes and plasmon resonance effects of the AuNPs were investigated for various molar concentrations and volumes of the gold precursor and reducing agent. The surface morphology of the AuNPs were examined by scanning electron microscopy, the crystallinity of AuNPs were studied by measuring X-ray diffraction pattern, and the plasmon resonance effects of AuNPs were investigated by optical absorption spectroscopy. The AuNP thin films were deposited on a glass substrate by soaking over night. (3-Aminopropyl) triethoxysilane was used as a binder between AuNPs and glass substrate. The prepared AuNPs were annealed at a temperature higher than 300℃ to remove residual impurity. The biomaterials were coated on the AuNPs. Their optical sensing properties of AuNPs were compared with those of bare glass without AuNPs.

Keywords: Plasmon resonance effects, Optical sensing, Gold nanoparticles, Sodium citrate.

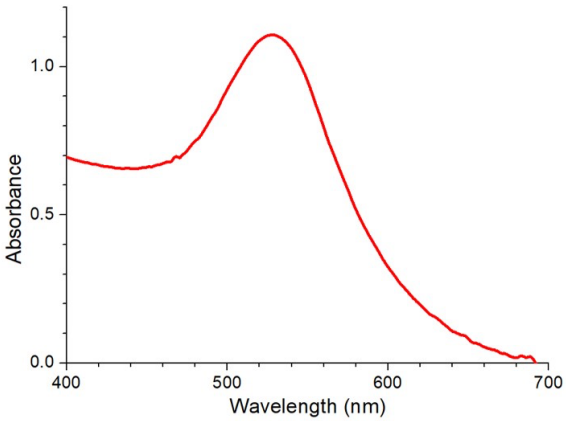

Figure 1: Typical optical absorption spectrum of gold nanoparticles synthesized by citrate reduction method.

References:

1. G. J. Lee, M. Kang, Y. Kim, E. H. Choi, M. J. Cho and D. H. Choi (2020), Optical assessment of chiral–achiral polymer blends based on surface plasmon resonance effects of gold nanoparticles, *J. Phys. D: Appl. Phys.* **53**, 095102.
2. G. J. Lee, P. Attri, E. H. Choi, Y. W. Kwon, I. Krasnikov and A. Seteikin (2014), Optical and Structural Properties of Nanobiomaterials, *J. Nanosci. Nanotechnol.* **14**, 221–249.

Facile fabrication of Cuprous Oxide QDs-Afr 2D array as a sensor media for neurotransmitter

Ho Kyung Lee, Sang Joon Park*

[1] Gachon University, Department of Chemical and Biological Engineering, Seongnam-si, Republic of Korea

Abstract:
Protein is a versatile material in many research fields such as bioelectronics, catalysis, batteries, bio-sensor and labeling. Among them, bio-sensor and labeling areas have been extensively investigated with protein due to its bio-compatibility, abundance of functional groups and unique reactivity. Apoferritin, derivative of ferritin, is one kind of protein with a function of iron storage and transportation in all life forms and this protein has high physical and chemical stability, i.e., the heat endurance up to 85°C and the broad available pH range of 2.0 ~ 11.0. Here, we prepared Cu_2O QDs in apoferritin cavity and 2D array onto ITO glass electrode with pre-synthesized QDs material for neurotransmitter sensing. To construct covalent bond between ITO and QDs, EDC/NHS coupling agents were utilized. By employing HR-TEM, SEM XRD and XPS, the fabricated film was investigated to characterize morphology and film structure. FT-IR measurement was also used to prove amide bond for covalent bond between ITO and QDs. To characterize its optical property, Uv-Vis and Photolominescence measurement were used. After characterization, the fabricated sensor array was conjugated with dopamine and PL measurements were performed as a function of dopamine concentration for evaluating the array as a sensor media. In addition, to investigate the selectivity for dopamine, the sensing performance was evaluated with other compounds such as ascorbic acid (AA), uric acid (UA), histamine (HA), and γ-amino butyric acid (GABA).

Keywords: protein, bio-template, Quantun dots, Cuprous Oxide, bio-sensor, photoluminescence, photoelectrochemical system.

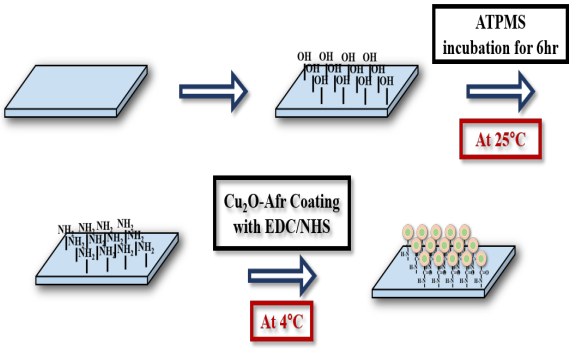

Figure 1: Schematic diagram of 2D array fabrication onto ITO glass electrode.

References:

1. Christopher D Bostick, Sabyasachi Mukhopadhyay, Israel Pecht, Mordechai Sheves, David Cahen, David Lederman, (2018) Protein bioelectronics: a review of what we do and do not know, *Rep. Prog. Phys*, 81, 026601-026657.
2. Katherine A. Brown, Derek F. Harris, Molly B. Wilker, Andrew Rasmussen, Nimesh Khadka, Hayden Hamby, Stephen Keable, Gordana Dukovic, John W. Peters, Lance C. Seefeldt, Paul W. King, (2016) Light-driven dinitrogen reduction catalyzed by a CdS:nitrogenase MoFe protein biohybrid, *Science*, 352, 448-450.
3. Jun-Seo Lee, Hyun-Soo Kim, Won-Hee Ryu, (2019) Iron/carbon composite microfiber catalyst derived from hemoglobin blood protein for lithium-oxygen batteries, *Applied Surface Science*, 466, 562-567

Photoluminescence and structural defects of ZnO films deposited by reactive magnetron sputtering with unconventional Ar-O_2 gas mixture formation

K. Bockute[1,2*], E. Demikyte[2,3], S. Tuckute[2], M. Urbonavicius[2], S.Varnagiris[2], G. Laukaitis[1,2], M. Lelis[2]
[1] Department of Physics, Kaunas University of Technology, Kaunas, Lithuania
[2] Centre for Hydrogen Energy Technologies, Lithuanian Energy Institute, Kaunas, Lithuania
[2] Department of Biochemistry, Vytautas Magnus University, Kaunas, Lithuania

Abstract:
Zinc oxide is a well-known traditional industrial material which has high potential to become one of the key components for the next generation of future electronics], LED emitters and visible light photocatalysis etc [1, 2]. In its pristine form ZnO has relatively wide band gap of approximately 3.4 eV and is not suitable for the visible light applications but it was shown that there is a lot various defect species in this system [3, 4]. Interstitial and vacancy defects of zinc and oxygen introduce various new electron levels in between the conduction and valent bands of ZnO [1] and makes ZnO capable to absorb/emit visible light radiation.
In current, study zinc oxide films were deposited using reactive magnetron sputtering with the unconventional Ar-O_2 gas mixture supply control method. Ar gas flow rate was controlled to maintain the total gas mixture pressure at $1x10^{-2}$ mbar, whereas O_2 gas flow rate was actively adjusted to maintain the selected intensity of optical zinc emission from the working cathode zone. It was demonstrated that by applying such Ar-O_2 gas mixture formation method it is possible to stabilise reactive magnetron sputtering process over were wide oxygen flow rate range (Figure 1.).
Interestingly, this method allowed to do conduct ZnO based film deposition at nearly identical Ar:O_2 gas ratios but with different zinc emission line intensity. These films had nearly the same elemental composition but some of their properties differed significantly. In this work differences in film optical properties and their photoluminescence spectra as well as presence of various types of ZnO structure defects are discussed in more details.

Keywords: ZnO films, reactive magnetron sputtering, photoluminescence, structural defects, energy levels, optical properties.

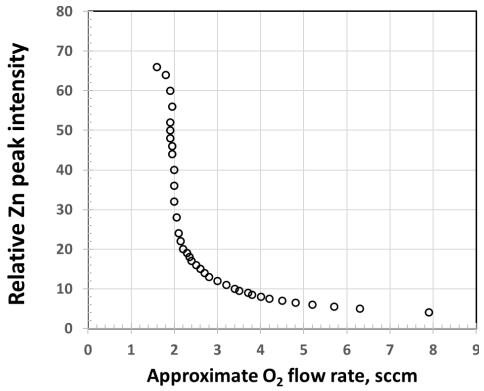

Figure 1: Intensity of Zn emission line at 481 nm measured in the working zone of the magnetron cathode (Zn target). Vertical region of the curve has nearly identical Ar:O_2 gas flow ratios but leads to the formation ZnO films with significantly different optical properties.

References:

1. S.Vempati, J.Mitra and P.Dawson, One-step synthesis of ZnO nanosheets: a blue-white fluorophore, *Nanoscale Research Letters*, 7 (2012) 470.
2. K.S.Ranjith, P.Manivel, R.T.Rajendrakumar, T.Uyar, Multifunctional ZnO nanorod-reduced graphene oxide hybrids nanocomposites for effective water remediation: Effective sunlight driven degradation of organic dyes and rapid heavy metal adsorption, *Chemical Engineering Journal*, 325 (2017) 588-600.
3. K.Wetchakun, N.Wetchakun, S.Sakulsermsuk, An overview of solar/visible light-driven heterogeneous photocatalysis for water purification: TiO2- and ZnO-based photocatalysts used in suspension photoreactors, *Journal of Industrial and Engineering Chemistry* 71 (2019) 19–49.
4. S.Dutta, S.Chattopadhyay, A.Sarkar, M.Chakrabarti, D.Sanyal, D.Jana, Role of defects in tailoring structural, electrical and optical properties of ZnO, *Progress in Materials Science*, 54 (2009) 89-136.

Study on the Quantum Dot Organic-Inorganic Hybrid Photodetector Using Low Temperature Conbustion Process Based NiO_x as an Electron Blocking Layer

Kee-tae Kim [1], Woo-Seong Kim [2], Se-young Oh [2 *]

[1] Sustainable Energy and Environmental Research Institute, Sogang University, Seoul 04107, Korea
[2] Department of Chemical and Biomolecular Engineering, Sogang University, Seoul 04107, Korea
* *E-mail:* syoh@sogang.ac.kr

Abstract:
In the present work, we have fabricated organic-inorganic hybrid photodetector consisting of ITO/ NiO_x/ CdSe@ZnS/ P3HT:PCBM/ Yb/ Al. The bilayers of quantum dots and P3Ht active layers are used to enhance the photocurrent of device due to Förster resonance energy transfer (FRET) effect between quantum dots and P3HT layers.[1]
We have investigated the current-voltage characteristics, external quantum efficiency and transient photocurrent response. Especially, we have explored the physical effects of quantum dot layer on the device performance through the measurement of photoluminescence and impedance.

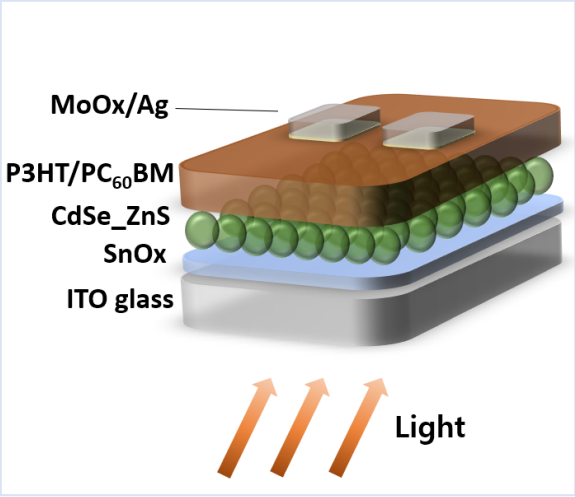

Figure 1: Configuration of quantum dot hybrid photodetector

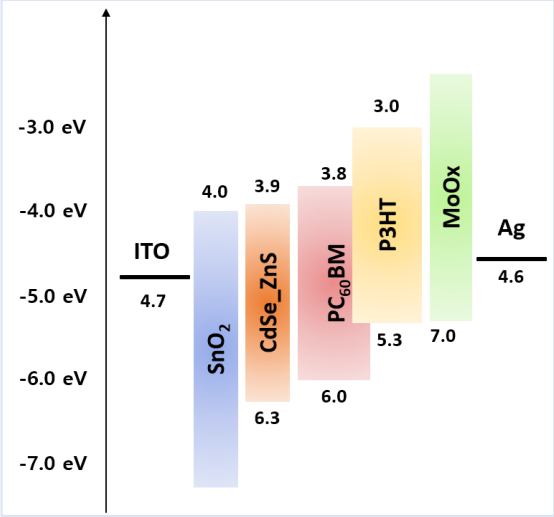

Figure 2: Energy diagram of quantum dot hybrid photodetector

Keywords: Quantum dot, Organic Photodetector, FRET effect, Nickel oxide

References:

1. Dong Ick Son, Adv. Energy Mater. 2014, 1401130
2. TobinJ.Marks , NATUREMATERIALS | VOL 10 | MAY 2011

Improved Dark Current of Organic Photodetector By inserting of Hf-SnO_2 Layer as an Electron Transport Material

Seri Lee[1], Gyu-min Kim[2], Seyoung Oh[1]*

[1] Department of Chemical and Biomolecular Engineering, Sogang University, Seoul 04107, Republic of Korea
[2] Department of Chemical Engineering, Hankyong National University, Seoul 17579, Republic of Korea

Abstract:
The dark current is a critical physical point for achieving high-detectivity in organic photodetectors. It is effective to insert a buffer layer that blocks the reverse-biased dark current. Many studies have been carried out using metal oxides as buffer layers that show excellent charge transport properties and stability. In the present work, we have fabricated an inverted organic photodetector using a Hf-doped SnO_2 buffer layer as electron transport material. The device configuration is ITO / SnO2 / P3HT: PC60BM / MoOx / Ag. Here, the Hf-doped SnO_2 plays role in hole blocking and light soaking buffer layer. Especially, the SnO2 ultra-thin film was fabricated at low temperature through the solution combustion process method in the prepared device shows a high detectivity of 8.70×10^{11} Jones. We also investigated the physical effect of the Hf-doped SnO_2 buffer layer on the performance of organic photodetector through the measurements of Impedance, band width, and surface morphology.

Keywords: SnO_2, Inverted Photodetector, Organic Photodetector, Hole Blocking Layer, Electron Transport Layer, Hf-SnO_2

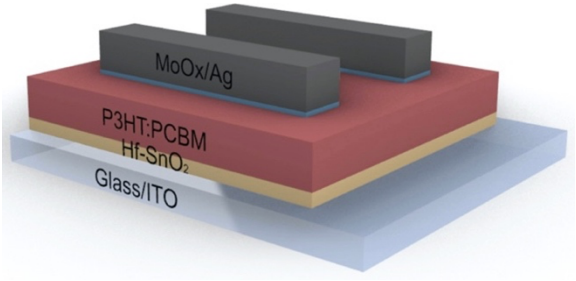

Figure 1: Configuration structure of the prepared inverted organic photodetector.

References:

1. Kwang-Hee Lee, Dong-Seok Leem, Jeffrey S. Castrucci, Kyung-Bae Park, Xavier Bulliard, Kyu-Sik Kim, Yong Wan Jin,*, Sangyoon Lee, Timothy P. Bender and Soo Young Park, ACS Appl. Mater. Interfaces, 5, 13089 (2013).

Water-processable $LiFePO_4$/graphene hybrid cathodes for high power Lithium Ion Batteries

Ju-Won Jeon [1,2,*], Manik Biswas[2]

1 Department of Applied Chemistry, Kookmin University, Seoul, Republic of Korea States
2 Department of Chemical & Biological Engineering, The University of Alabama, Tuscaloosa, Alabama 35487, United States

Abstract:
Currently cathodes for lithium ion batteries (LIBs) are manufactured with an organic solvent, usually N-methyl-2-pyrrolidone (NMP). If water can be used as a solvent, electrode fabrication cost would be largely reduced. Here, we report facile water-processable fabrication methods for LiFePO4/graphene hybrid cathodes in lithium ion batteries (LIBs). Graphene oxide (GO) plays roles of dispersant, binder, and precursor of conductive graphene. Therefore, additional polymeric binder and additional conductive carbon were not necessary. At high current rates, the water-processed LiFePO4/rGO (LFP/rGO) had larger capacity than conventional LiFePO4 cathodes produced by the previously formulated method. The LFP/rGO electrodes were successfully prepared through water-based spray coating methods without an organic solvents. It turned out that thermal reduction yields cathodes having improved rate capability. We expect that the developed electrodes can be applied in high-power batteries with a significantly reduced electrode fabrication cost.

Keywords: lithium iron phosphate, cathodes, lithium-ion batteries, water-processable

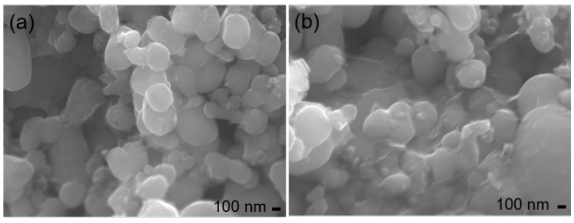

Figure 1: (a) SEM images of LFP particle and (b) LFP-rGO reduced at 300 oC.

References:

1. Bresser, D.; Buchholz, D.; Moretti, A.; Varzi, A.; Passerini, S. Alternative binders for sustainable electrochemical energy storage – the transition to aqueous electrode processing and bio-derived polymers. Energy & Environmental Science 2018, 11, 3096-3127.
2. Wood, D. L.; Quass, J. D.; Li, J. L.; Ahmed, S.; Ventola, D.; Daniel, C. Technical and economic analysis of solvent-based lithium-ion electrode drying with water and NMP. Dry. Technol. 2018, 36, 234-244.
3. Gainese, J.; R., C. Costs of lithium-ion batteries for vehicles; Argonne National LAboratory: Argonne, IL. 2000.

Immobilization of viable proteins onto plasma modified nanofibers investigated by XPS analysis

A. Manakhov [1*], A. Solovieva [1,2]

[1] Research Institute of Clinical and Experimental Lymphology– Branch of the ICG SB RAS, Novosibisk, Russia

Abstract:
Biocompatible and biodegradable materials are of high interest for tissue engineering, drug delivery and wound healing and their development is required for a new generation healthcare materials.
Recently it was found that the immobilization of ensemble of viable biomolecules, e.g. Platelet-rich Plasma (PRP) or different growth factors may induce superior bioactivity of polymeric nanomaterials [1]. Moreover, even single proteins immobilization (e.g. fibronectin, apoliprotein, etc.) was found to be responsible for enhanced bioactivity of the surfaces.
Nevertheless, to date, there is lack of understanding regarding the chemical linkages between the proteins and surface. The majority of the surface analyses dedicated to the investigation of protein-surface interactions are focused on the analysis of immobilized fibronectin. The methodology of fibronectin detection is quite complex and requires antibody staining. In the majority of the manuscripts the immobilization of the fibronectin is confirmed only qualitatively by some changes in the atomic concentrations, e.g. increase of the nitrogen or by small changes in the carbon environment derived from the C1s XPS curve fitting. However, no quantitative calculation methodology can be found.
The situation became more complicate when the researcher is searching the information regrading the immobilization of less abundant proteins. For example, the surface with immobilized APO-A1 or angiogenin never analyzed by X-ray Photoelectron Spectroscopy (XPS) or IR spectroscopy.
In this work, the immobilization of Apoliprotein A1 and Angiogenin on biodegradable nanofibers is carefully investigated by using XPS, FT-IR, SEM and special XPS curve fitting using the simulation of protein spectra. We will demonstrate that the combination of XPS curve fitting and simulation is a new powerful method to quantify the immobilized protein at the surface of nanofibers. These results will be a basis for further fundamental research of protein-surface interactions.

Keywords: XPS, plasma polymers, nanofibers, Apoliprotein A-I, angiogenin, immobilization, tissue engineering.

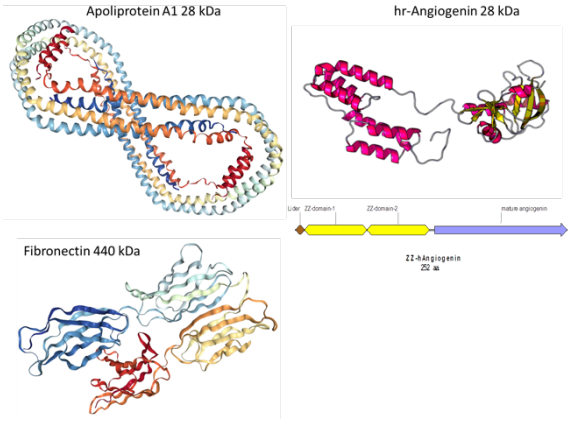

Figure 1: Structures of viable proteins: Fibronectin, Apoprotein AI and Angiogenin.

Acknowledgements
Authors gratefully acknowledge the financial support of the Russian Science Foundation (grant No. 18-75-10057)

References:

1. S Miroshnichenko, V Timofeeva, E Permyakova, S Ershov et al *Nanomaterials* 2019, 9 (4), 637

Phototransistor with Heterogeneous Double Layer Consisted of Inorganic $CsPbI_xBr_{3-x}$ Perovskite and In-Ga-Zn-O Semiconductor for Visible Light Detection

Hyun-Jae Na[1], Sung-Eun Lee,[1] and Youn Sang Kim[1,2]

[1] Seoul National University, Graduate School of Convergence Science and Technology, Seoul, Korea
[2] Advanced Institute of Convergence Technology, Suwon, Korea.

Abstract:
All inorganic perovskites with good excellent physical properties received a considerable attention in optoelectronic applications. Despite the high performance photoelectric properties of all inorganic cesium lead iodide ($CsPbI_3$) perovskites retaining the black α-phase, the phase instability in the ambient condition and the high annealing temperature process inhibit their further development. To improve the availability and long-term stability of $CsPbI_3$, multi-anion structures have been studied in the ABX_3 structure of $CsPbI_3$. Herein, we suggest inorganic heterojunction with $CsPbI_xBr_{3-x}$ and In-Ga-Zn-O (IGZO) semiconductor which applied bi-anion I_xBr_{3-x} instead of I_3 in $CsPbI_3$. Using this hetero-junction, we demonstrate a new phototransistor with a structure of p^{++} Si / SiO_2 / IGZO / $CsPbI_xBr_{3-x}$ / Ti-Al-Ti where IGZO is a charge transfort layer and $CsPbI_xBr_{3-x}$ is a light absorption layer. The material stable properties of $CsPbI_xBr_{3-x}$ were confirmed by changing the ratio of I : Br from 10: 0 to 0:10. When the ratio of $CsPbI_xBr_{3-x}$ perovskite I: Br is 8: 2, the inorganic perovskite maintains the black α phase in the ambient condition. Phototransistor based on $CsPbI_xBr_{3-x}$ perovskite/IGZO heterojunction shows excellent responsivities both ultraviolet region and entire visible light region, unlike the single-IGZO phototransistor reacting only in the ultraviolet region. Furthermore, long term reliability was confirmed by maintaining the α-phase of the IGZO/ $CsPbI_xBr_{3-x}$ heterojunction layer well up to 300 hours.

Keywords: inorganic perovskite, IGZO, $CsPbIxBr_{3-x}$, heterojunction phototransistor, stability

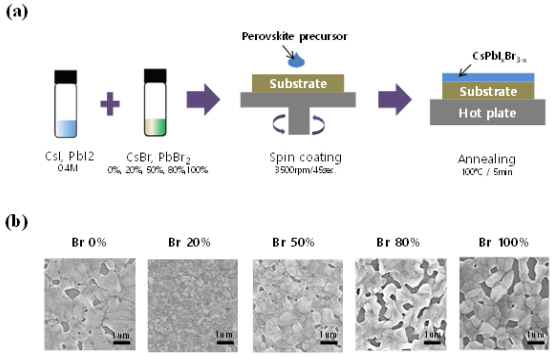

Figure 1: (a) Simplified schematics of Perovskite film procedures (b) SEM images of the $CsPb_xBr_{3-x}$ films fabricated with different Br concentrations of Br 0%, 20%, 50%, 80% and 100%

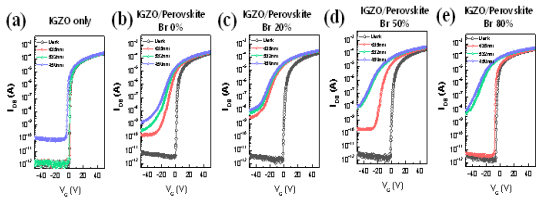

Figure 2: Transfer characteristics of phototransistor under different wavelenght of light. (a) only-IGZO film, (b) IGZO/$CsPbI_3$ (Br 0%) film, (c) IGZO/$CsPbI_xBr_{3-x}$ (Br 20%) film, (d) IGZO/$CsPbI_xBr_{3-x}$ (Br 50%) film, and (e) IGZO/$CsPbI_xBr_{3-x}$ (Br 80%) film. (V_{ds} = 1 V)

References:

1. H. J Na, N. K Cho, J. Park, S. E Lee, E. G Lee, C. Im and Y. S Kim (2019), A visible light detector based on a heterojunction phototransistor with a highly stable inorganic $CsPbI_xBr_{3-x}$ perovskite and In–Ga–Zn–O semiconductor double-layer, *J. Mater. Chem. C*, 7, 14223

Enhanced wear performance of surface layer of some cold working tool steels after combined finishing processes

Daniel Toboła *, Aneta Łętocha

Łukasiewicz Research Network - Krakow Institute of Technology, Zakopianska 73 Str., 30-418 Krakow, Poland, daniel.tobola@kit.lukasiewicz.gov.pl

Abstract:
The mechanical and/or tribological properties of machined components (e.g. tools for cold working) depend on machining processes because the surface layer of the workpiece is altered due to the interaction of the tool and the material. The surface properties of components, as a result of the machining process or combined processes of surface engineering are needed to understand the relationship between the treatment applied and the component functional performance [1].
Increase of wear resistance can be obtained by choosing more durable tool materials, but we provide options for working with a material already available. In order to increase utility properties (durability) of the product, a new state of the material is formed with changed physical and sometimes chemical properties in relation to the core as a result of various types of surface treatments on their surface [2,3]. We applied multistage processes of surface layer modification, as eg.: turning-burnishing, turning-burnishing-PVD, grinding-nitriding, turning-burnishing-nitriding, turning-nitriding-polishing, turning-burnishing-nitriding-polishing as well turning or grinding only.
We have studied the relationship between phase transformations and changes in wear resistance in the surface layer of Vanadis 6 and Vancron 40 tool steels obtained after different treatments. Heat treatment was carried out in vacuum furnaces with gas quenching and tempering until the hardness of ≈ 62±1 HRC (Vanadis) and ≈ 64±1 HRC (Vancron) was achieved. Optical and scanning electron microscopy observations, X-ray diffraction and residual stress le-vels analysis and finally ball-on-disc tribological tests against Al_2O_3 pins as counterparts provide information about wear and friction values. Selected wear values for samples after mechanical processes and along with deposition of PVD coating, as shown in Figure 1.

Keywords: wear resistance, P/M tool steel, burnishing, nitriding, PVD coating.

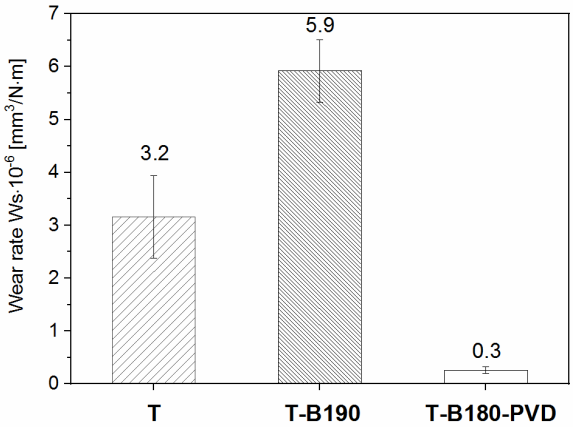

Figure 1: Wear rates obtained in pin-on-disc testing of Vanadis 6 steel after: turning (T), turning-burnishing with 190N force (T-B190), as well as turning-burnishing with 180N force and PVD coating deposition (T-B180-PVD).

Samples wear rates were significantly decreased after some combined finishing processes.

Acknowledgments
The support from the National Centre for Research and Development of Poland, Grant no. LIDER/13/0075/L7/15/NCBR/2016 is gratefully acknowledged.

References:

1. Jawahir, I.S., Brinksmeier, E., M'Saoubi, R., et al. (2011) Surface integrity in material removal processes: Recent advances, *CIRP Ann Manuf. Technol.* 60, 603-626.
2. Dearnley, P.A., Liskiewicz, T. (2013) Vapor Deposition Coating Technologies (CVD, PACVD, PVD, and Hybrid PVD-CVD) and Their Tribological Application. In: Wang, Q.J., Chung, Y-W. (Ed.). *Encyclopedia of Tribology*, Springer, New York.
3. Toboła, D., Brostow, W., Czechowski, K., et al. (2017) Improvement of wear resistance of some cold working tool steels, *Wear* 382-383, 29-39.

Phosphate and Flouride Bath Electrolyte for Low-energy PEO Coatings on Mg-based Biodegradable Materials

Y. Husak, B. Dryhval

Sumy State University, Medical Institute, 40018 Sumy, Ukraine

Abstract:
Magnesium (Mg) and its alloys are widely used in biomedical applications. The major problem of its usage remains the high degradation rate and corresponding hydrogen gas evolution adjacent to the implant. Therefore, In-vivo application of the Mg-based materials requires stable biological and mechanical properties. Porous ceramic coatings on the Mg-based biodegradable materials fabrication by Plasma Electrolytic Oxidation (PEO) have particular relevance due to the capacity to influence the surfaces' characteristics. The type of electrolytes, their concentrations, and applied voltage could influence to the morphology and microstructure of PEO coatings. The incorporation of bioactive elements such as Phosphates and Fluorides could decrease the degradation rate, develop surface morphology, and provide bioactive functional groups. The morphology, microstructure, and roughness are affected by the mechanisms of the cell interaction with coatings. The film compactness and pore characteristic are essential for cell adhesion and their further proliferation. The presence of deep pores and cracks in the surface that negatively affect the coatings' corrosion resistance is one of the PEO procedure limitations. Our previous results suggest electrolyte chemistry can influence the voltage profile (Figure 1). Our study aims to address the low-energy formation of PEO coatings as a relatively new, environmentally friendly, and low-cost process for effective surface modification of Mg-based biodegradable materials. Selecting the optimum electrolyte composition based on sodium phosphate and ammonium fluoride and electrical parameters will produce the coating with improved bio-functional properties.

Keywords: Magnesium, plasma electrolytic oxidation, coatings, surface morphology, degradation rate, electrolyte bath, biomedical applications.

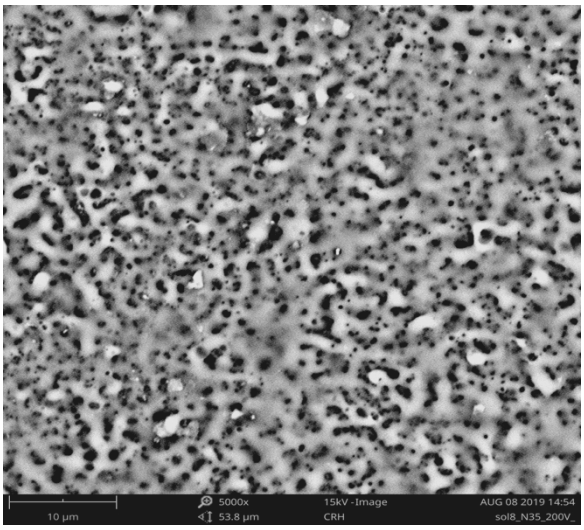

Figure 1: Scanning electron microscopy, illustrating the fundamental issue of our investigation: using the sodium phosphate and ammonium fluoride electrolyte bath makes it possible to create highly porous surface morphology without cracks with low voltage applying.

References:

1. Sampatirao, H., Radhakrishnapillai, S., Dondapati, S., Parfenov, E., Nagumothu, R. (2021) Developments in plasma electrolytic oxidation (PEO) coatings for biodegradable magnesium alloys, *Mater Today Proc.,* Published online.
2. Dehnavi, V., Binns, W.J., Noël, J.J., Shoesmith. D.W., Luan, B.L. (2018) Growth behaviour of low-energy plasma electrolytic oxidation coatings on a magnesium alloy. *J Magnes Alloy*., 6(3), 229-237.

Acknowledgements:
This research supported by H2020 MSCA-RISE-2017 project “NanoSurf 777926” and Ukraine MESU Grant # 0119U100770.

Temperature and Iodine Effects on Hydrogen Oxidation

Hee-Jung Im [1,*], Jei-Won Yeon [2]

[1] Department of Chemistry, Jeju National University,
102 Jejudaehak-ro, Jeju-si, Jeju Province 63243, Republic of Korea
[2] Nuclear Chemistry Research Division, Korea Atomic Energy Research Institute,
150 Deokjin-dong, Yuseong-gu, Daejeon 305-353, Republic of Korea
*E-mail: imhj@jejunu.ac.kr, tel: +82-64-754-3544, fax: +82-64-756-3561

Abstract:
After the hydrogen explosion during Fukushima accident in 2011, the establishment of Passive Autocatalytic Recombiner (PAR) is highly recommended in every nuclear power plant for effective hydrogen mitigation or removal. However, the catalytic performances decrease, which may be due to the poisoning on the surfaces of the PAR such as by iodine, but the mechanisms are not known and cannot explain the reason exactly.
Pt/Al_2O_3 catalyst in contact with various iodine compounds was studied by several physicochemical methods, including X-ray photoelectron spectroscopy, X-ray diffreaction, diffuse reflection UV-vis, and dispersive Raman spetra measurements. The binding energies of I 3d for Pt/Al_2O_3 catalytic pellets in contact with CsI solid (containing some drops of water), I_2 gas, and CH_3I gas were all very similar regardless of their iodine sources and 4% H_2 or air conditions at room temperature. Their positions were assigned to I_2. However, HIO_3 containing some drops of water showed two species of iodine on the Pt/Al_2O_3 catalyst, which correspond to the higher binding energies assigned to IO_3^- and the lower binding energies ascribed to I_2. For I^- of CsI, I^- remains only under H_2 condition at 200 ºC. Except that, all were oxidized to I_2. In case of HIO_3, 2~3 species exist together on the surface of Pt/Al_2O_3 catalyst and go to the more amounts of I_2 (& finally I_2 only) after the period.
It has been reported in Angew. Chem. Int. Ed. 2014, 53, 12426-12429 that "oxidation of carbon monoxide (CO) on the catalyst may result in partial inhibition of the catalyst with respect to oxidation of hydrogen, since carbon monoxide molecules occupy some hydrogen adsorption sites." The behavior of iodines is similar to the CO, so iodines are oxidized and occupy some hydrogen adsorption sites. Therefore the number of H attached on Pt/Al_2O_3 is smaller than expected.

Keywords: hydrogen removal, platinum catalyst, iodine species, temperature effect, reduction, dissociation of iodine, on the catalyst surfaces.

References:

1. Im, H.-J., Park, K.M., Yeon, J.-W. (2020), Investigation of the iodine species on platinum catalyst used as hydrogen oxidation, *Int. J. Energy Res.,* 44, 8221-8228.
2. Im, H.-J., Thang, P.T., Kim H.-H. (2019), Cleavage of functionalized organic group and role of active sites for very low concentration of gaseous wet methyl iodide in the presence of Ag nanoparticles in organofunctional silica-gel network, *Appl Surf Sci.,* 477, 15-21.
3. Im, H.-J., Pham, T.T., Kim, H.-H., Yeon, J.-W. (2018), Effect of water-droplet sizes and radiation-field exposure on the transfer of I_2 and CH_3I gases adsorbed in water, *J Radioanal Nucl Chem.,* 317, 667-673.

Stability of polyacid-doped polyaniline-based layer-by-layer films

Ju-Won Jeon*[1], Putri Bintang Dea Firda[1], Yoga Trianzar Malik[1]
1Department of Applied Chemistry, Kookmin University, Seoul, Republic of Korea States

Abstract:
Polyaniline (PANI) have been widely used as an electroactive material in electrochemical energy storage system owing to PANI's unique redox properties. However, the electrochemical stability of PANI-based electrodes still remains a challenge. Herein, a comparative study between three different polyacid-doped polyaniline-based layer by layer electrode is presented. Polyacids with different functional groups and acidity i.e., poly(acrylic-acid) (PAA), polystyrene sulfonate (PSS), and tannic acid (TA), were used. The results indicate that the stability of the electrode affected by the secondary interactions between PANI and polyacid. The weak secondary interaction between PANI and TA is not strong enough to stabilize the PANI. While strong secondary interaction between PANI and PSS might hinder the reversible redox reaction of PANI, result in unstable performance. The PANI/PAA electrodes have higher electrochemical stability compared to PANI/PSS and PANI/TA.

Keywords: polyaniline, layer-by-layer assembly, polyacid, charge storage, secondary interaction.

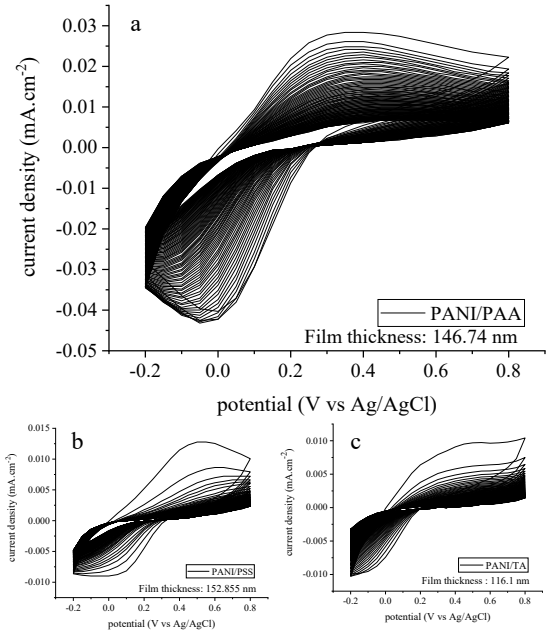

Figure 1: Cyclic voltammetry of PANI/PAA (a), PANI/PSS (b), PANI/TA (c) cycled at 50mV/s vs Ag/AgCl with 1M Na_2SO_4.

References:

1. Ju-Won Jeon, Yuguang Ma, Jared F. Mike, Lin Shao, Perla B. Balbuena, and Jodie L. L utkenhaus, "Oxidatively stable polyaniline:p olyacid electrodes for electrochemical energ y storage", Physical Chemistry Chemical Ph ysics. 2013, 15, 24, 9654-9662.